

THE EFFECT OF A  
CYLINDRICAL HEAT  
SOURCE IN CLAY

K. LAWRENCE-HAYNES  
1989

**Civil Engineering IV**

**Honours Thesis**

**The Effect of a  
Cylindrical Heat  
Source in Clay**

**K. Lawrence-Haynes**

**November 1989**

**University of Sydney**

## Abstract.

The possibility of disposing of nuclear waste in the ocean bed has led to investigations into the effect of heat upon clay. In this thesis analytic closed form solutions have been developed for a cylindrical heat source in clay. These solutions provide expressions for the increase in temperature of the soil, increases in pore pressure, displacements and stresses. Increases in pore pressure may lead to reduction in effective stresses which could cause cracks to appear in the soil allowing nuclear waste to escape.

Various cases were studied, including a constant power source, an exponentially declining with time, power source and a constant temperature source, all cylindrical in shape with the source contained within the soil. In addition the case of a cylindrical heat source around the soil body was considered for a constant power source, a constant temperature source and a temperature source linearly increasing with time. Finally, two coaxial sources were considered with the soil between the sources studied.

From this study it was found that permeable soils allow the passage of pore water through the soil from areas of high pressure to low pressure which serves to minimise the build up of pore pressures. In addition the temperature response of the soil for various cases is presented. The various conclusions were in agreement with those of other researchers including the finding that the pore water response to heating was very rapid.

### **Preface .**

. This thesis was made possible through the guidance of my supervisor Professor John Booker who provided clear, helpful and patient advice throughout the duration of my work. I am most grateful to my husband, Philip Haynes, for aiding with the computer work, and in typing the work. My parents Joan and Ron Lawrnce were also of great assistance in typing the material and in the preparation of figures.

K. Lawrence-Haynes.

List of Symbols.

- a coefficient of volumetric thermal expansion.  
a' coefficient of volumetric thermal expansion of the soil skeleton.  
 $a_u$  coefficient of volumetric thermal expansion.  
 $b'$   $B-a'$   
c specific heat.  
 $c_v$  coefficient of consolidation.  
d part of exponent for exponentially declining power source.  
e void ratio.  
h heat flux  
k coefficient of permeability.  
q thermal energy of source per unit time; per unit length.  
r radial distance.  
 $r_o$  radius of cylindrical source.  
 $r_i$  radius of coaxial cylindrical source.  
 $\Delta$  Laplace operator.  
t time.  
u excess pore water pressure.  
 $u_N$  reference excess pore pressure  $X_{\theta N}$   
 $u_0$  reference excess pore pressure  $X_{\theta 0}$   
v superficial velocity of the pore water relative to the soil.  
 $x, y, z$  Cartesian coordinate axes.  
B Bulk modulus.  
C volumetric specific heat.  
 $E'$  effective stress Youngs modulus  
F a constant  
G elastic shear modulus  
K coefficient of thermal conductivity  
 $R_s$  Rayleigh Number  
T dimensionless time constant  $\kappa t/r_o^2$   
 $T^*$  dimensionless time constant  $\kappa r/r_a^2$

$U_{xx}$  etc components of displacement.

$V$  total volume

$V_v$  volume of voids

$V_s$  volume of soil particles

$X = (\lambda + 2G) u_x - b'$

$\gamma$  bulk unit weight.

$\epsilon_v$  volumetric strain

$\epsilon_{xx}$  etc components of strain.

$\eta$  porosity

$\kappa$  coefficient of thermal diffusivity

$\lambda$  Lame's modulus

$\nu'$  Poisson's ratio in terms of effective strength

$\epsilon = s^{1/2}$

$\sigma_{xx}$  etc components of total stress

$\sigma'$  etc components of effective stress.

$\theta$  temperature increase

$\theta_0$  reference temperature

$\theta_s$  surface temperature of constant temperature source

$\nabla \cdot (\text{del}) = (\delta/\delta x, \delta/\delta y, \delta/\delta z)$

$\nabla^2 = \nabla \cdot \nabla = \delta^2/\delta x^2 + \delta^2/\delta y^2 + \delta^2/\delta z^2$

Subscripts :

$zz$  along source line

$rr$  radial

$vv$  circumferential.

## **Background to the Problem.**

The need to dispose of nuclear waste, in isolated stable areas, has lead to the suggestion that canisters of nuclear waste may be buried in places such as the ocean bed. These canisters emit heat which generally declines as the radionuclides decay. While the cannisters remain hot the surrounding soil suffers detrimental effects because the heat source causes increases in the temperature of the soil. This leads to increased pore water pressure and displacements and possibly a reduction in effective stress which may lead to cracking and destabilisation of the soil body.

In recent years it has been prudent to learn more about this situation. Such investigations are necessary because nuclear waste exists and must be disposed of safely.

Studies have been undertaken in this area through the modelling of the canisters of nuclear waste as hot sources in clay. A primary objective of the research has been to discover whether the natural barrier, provided by the ocean bed, to the passage of radionuclides, remains under the conditions of heating.

The nuclear waste materials are commonly classified as low, medium or high-level in accordance with their radionuclide content, heat generation rates and methods of treatment. High level wastes must initially be stored in water ponds or air cooling chambers before a permanent repository can be found. Medium and low level wastes can usually be placed in permanent storage soon after production.

For transporation, metal canisters are a popular choice and are typically 6 metres long and 0.6 metres in diameter. However it is not safe to depend on such canisters to contain the radioactive waste until it

becomes harmless as this may take hundreds or thousands of years, before which, corrosion will have become significant. It is thus necessary that the environment in which the canisters are stored provides a long term barrier to the migration of radionuclides.

At an early stage the idea was put forward to dispose of radioactive waste canisters in stable geological formations and provide isolation of the waste via various engineering and natural barriers. Disposal in deep continental geological formations and argillaceous formations have been considered but it is the disposal of the waste in ocean beds that is relevant to this study.

If waste is to be buried in sediments on the ocean floor it would be appropriate for the sediment to have a large sorption coefficient for radionuclides and low permeability to minimise the migration of waste. It is also important that placement of the canisters does not affect the integrity of the deposit and thus good healing properties and low strength would be desirable. To ensure long term stability any deposit chosen for the disposal of radioactive waste should be remote from disturbances due to ocean currents, volcanoes, tectonic movements and disturbances due to another ice-age.

Generally the ocean floor displays a long stable geological history and if deposits can be found satisfying the requirements they would provide a practical disposal option due to the relative ease of placement of canisters.

Canisters may be placed on the ocean floor by projectile emplacement, winch controlled placement with freefall or via a drilled hole. (Figure 1.1).

For the simplest method, of free fall after dropping from a ship it is expected a terminal velocity of approximately 50 metres per second would be achieved resulting in penetration of the order of 30m; a depth considered adequate to provide a suitable barrier. It is expected any disruption caused by placement would be sufficiently healed before waste materials began their migration due to disintegration of the canisters.

### Outline of Study.

In this study the primary aim is the development of analytic solutions to the problem of a hot source in saturated clay. Previous researchers have undertaken similar solutions including Booker & Savvidou (1984). This Thesis attempts to supplement these solutions to provide a broader understanding of the behaviour of heat sources in clay.

In devising analytic solutions, non dimensional formulations, independent of particular soil parameters, are used wherever possible. The solutions can never be exact but should provide an accurate indication of the trends to be found in particular situations.

In the analytic solutions developed by Booker & Savvidou (1984) a spherical source, of constant power output, was studied and changes in temperature, pore water pressure and stress in the neighbourhood of the source were predicted.

This study looks at an infinitely long cylindrical heat source with mathematical models following those of Booker & Savvidou. A study such as this is relevant because the canisters used to store nuclear waste are commonly cylindrical. The infinite cylinder was studied rather than a finite cylinder because the extremely complicated boundary conditions in

the latter case, making solution very difficult. The case of a finite cylinder would be expected to lie somewhere between that of the infinite cylinder and the sphere.

In the study of the infinite cylinder the cases examined were:

(i) A radiating constant power heat source of radius  $r_0$  where pore pressure, temperature and displacement changes were found at  $r > r_0$ .

The original surface temperature of the sphere was assumed to be that of the surrounding soil.

(ii) A source of the type discussed in (i) with a constant power output replaced by an exponentially decaying power source. This case is examined because as mentioned a radioactive source will decay over time. The decay is exponential and at varying rates depending on the type of radioactive source. If the decay is very slow the source may be approximately constant power while greater rates of decay would be better approximated by the exponentially decaying power source.

(iii) A radiating constant surface temperature source of radius  $r_0$  where pore pressure, temperature and displacement changes were found for  $r > r_0$  as a case intermediate to the above two.

(iv) The effect on soil inside a heat source in soil was examined as this may have significance to laboratory examinations. The heat sources studied here were again cylindrical with the cases of a constant power, linearly increasing temperature and constant temperature being examined. Again the changes in temperature, pore water pressure and displacement were examined.

(v) The case of 2 concentric cylindrical sources in the soil was examined with pore pressure and temperature changes found in the region between the two sources. A constant power and insulator source pair was examined followed by a constant temperature and insulator source pair. A constant power and zero temperature source pair were also examined. Again this study may be of significance in laboratory investigations undertaken in this field, as models of soil behaviour due to heating are considered under various circumstances.

### Literature Survey.

Studies on the thermal behaviour of soils and research relevant to the heat transfer aspect of the radioactive waste disposal problem are summarised here to give an indication of how this study relates to previous research and to provide a basis for comparison of results.

Problems such as those encountered in this examination involve strong coupling between heat transfer, pressurization, the motion of interstitial pore water and the deformation of the porous material. (Figure 1.2.) The pioneering work on such isothermal porous media was performed by Biot (1941) and (1946.) Rice and Cleary (1976) extended Biot's work with straight forward physical interpretations and general solution methods.

The effect of heat on a saturated clay is to generate excess pore pressures and triaxial tests performed on clay by Mitchell and Campanella (1963) and Plum (1968) have shown these pressure changes to be significant. The primary factory in the generation of excess pore pressure is the very high coefficient of thermal expansion of pore water relative to that of the soil particles.

Numerical predictions of the increase in temperature, pore pressure, displacement and stresses around a heat source buried in domal salt were compared with field measurements by Wagner (1982.) These agreed to within 10% for parameters other than stress. It was thought the differences in stresses may have been due to errors in the stress meters used.

Sandia Laboratories of New Mexico, USA has undertaken extensive studies in the field of heat transfer around a heat source. Hickox and Watts (1980) performed studies which included the effect of convection in addition to conduction for heat transfer. It was found for soils with low Raleigh Numbers, which includes clay, that convection was insignificant compared to conduction.

Hickox (1980) produced analytic solutions for the steady state thermal & flow fields around a point & line source of constant power in addition to around a constant temperature sphere. These studies led to the conclusion that one year after burial temperature increases, even close to the source, are small.

Sandia Laboratories also undertook an insitu heat transfer experiment which was reported by Percival (1982.) The insitu experiment used a 45 cm long, 8.3cm diameter cylinder of constant power output 60cm below the sediment water interface. A laboratory simulation produced similar results but outer isotherms were distorted due to the boundaries of the laboratory tank.

Wickens (1982) working at Harwell Laboratories confirmed the differential thermal expansion between pore water and soil particles to be the dominant driving force behind the pore fluid flow field by undertaking a numerical study and analytic solution of temperature and pore pressure changes in the soil surrounding a heat source. Here convection was ignored and the soil was treated as a saturated rigid porous matter.

Other researchers assumed the soil skeleton to be compressible and this was found to be significant as consolidation occurred. Wickens found that the pressure fields extended large distances away from the source and the pore pressure response to temperature is very rapid, occurring before the temperature response. However these effects might not be so extreme in reality due to the effects of consolidation.

The problem of heat and mass transfer around buried cables that act as heat sources in partly saturated soils has also been studied by Liukor (1975), Ravdkivi and Van U'u (1976) and Abdel Hadi & Mitchell (1981). Here the porous media was assumed rigid and evaporation was included. This work is of limited relevance to the problem under consideration because in this study the soil is assumed to remain saturated and the hot source is buried deep within the clay thus evaporation would not be significant.

Finite Element Formulations have been common in this field with Borsetto et al (1981) suggesting ways of formulating finite element solutions for heat transfer and consolidation around a hot source. Dawson & Chavez (1982) produced a finite element analysis for a heat source buried in a fully saturated compressible porous medium with the medium treated as a highly viscous fluid. Additionally Hickox et al (1980) working for Sandia Laboratories produced a finite element analysis for a decaying power source which showed a rapid drop in temperature away from the canister and the symmetry of the predicted isotherms led to the conclusion for a Raleigh Number of 0.001 or less thermal conduction alone was responsible for heat transfer. Most soils used for the disposal of nuclear waste are clays with Raleigh Numbers less than 0.001 and thus it is generally acceptable to ignore convective heat transfer components in favour of conductive heat components.

As mentioned Booker & Savvidou (1984) produced analytic solutions for a distributed and radiating constant spherical power hot source and showed that pore pressures rise to a small fraction of the value for an impermeable soil, in permeable soil. In addition measurements of pore water pressure and temperature changes close to model canisters in kaolin clay, were obtained by Savvidou (1984).

The outlined research establishes several points relevant to the study undertaken here:

- (i) For fine grained soils with low Raleigh number, such as clay, convection can be ignored in favour of conduction.
- (ii) The temperature drop with time is steep at points close to the heat source.
- (iii) The driving force behind the response to heating is the much greater coefficient of thermal expansion of pore water compared to soil particles.
- (iv) The pore pressure response to temperature is rapid, occurring even before the peak temperature response.
- (v) For correct modelling of the soil behaviour it is important that the compressibility of the soil is considered in the prediction of the generation and dissipation of excess pore water pressures.
- (vi) The permeability of the soil is significant in providing a mitigating effect to the heating of the soil. If pore water is able to flow from areas of high pressure to those of lower pressure, due to a sufficiently

permeable soil, then the rise in pore pressure is not as severe as it would be otherwise.

(vii) In assessing the suitability of a deposit for the burial of radioactive waste the reduction in effective stress due to the increase in pore pressure must be considered. A significant reduction in effective stress may lead to cracking of the soil which may allow the migration of nuclear waste materials.

### The Analytic Solutions.

As discussed analytic solutions will be developed for an infinitely long cylinder for different cases of power output. This theory is not exact and is intended to provide an indication of the trends in temperature, pore pressure, displacement and stress in response to a heat source in clay.

The assumptions made in order that such a theory be developed are presented below.

(i) The convective components of heat transfer are neglected in favour of conduction. That is heat is transferred from one part of the body to another through direct contact.

(ii) The determination of temperatures is completely uncoupled from that of pore pressures and displacements. The effect of strain on temperature is not included.

(iii) The theory of consolidation of soil for non-isothermal conditions includes the differential thermal expansion of the pore water and the soil particles and is based on the simple concepts of volume constraint and on

the effective stress principle. It is assumed that temperature increase will cause expansion of the pore water and of the soil particles. This differential expansion will cause an increase in total stress and pore water pressure. If the permeability of the soil is high enough the pore pressures will dissipate.

(iv) The soil particles and the pore water are assumed to have infinite stiffness in comparison to the stiffness of the soil skeleton this volume changes of pore water due to changes in pore pressure are neglected. The only volume changes of a soil element considered will be those due to temperature changes and water flow.

(v) Changes in the density of the soil particles and water, due to thermal expansion, are neglected. However the soil is assumed compressible and able to deform under changes in effective stress.

## 1. Preliminary Formulations

The equations used are those governing the consolidation of a saturated thermo-elastic soil.

### 1.1 Equations of Equilibrium

The condition of stress equilibrium leads to:

$$\frac{\partial \sigma_{xx}}{\partial x} + \frac{\partial \sigma_{xy}}{\partial y} + \frac{\partial \sigma_{xz}}{\partial z} = 0 \quad (1.1)$$

$$\frac{\partial \sigma_{yx}}{\partial x} + \frac{\partial \sigma_{yy}}{\partial y} + \frac{\partial \sigma_{yz}}{\partial z} = 0$$

$$\frac{\partial \sigma_{zx}}{\partial x} + \frac{\partial \sigma_{zy}}{\partial y} + \frac{\partial \sigma_{zz}}{\partial z} = 0$$

where  $\sigma_{xx}, \sigma_{yy}, \sigma_{zz} \dots$  etc denote the increase in total stress components over the initial state. Compressive stresses are considered positive.

### 1.2 The Strain Displacement Relations

The strains are related to the displacement coefficients by the following relations. Compressive strains are considered positive.

$$\epsilon_{xx} = -\frac{\partial u_x}{\partial x} \quad \gamma_{yx} = -\left[\frac{\partial u_y}{\partial x} + \frac{\partial u_z}{\partial y}\right] \quad (1.2)$$

$$\epsilon_{yy} = -\frac{\partial u_y}{\partial y} \quad \gamma_{yz} = -\left[\frac{\partial u_y}{\partial z} + \frac{\partial u_x}{\partial z}\right]$$

$$\epsilon_{zz} = -\frac{\partial u_z}{\partial z} \quad \gamma_{xz} = -\left[\frac{\partial u_z}{\partial x} + \frac{\partial u_y}{\partial x}\right]$$

$u_x, u_y, u_z$  are the Cartesian components of deformation.  
 $\epsilon_{xx}, \epsilon_{yy}, \epsilon_{zz}$  are the Cartesian strains.

$\gamma_{xx}$ ,  $\gamma_{yy}$ ,  $\gamma_{zz}$  are the shear strains.

### 1.3 Effective Stress Strain Temperature Relation.

The stress strain relation for an isotropic thermo elastic medium which includes the effect of an increase in the temperature  $\theta$ .

$$\epsilon_{xx} + \frac{\alpha' \theta}{3} = \frac{1}{E'} [\sigma'_{xx} - \nu'(\sigma'_{yy} + \sigma'_{zz})]$$

$$\epsilon_{yy} + \frac{\alpha' \theta}{3} = \frac{1}{E'} [\sigma'_{yy} - \nu'(\sigma'_{xx} + \sigma'_{zz})] \quad (1.3)$$

$$\epsilon_{zz} + \frac{\alpha' \theta}{3} = \frac{1}{E'} [\sigma'_{zz} - \nu'(\sigma'_{xx} + \sigma'_{yy})]$$

$$\gamma_{yx} = \frac{\sigma_{yx}}{G} \quad \gamma_{zx} = \frac{\sigma_{zx}}{G} \quad \gamma_{xy} = \frac{\sigma_{xy}}{G}$$

$E'$  = drained Young's modulus of the soil.

$\nu'$  = drained Poisson's ratio of the soil

$G$  = shear modulus ( $E/2(1+\nu')$ )

$\alpha'$  = thermal volumetric expansion coefficient of the soil skeleton.

The effective stresses are given by:

$$\begin{aligned}\sigma'_{xx} &= \sigma_{xx} - u \\ \sigma'_{uu} &= \sigma_{uu} - u \quad (1.3b) \\ \sigma'_{zz} &= \sigma_{zz} - u\end{aligned}$$

where  $u$  = excess pore water pressure.

Equations 1.3(a) and 1.3(b) may be rearranged to give:

$$\begin{aligned}\sigma_{xx} &= u + b'\epsilon + \lambda\epsilon_v + 2G\epsilon_{xx} \\ \sigma_{uu} &= u + b'\epsilon + \lambda\epsilon_v + 2G\epsilon_{uu} \quad (1.3c) \\ \sigma_{zz} &= u + b'\epsilon + \lambda\epsilon_v + 2G\epsilon_{zz} \\ \sigma_{uz} &= G\gamma_{uz} \\ \sigma_{zx} &= G\gamma_{zx} \\ \sigma_{uy} &= G\gamma_{uy}\end{aligned}$$

where  $\epsilon_v$  = volumetric strain =  $\epsilon_{xx} + \epsilon_{yy} + \epsilon_{zz}$   
and  $\lambda$  = Lamé modulus =  $\frac{2G\nu'}{(1-2\nu')}$   
 $G$  = elastic shear modulus,  $b' = 3 - a'$

#### 1.4 The Volume Constraint Equation.

The effect of temperature is considered by examining the pore water and soil particles separately; see figure 1.2. The increase in temperature causes the soil particles and the pore water to expand and inflow or outflow of pore water may occur at the same time or soon after.

Suppose that the initial volume of pore water is  $V_u$ , then a temperature rise of  $\alpha$  will cause the water to expand to a volume of

$$V_w(1 + 3\alpha_w\theta) \quad (1.4a)$$

where  $\alpha_w$  = linear coefficient of thermal expansion of pore water. (Assumed the same in all three directions)  $3\alpha_w = a_s$

Suppose that the initial volume of the solid particles is  $V_s$ . Due to a temperature rise of  $\theta$  the water expands to volume of

$$V_s(1 + 3\alpha_s\theta) \quad (1.4a)$$

where  $\alpha_s$  = linear coefficient of thermal expansion of soil particles. ( $3\alpha_s = a_s$ ).

The inflow of water per unit time into a soil element can be represented as

$$\left( \frac{\partial V_x}{\partial x} + \frac{\partial V_y}{\partial y} + \frac{\partial V_z}{\partial z} \right) = -\nabla^T v$$

The total inflow is obtained by integration:

$$\text{total inflow / unit volume} = - \int_0^t \nabla^T v dt$$

$$\text{total inflow} = -V \int_0^t \nabla^T v dt \quad (1.4c)$$

where  $V$  is the volume of the element =  $V_w + V_s$

The volume strain is the change in volume divided by the initial volume:

$$\epsilon_v = \frac{V_w(1+3\alpha_w\theta) + V_s(1+3\alpha_s\theta) - V \int_0^t \nabla^T v dt - V}{V}$$

where  $3\alpha_w = a_w$  and  $3\alpha_s = a_s$ .

Leading to

$$\int_0^t \nabla^T v dt = (n a_w + (1-n)a_s)\theta + \epsilon_v$$

where  $n$  = porosity =  $V_w/V$ ,

or alternately

$$\int_0^t \nabla^T v dt = a_w\theta + \epsilon_v (1.4(d))$$

where  $a_w = n a_w + (1-n)a_s$

### 1.5 Darcy's Law.

The flow of pore water in the soil is assumed to be governed by Darcy's Law.

$$\mathbf{v} = \frac{\mathbf{k}}{\gamma_w} \cdot \nabla u \quad (1.5)$$

$$\nabla u = \left[ \frac{\partial u}{\partial x}, \frac{\partial u}{\partial y}, \frac{\partial u}{\partial z} \right]^T$$

where

$\gamma_w$  = unit weight of water

$k$  = coefficient of permeability

### 1.6 Thermal Energy Balance.

The net rate of inflow of energy into an element of soil will be exactly balanced by the increase in internal energy contribution

$$\text{In this case } -\nabla^T h = C \frac{\partial e}{\partial t} \quad (1.6)$$

where

$C$  = specific heat of soil composite

$h$  = heat flux vector.

### 1.7 Fourier's Law of Heat Conduction

The flow of heat in the soil composite is governed by Fourier's Law of heat conduction thus  $h = -K\nabla e$  (1.7)

where  $K$  = coefficient of thermal conductivity and is assumed the same in all directions.

### 1.8 Equations for a Homogeneous Soil

Equations 1.1, 1.2, and 1.3(c) may be combined by substituting for the strains in equation 1.3(c)

This results in the equations:

$$\sigma_{xx} = u + b'e + \lambda e_v + 2G \left( -\frac{\partial U_x}{\partial x} \right) \quad (1.8a)$$

$$\sigma_{yy} = u + b'e + \lambda e_v + 2G \left( -\frac{\partial U_y}{\partial y} \right) \quad (1.8b)$$

$$\sigma_{zz} = u + b'e + \lambda e_v + 2G \left( -\frac{\partial U_z}{\partial z} \right) \quad (1.8c)$$

$$\sigma_{yx} = -G \left( \frac{\partial U_y}{\partial z} + \frac{\partial U_z}{\partial y} \right) \quad (1.8d)$$

$$\sigma_{xz} = -G \left( \frac{\partial U_x}{\partial z} + \frac{\partial U_z}{\partial x} \right) \quad (1.8e)$$

$$\sigma_{xy} = -G \left( \frac{\partial U_x}{\partial y} + \frac{\partial U_y}{\partial x} \right) \quad (1.8f)$$

Upon combining equations 1.8a to f it can be shown

$$G\nabla^2 U_x - (\lambda + G) \frac{\partial e_v}{\partial x} = \frac{\partial u}{\partial x} + b' \frac{\partial e}{\partial x} \quad (1.8g)$$

$$G\nabla^2 U_y - (\lambda + G) \frac{\partial e_v}{\partial y} = \frac{\partial u}{\partial y} + b' \frac{\partial e}{\partial y} \quad (1.8h)$$

$$G\nabla^2 U_z - (\lambda + G) \frac{\partial e_v}{\partial z} = \frac{\partial u}{\partial z} + b' \frac{\partial e}{\partial z} \quad (1.8i)$$

Upon Combining appropriate derivatives of equations 1.8g, 1.8h, 1.8i it is found

$$\nabla^2 [u + b'e + (\lambda + 2G)e_v] = 0 \quad (1.8j)$$

Finally on combining equations 1.4d and 1.5

$$\int_0^T \nabla^T v dt = \epsilon_v + a_{v\theta}$$

$$v = - \frac{k}{\gamma_w} \cdot \nabla u$$

$$\text{Then } \int_0^T \nabla^T \nabla u dt = - \frac{k}{\gamma_w} dt = \epsilon_v + a_{v\theta}$$

$$\text{Now } \nabla^T \nabla u = \nabla^2 u$$

$$\text{thus } - \frac{k}{\gamma_w} \int_0^T \nabla^2 u dt = \epsilon_v + a_{v\theta} \quad (1.8k)$$

Where initially  $\epsilon_v + a_{v\theta}$  is zero.

$$\text{upon differentiation } - \frac{k}{\gamma_w} \nabla^2 u = \frac{\partial \epsilon_v}{\partial t} + a_{v\theta} \frac{\partial \theta}{\partial t} \quad (1.81)$$

using equations 1.6 and 1.7

$$\nabla^T k \nabla \theta = \frac{d \theta}{dt}$$

$$k \nabla^2 \theta = C \frac{d \theta}{dt}$$

$$\kappa \nabla^2 \theta = \frac{d \theta}{dt} \quad (1.8m)$$

where  $\kappa = \frac{k}{c}$  = coefficient of thermal diffusivity.

c

## 2. The Infinitely Long Cylindrical Power Source.

The infinitely long cylindrical constant power source is examined first. Initially the surface temperature of the source is assumed to be the same as the surrounding soil. From this the solutions for a line source can be developed by allowing the radius of the cylinder to approach zero.

The source is assumed to be rigid and impermeable and buried deep in a homogenous, saturated, thermo-elastic infinite medium.

As the source is cylindrical, cylindrical coordinates will be used. The infinite source results in symmetry with respect to  $z$  in addition to  $\phi$ . See figure 1.4.

### 2.1 The Cylindrical Coordinates.

The conversion from cartesian coordinates can be represented as: (see figure 3.).

$$U_x = U_r \cos \phi \quad \cos \phi = x/r$$

$$U_\omega = U_r \sin \phi \quad \sin \phi = y/r$$

$$\text{then } U_x = \frac{U_r x}{r} \quad U_\omega = \frac{U_r y}{r}$$

$U_z = 0$  as the source is of infinite length in the  $z$  direction and thus  $U_z$  may be ignored thus

$$(U_x, U_\omega) = \frac{1}{r}(x, y) U_r(r, t) \quad (2.1)$$

## 2.2 The Omega Function.

The function omega is introduced for ease of solution of the problem with the property

$$U = \nabla \Omega = \left( \frac{\partial \Omega}{\partial r}, \frac{1}{r} \frac{\partial \Omega}{\partial \psi} \right) , \quad \Omega = \Omega(R, t)$$

following from 2.1

$$\text{thus } U_r = \frac{\partial \Omega}{\partial r} \quad (2.2),$$

other components are zero due to symmetry.

## 2.3 Strains in Cylindrical Coordinates

For the cylindrical source the only non-zero strains are

$$\epsilon_{rr} = -\frac{\partial U_r}{\partial r} \quad \epsilon_{yy} = -\frac{U_r}{r}$$

$$\text{thus } \epsilon_{\psi} = -\frac{\partial U_r}{\partial r} - \frac{U_r}{r} \quad (2.3a)$$

using equation 2.2 this becomes

$$\epsilon_{\psi} = -\frac{\partial^2 \Omega}{\partial r^2} - \frac{1}{r} \frac{\partial \Omega}{\partial r}$$

or

$$\epsilon_{\psi} = -\nabla^2 \Omega \quad (2.3b) \text{ (cylindrical coordinates)}$$

## 2.4 The Laplace Transform

To aid the solution of the differential equations the Laplace Transform of the equation may be taken. The Laplace Transform of the function  $e$  with respect to time is denoted as  $\bar{e}$  and is defined as

$$\bar{e} = \int_0^{\infty} e^{-st} e(t) dt \quad (2.4a)$$

with the Laplace variable being  $s$ .

The equation of heat conduction (1.8m) becomes

$$\kappa \nabla^2 \theta = \frac{\partial \theta}{\partial t}$$

This is solved subject to the initial condition that  $\theta = 0$  at  $t = 0$  and under the Laplace Transform  $\frac{\partial \theta}{\partial t}$  transforms to  $s\bar{\theta} - \theta(0) = s\bar{\theta}$ ,  
and so it is found that :

$$\nabla^2 \bar{\theta} = \frac{s\bar{\theta}}{\kappa}$$

or alternatively, taking account of the cylindrical symmetry

$$\frac{\partial^2 \bar{\theta}}{\partial r^2} + \frac{1}{r} \frac{\partial \bar{\theta}}{\partial r} = \frac{s\bar{\theta}}{\kappa}$$

or

$$(\xi r)^2 \frac{\partial^2 \bar{\theta}}{\partial \xi^2} + \xi r \frac{\partial \bar{\theta}}{\partial \xi} - \xi^2 r^2 \bar{\theta} = 0 \quad (2.4b)$$

where  $\xi = \frac{z}{r}$

This is known as the Modified Bessel Equation of

order zero as its solution the linear combination of two complex series expansion functions  $I_0$  and  $K_0$ .

$$\theta = AI_0(\xi r) + BK_0(\xi r) \quad (2.4c)$$

where  $A$  and  $B$  are the constants to be determined by the boundary conditions.

### 2.5 Dimensionless Form.

Before proceeding with the final solution it is necessary to convert the equation to a non dimensional form so meaningful results can be obtained without the knowledge of particular soil properties.

Firstly a non dimensional time  $T$  is introduced where

$$T = \frac{\kappa t}{r_o^2}$$

$r_o$  = radius of the cylindrical source.

Upon applying the Laplace Transform the equation 1.8m

$$\nabla^2\tilde{\theta} = \frac{\tilde{g}\tilde{\theta}}{r_o^2} \quad (2.5b)$$

And the solution to the equivalent Modified Bessel Equation of order zero is

$$\tilde{\theta} = A I_0(\xi' \frac{r}{r_o}) + B K_0(\xi' \frac{r}{r_o}) \quad (2.5d)$$

where  $\xi' = i\beta$

## 2.6. The Boundary Conditions.

In this initial examination the effect of the cylindrical source at  $r = r_0$  is examined. For away from the source the effect will be negligible. However the  $I_0$  function approaches infinity as its argument approaches infinity and therefore cannot be considered a valid solution.

The solution thus becomes:

$$\bar{\theta} = \frac{BK_0(\xi' r)}{r_0} \quad (2.6a)$$

The Boundary Condition which enables  $B$  to be determined depends upon the nature of the source. In this case it is assumed there is a specified power source of intensity  $\bar{q}$  thus:

$$\frac{K_0}{\delta r} = -\frac{\bar{q}}{2\pi r_0} \quad \text{at } r = r_0 \quad (2.6b)$$

where  $\bar{q}$  is the Laplace Transform of the power per unit length of cylinder and  $2\pi r_0$  is the surface area of the cylinder per unit length.

It is noted that the derivative of  $K_0(z)$  is  $-K_1(z)$  a Modified Bessel Function of the first order. Then upon applying the boundary condition:

$$KB K_1(\xi' r/r_0) \frac{\xi'}{r_0} = -\frac{\bar{q}}{2\pi r_0} \quad \text{at } r = r_0$$

$$B = \frac{\bar{q}}{2\pi K_1(\xi' r/r_0)}$$

$$B = \frac{\bar{q}}{2\pi K \xi' K_1(\xi')} \quad (2.6 \text{ c})$$

and hence that

$$\bar{\theta} = \frac{\bar{q}}{2\pi K} \frac{1}{\xi'} \cdot \frac{K_0(\xi' r/r_\infty)}{K_1(\xi')} \quad (2.6 \text{ d})$$

For the purposes of plotting and calculation it is meaningful to compare  $\bar{\theta}$  to a dimensionless temperature increase

$$\theta_M = \frac{q}{2\pi K}$$

A constant such as this can be moved in or out of the Laplace Transform and remains the same.

## 2.7 The Constant Power Solution.

If the power source is constant the power per unit length  $q$  is a constant and thus the Laplace Transform of this constant becomes  $\tilde{q} = \frac{q}{s} = \frac{q}{\xi'^2}$

$$\text{thus } \tilde{\theta} = \frac{q}{2\pi K} \cdot \frac{1}{\xi'^3} \cdot \frac{K_0(\xi' r/r_0)}{K_1(\xi')} \quad (2.7a)$$

where  $\xi' = js$ ,  $s$  is the Laplace Transform Variable.

or

$$\frac{\tilde{\theta}}{\theta_H} = \frac{K_0(\xi' r/r_0)}{\xi'^3 K_1(\xi')} \quad (2.7b)$$

## 2.8 The Inversion.

The solution for the constant power source in the form of equation 2.7(b) is in the Laplace domain. To obtain the increase in temperature, a function dependent on time and radial distance from the source, the inverse Laplace Transform must be taken.

There is no simple method to obtain the inverse Laplace Transform of a general function. Mathematical Tables of functions and their inverses do exist but the function 2.7b is not to be found amongst them.

The only option that remains is to perform a numerical inversion. A program to do this for functions involving Bessel Functions was obtained from Talbot (1979) and modified to suit this application. The program evaluates the  $K_0$  and  $K_1$  Bessel functions by a means appropriate to their arguments and inverts the equation (2.7b) via a numerical interpretation of the Complex Inversion

Theorem.

The program can be seen in Appendix 2 and the modifications primarily consists of writing the subroutine LTFORM, which calls the subroutine to evaluate the Bessel Functions, and then evaluates the function to be inverted. Additionally arrays of dimensionless time values and values of dimensionless distance were produced so that the dimensionless temperature rise could be evaluated for all combinations of 5 dimensionless distances and 8 dimensionless time values. The results, thus, did not depend on the particular parameters of a soil.

The program was written in FORTRAN 77 and run using Microsoft Fortran 77 Version 4.0 on an IBM AT compatible computer equipped with a 80287 coprocessor with the results plotted using Lotus 123.

The program uses complex arithmetic and thus is able to perform the inversion across the complex plane as required. In order that there was a reasonable degree of confidence in the results the program was tested using the function  $K_0(j\bar{s})$ ; see appendix 3. In addition where trends did not follow those predicted by common sense the program and functions were thoroughly checked and commonly an error was detected.

The output values of the temperature increase chosen were  $r/r_o = 1, 2, 5, 10, 50$  and  $T = 0.1, 0.5, 1.0, 10, 100, 1000$  and  $10,000$ .

Results are presented in Appendix 3.

### 3. The Infinitely Long Cylindrical Exponentially Declining Power Source.

This examination followed that of the constant power source with only the final boundary condition changed.

#### 3.1 The Equation.

The basic equation describing the rise in temperature remains unchanged from that in equations (2.6a)

$$\bar{\theta} = \frac{B K_0(\xi' r)}{r_0}$$

In addition the boundary condition for the power source exist in the same form.

$$B = \frac{\bar{q}}{2\pi K_0(\xi' K_1(\xi'))}$$

However for an exponentially declining power source (to model the exponential decay of a radioactive source)

$$q = q_0 e^{-dt} \quad (3.1a)$$

where  $d$  is a constant and  $q_0$  is the initial power source per unit lenght of the source and  $T = \kappa t / r_0^2$

For this  $\bar{q} = \frac{q_0}{s + d} \quad (3.1b)$

Thus  $\frac{\bar{\theta}}{\theta_N} = \frac{K_0(s' \xi / r_0)}{\xi (s'^2 + d) K_1(\xi')}$

### 3.2 The Inversion.

The computer program is again used with LTFORM modified appropriately, see appendix 3, to accomodate the new function.

Various values of  $\alpha$  were examined to obtain the trend for an exponentially declining power source. The same values of  $r/r_0$  and the dimensionless time were used. Results are presented in Appendix 3.

#### 4. The Line Source

As mentioned previously a line source in the soil, such as might approximate a buried cable, as examined by other researchers, can be examined by allowing  $r_0$  to become very small.

##### 4.1 The Constant and Exponentially Decaying Power Line Source.

In order that the behaviour of a soil subject to heat from an infinitely long line may be examined, a new reference radial position,  $r_a$ , may be used.

Here a new dimensionless time is used where

$$T^* = \kappa t / r_a^2$$

Following the method used in §2.5 the transformed increase in temperature is found to be:

$$\tilde{\theta} = A I_0(\xi' \frac{r}{r_a}) + B K_0(\xi' \frac{r}{r_a}) \dots (4.1a)$$

where the function  $I_0$  is disregarded as previously

thus

$$\tilde{\theta} = A K_0(\xi' r / r_a) \quad (4.1b)$$

with the boundary condition for a constant power source (or exponentially declining power source) being

$$\frac{\partial \theta_{\text{so}}}{\partial r} = -\frac{\tilde{\theta}}{2\pi r_0} \quad \text{at } r = r_0 \quad (4.1c)$$

This leads to the final solution

$$\bar{\theta} = \frac{\bar{q}}{2\pi K} \frac{K_0(\xi' r/r_a)}{\xi' r_a K_1(\xi' r_a)} \quad (4.1d)$$

In examining the behaviour of a line source, the behaviour as  $r_a \rightarrow 0$ , where  $r_a$  is the radius of the source, is analysed.

Due to the fact that  $\lim_{z \rightarrow 0} z K_1(z) = 1$

the transformed temperature increase for the line source is

$$\bar{\theta} = \frac{\bar{q}}{2\pi K} K_0(\xi r/r_a) \quad (4.1e)$$

Using the expressions for  $\bar{q}$  previously:

$$\frac{\bar{q}}{\theta_N} = \frac{K_0(\xi' r/r_a)}{\xi'} \text{ for a constant power source.}$$

$$\text{where } \theta_N = \frac{q}{2\pi K}$$

$$\text{and } \frac{\bar{q}}{\theta_N} = \frac{K_0(\xi' r/r_a)}{(\xi'^2 + d)} \text{ for the exponentially declining power source.}$$

In examining the temperature increases in this case values of  $r/r_a$  may range between zero and infinity. The discontinuity of the  $K_0$  function when it has a zero argument is in keeping with being inside the line source at this point.

LTFORM is modified appropriately and results presented in Appendix 3.

## 5. The Constant Temperature Source.

Another case worth considering is that of a cylindrical source with a constant surface temperature of  $\theta_0$ . The development is identical to that of the cylindrical constant power source with the only difference being in the final boundary condition.

Again the source is assumed to be rigid and impermeable and buried deep in a homogenous, saturated, thermoelastic infinite medium.

### 5.1 The Solution.

Again the equation 2.6a applies.

$$\bar{\theta} = \frac{3K_0(\xi'E)}{r_0} \quad (2.6(a))$$

in the non-dimensional form.

If the temperature of the source remain constant then at  $r = r_0$   $\theta = \theta_0$ . The Laplace Transform means that

$$\bar{\theta} = \frac{\theta_0}{s} \text{ at } r = r_0$$

thus  $\frac{\theta_0}{s} = \frac{3K_0(\xi')}{r_0}$

then  $\bar{\theta} = \frac{\theta_0}{s} \frac{K_0(\xi'r/r_0)}{K_0(\xi')}$

For purposes of plotting and solution  $\theta$  is compared to  $\theta_0$  then

$$\frac{\bar{\theta}}{\theta_0} = \frac{K_0(\xi' r/r_0)}{\xi'^2 K_0(\xi')} \quad (5.1a)$$

Again LTPORM is appropriately adjusted and the results produced for various  $r/r_0$  and dimensionless time values as before. The results are presented in Appendix 3.

## 6. Pore Pressure and Displacement For The Various Cases

The case of an impermeable soil will be examined in addition to that of permeable soil for various values of ratio of coefficient of permeability  $k$  and the coefficient of consolidation  $c_v$ .

### 6.1 Impermeable Soil For all Power Sourced.

Source: Pore Pressure.

Consider equation 1.8j

$$\nabla^2[u + b'\theta + (\lambda + 2G)\epsilon_v] = 0$$

all field quantities must vanish as the value of  $r$  approaches infinity thus :

$$\bar{u} = -[(\lambda + 2G)\bar{\epsilon}_v + b'\bar{\theta}] + \bar{T} \quad (6.4a)$$

where  $\bar{T}$  is a constant and equals zero for an infinite region such as this then

$$\bar{u} = -[(\lambda + 2G)\bar{\epsilon}_v + b'\bar{\theta}].$$

For the undrained case from equation (1.8l) as  $k = 0$  (for the impermeable soil)

$$c_v = -a_{uv} \theta \quad (6.1b)$$

Thus substituting equation 6.1b into 6.1a

$$\bar{u} = -[(\lambda + 2G) - a_{uv} + b']\bar{\theta}$$

$$\bar{u} = x\bar{\theta} \quad (6.1c)$$

where  $X = (\lambda + 2G)a_w - b'$

Thus for the case of an impermeable soil the pore pressure increase is directly proportional to the rise in temperature.

#### 6.2 Displacements for the Impermeable Soil with Constant and Exponentially Declining Power Source.

Consider equation 2.3

$$\epsilon_v = -\nabla^2 \tilde{\eta}$$

thus using equation 6.1b for the impermeable soil

$$\nabla^2 \tilde{\eta} = a_w \epsilon \quad (6.2a)$$

$$\text{or} \quad \nabla^2 \tilde{\eta} = a_w \bar{\epsilon} \quad (6.2a)$$

$$\text{but from equation 2.5b } \bar{\epsilon} = \frac{r_0^2}{s} \nabla^2 \tilde{\epsilon}$$

$$\text{thus } \nabla^2(\tilde{\eta} - \frac{a_w r_0^2}{s} \tilde{\epsilon}) = 0 \quad (6.2b)$$

the solution to this equation is

$$\tilde{\eta} - \frac{a_w r_0^2 \tilde{\epsilon}}{s} = D + E \ln r \quad (6.2c)$$

where D and E are constants

$$\text{but } U_r = \nabla \tilde{\eta} = \frac{\partial \tilde{\eta}}{\partial r} \text{ thus}$$

$$U_r = \frac{\partial \bar{u}}{\partial r} = \frac{a_0 r_0^2}{s} \frac{\partial \bar{u}}{\partial r} + \frac{E}{r} \quad (6.1d)$$

$U_r = 0$  when  $r = r_0$  and for the case of constant or exponentially declining power source

$$\frac{\partial \bar{u}}{\partial r} = \frac{-\bar{q}}{2\pi K r_0} \quad \text{at } r = r_0$$

$$0 = \frac{a_0 r_0^2}{s} \cdot \frac{-\bar{q}}{2\pi K r_0} + \frac{E}{r_0}$$

$$E = \frac{\bar{q} a_0 r_0^2}{2\pi K s}$$

Thus

$$U_r = \frac{a_0 r_0^2}{s} \frac{\partial \bar{u}}{\partial r} + \frac{a_0 r_0^2}{s} \frac{\bar{q}}{2\pi K} \cdot \frac{1}{r}$$

$$\bar{u} = \frac{\bar{q}}{2\pi K} \frac{K_0(\xi r/r_0)}{\xi K_1(\xi)}$$

then

$$\frac{U_r}{r} = \frac{a_0}{s} \cdot \frac{\bar{q}}{2\pi K} \left[ \frac{r_0^2}{r^2} - \frac{r_0}{r} \frac{K_1(\xi r/r_0)}{K_1(\xi)} \right] \quad (6.2d)$$

Note: for a constant power source  $\bar{q} = q_{\infty}$

for the exponentially declining power source  $\bar{q} = q_{\infty} e^{-\xi r}$

### 6.3 Displacements for the Constant Temperature Source.

#### Impervious Soil.

This follows 6.2 but

$$\frac{\partial \bar{u}}{\partial r} = \theta_0 + \frac{1}{\xi^2} + \frac{\xi}{r_0} + \frac{-K_1(\xi r/r_0)}{K_0(\xi)}$$

and again  $U_r = 0$  at  $r = r_0$

$$0 = \frac{a u r_0^2}{\xi} + \frac{a_0}{\xi r_0} + \frac{-K_1(\xi)}{K_0(\xi)} + \frac{\xi'}{r_0}$$

$$\xi' = \frac{a u r_0^2}{\xi} \frac{a_0 K_1(\xi')}{K_0(\xi')}$$

$$\frac{U_r}{r} = \frac{a u r_0^2}{\xi} \left[ \frac{r_0^2}{r} \frac{K_1(\xi')}{K_0(\xi')} - \frac{r_0^2}{r} \frac{K_1(\xi' r/r_0)}{K_0(\xi')} \right] \quad (6.3a)$$

#### (6.4) Pore Pressure For a Permeable Soil for Constant and Exponential Declining Power Source

Here the non-dimensional time constant  $T$  and the dimensionless ration  $r/r_0$  are used but the parameter  $a_u/K$  must be a specific value. Consider equation (1.81)

$$-\frac{k}{\gamma_w} \nabla^2 u = \frac{\partial e_w}{\partial t} + \frac{a u \partial e}{\partial t}$$

which becomes

$$-\frac{k}{\gamma_w} \nabla^2 u = \frac{\partial e_w}{\partial t} + \frac{k}{r_0^2} + a u \frac{\partial e}{\partial t} \frac{k}{r_0^2}$$

$$\frac{k}{\gamma_w} (\lambda + 2G) \nabla^2 \bar{u} = (-\bar{e}_w - a u \bar{e}) \frac{k}{r_0^2} (\lambda + 2G)$$

using  $\bar{e}_w = -(\bar{u} + b' a)$  from equation 6.1(a)

$$a u \nabla^2 \bar{u} = ((\bar{u} + b' a) s - a u \bar{e}) \frac{k}{r_0^2} (\lambda + 2G)$$

$$a u \nabla^2 \bar{u} = s(\bar{u} - \lambda \bar{e}) \frac{k}{r_0^2} \quad \text{where } \lambda = (\lambda + 2G) a_u - b' \quad (6.4a)$$

Additionally it is known from equation 2.5(b)

$$\nabla^2 \bar{\theta} = \frac{s\bar{\theta}}{r_o^2}$$

Assume a solution to 6.4a of the form  $L\bar{\theta} = \bar{u}$  where  $L$  is a constant.

Then

$$c_v L + s\bar{\theta} - \frac{1}{r_o^2} = s(L\bar{\theta} - x\bar{\theta}) - \frac{x\bar{\theta}}{r_o^2}$$

and

$$L = \frac{x}{1 - c_v/\kappa}$$

it remains to solve

$$c_v \nabla^2 \bar{u} - \frac{s\bar{u}}{r_o^2} = 0 \quad (6.4c)$$

This is the Modified Bessel equation of order 0 with argument  $nr$  where  $n = 4(\frac{s\kappa}{c_v})^{1/2}$

Again the solution is:

$\bar{u} = AK_0(nr/r_o) + BI_0(nr/r_o)$  with the  $I_0$  function, not included as the pore pressure must disappear as  $r$  approaches infinity.

thus the full solution is

$$\bar{u} = AK_0(nr/r_o) + \frac{x\bar{\theta}}{1 - c_v/\kappa} \quad (6.4c)$$

The boundary condition again are

$$\frac{\partial \bar{u}}{\partial r} = 0 \text{ at } r = r_0$$

This boundary condition leads to the final solution

$$\bar{u} = \left( \frac{\chi}{1 - c_w/\kappa} \right) \left\{ \frac{\bar{q}}{2\pi K} \right\} \left[ \frac{K_0(\xi' r/r_0)}{\xi' k_1(\xi')} - \frac{K_0(nr/r_0)}{nk_1(n)} \right] \quad (6.4d)$$

The pore pressures may be presented in a dimensionless form by comparing to

$$U_{in} = -\frac{\chi q}{2\pi K}$$

then

$$\frac{\bar{u}}{U_{in}} = \left( \frac{1}{1 - c_w/\kappa} \right) \left[ \frac{-K_0(\xi' r/r_0) - K_0(nr/r_0)}{\xi' k_1(\xi') nk_1(n)} \right] + F \quad (6.4e)$$

$$F = \frac{1}{\xi'^2} \quad \text{for constant power, } \quad \frac{1}{\xi' + d} \quad \text{for exponentially}$$

declining power.

The pore pressure is evaluated using an appropriate modification to LTFORM. The pore pressure increases are calculated for the same dimensionless time constant and  $r/r_0$  values as for the temperature increase cases. However, in addition the ratio of  $c_w/\kappa$  is required. The values of the ratio  $c_w/\kappa$  chosen are shown in figure 11. The results of the pore pressure increase for these ratio values are presented in Appendix 3.

6.5 Displacement for a Permeable Soil for Constant and Exponential Declining Power Sources.

The non-dimensional formulation is again used. From equation 6.1(a):

$$\begin{aligned} -\bar{\epsilon}_v &= \frac{\bar{u} + b' \bar{\epsilon}}{\lambda + 2G} \\ &= \left[ 1 - \frac{x}{c_v/K} \right] \left[ \frac{\bar{q}}{2\pi K} \right] \left[ \frac{K_0(\xi r/r_0)}{\xi K_1(\xi)} - \frac{K_0(nr/r_0)}{n K_1(n)} \right] \cdot \frac{1}{(\lambda + 2G)} \\ &\quad + \frac{b' q}{2\pi K} \frac{K_0(\xi' r/r_0)}{\xi' K_1(\xi')} \cdot \frac{1}{(\lambda + 2G)} \end{aligned}$$

using 6.4(d) and 2.4(c).

or

$$-\epsilon_v = \frac{a_M \bar{q} T_n}{2\pi K}$$

where

$$T_n = Y \left[ \frac{K_0(\xi' r/r_0)}{\xi' K_1(\xi')} \right] - Z \left[ \frac{K_0(nr/r_0)}{n K_1(n)} \right]$$

$$\text{where } Y = \frac{b'}{a_u(\lambda + 2G)} + \frac{\lambda}{a_u(\lambda + 2G)(1 - c_v/R)}$$

$$Z = \frac{\lambda}{a_u(\lambda + 2G)(1 - c_v/R)}$$

and

$$-c_v = \frac{sU_c}{sr} + \frac{Ur}{r} \quad \text{from equation (2.3a)}$$

A trial part solution is

$$\frac{U_r}{r} = \text{const} \left[ \frac{K_1(\xi' r/r_0)}{\xi' K_1(\xi')} \frac{U_a}{r} + \frac{ra^2}{\xi' r^2} \right]$$

$$K_1(z) = - K_0(z) - \frac{1}{z} K_1(z)$$

in this case

$$\frac{\partial U_r}{\partial r} = \left[ \frac{K_0(\xi' r/r_0)}{K_1(\xi')} + \frac{r_0}{\xi' r} \frac{K_1(\xi' r/r_0) - r_0^2}{K_1(\xi')} \right]$$

$$\text{then } \frac{\partial U_r}{\partial r} + \frac{U_r}{r} = \text{const} \left[ \frac{K_0(\xi' r/r_0)}{K_1(\xi')} \right]$$

this is to equal

$$\frac{Y}{\xi'} \frac{K_0(\xi' r/r_0)}{K_1(\xi')} + \frac{a_w q}{2\pi k}$$

thus

$$\text{const} = \frac{a_w q Y}{2\pi k \xi'}$$

Similarly the remainder of the solution is

$$U_r = \frac{a_w q Z}{2\pi k} \left[ \frac{r_0^2}{nr^2} + \frac{K_1(nr/r_0)}{n K_1(n)} \frac{r_0}{r} \right]$$

The entire solution is:

$$U_r = \frac{a_w q}{2\pi k} \left[ \frac{Y}{\xi'} \left\langle \frac{-K_1(\xi' r/r_0)}{K_1(\xi')} \frac{r_0}{r} + \frac{r_0^2}{nr^2} \right\rangle + \frac{Z}{n} \left\langle \frac{K_1(nr/r_0)}{n K_1(n)} \frac{r_0}{r} - \frac{r_0^2}{nr^2} \right\rangle \right]$$

Note this satisfies the boundary condition of  $U_r = 0$

when  $r = r_0$  thus it is the full solution.

#### 6.6 The Pore Pressure for an Permeable Soil with a Constant Temperature Source.

This follows the method for 6.4 but the boundary condition is modified where the value of temperature at  $r = r_0$  is  $\theta_0$ .

$$\text{Again } \bar{u} = \Delta K_0(nr/r_0) + \frac{\chi}{(1-\epsilon_u/\kappa)} \bar{\theta}$$

and  $\partial u/\partial r = 0$  at  $r = r_0$  but the different expression for  $\bar{\theta}$  produces the solution

$$\frac{\bar{u}}{u_{n'}} = \frac{1}{(1 - \epsilon_u/\kappa)} \frac{1}{\xi} \left[ \frac{K_0(\xi' r/r_0)}{\epsilon' K_0(\xi')} - \frac{K_1(\xi') K_0(nr/r_0)}{K_0(\xi') n K_1(n)} \right]$$

Where  $u_{n'} = \chi \theta_0$

The pore pressures are evaluated for the same cyclic ratio value as for the constant and exponentially declining power sources. The results are shown in appendix 3.

#### (6.7) The Displacements for Permeable Soil for the Constant Temperature Source.

Following a similar process as for 6.5 it is found that:

$$\begin{aligned} \frac{u_r}{r} &= \frac{\chi \theta_0 n}{\xi} \left[ \frac{1}{\xi} \left( \frac{K_1(\xi' r/r_0) \epsilon_0}{K_0(\xi')} - \frac{K_1(\xi')}{K_0(\xi')} \frac{r \epsilon_0^2}{r^2} \right) \right] \\ &= \frac{\chi}{n \xi} \left( \frac{K_1(nr/r_0)}{K_0(n)} \frac{\epsilon_0}{r} - \frac{K_1(n)}{K_0(n)} \frac{r \epsilon_0^2}{r^2} \right) \end{aligned} \quad (6.7a)$$

which satisfies the boundary condition  $U_r = 0$  at  $r = r_o$   
and is thus the complete solution.

#### 6.8 Special Cases for Pore Pressures when $c_v = \infty$

See appendix for this development

#### 6.9 Pore Pressure for the Line Sources - Impermeable Soil.

For the constant power line source

$$\frac{\bar{e}}{e_n} = \frac{K_0(\xi' r/r_a)}{\xi}$$

For the exponentially declining power source

$$\frac{\bar{e}}{e_n} = \frac{K_0(\xi' r/r_a)}{(\xi'^2 + d)}$$

Again the non dimensional form is used following section 6.4 a similar solution is obtained with  $I_0$  ignored as previously thus the full solution is

$$\bar{u} = A K_0(nr/r_a) + \frac{X}{(1 - c_v/\kappa)} \bar{e}$$

The boundary condition  $\delta\bar{u}/\delta r = 0$  at  $r = r_o$

This leads to :

$$\frac{\bar{u}}{u_n} = \frac{1}{(1 - c_v/\kappa)} \left[ \frac{K_0(\xi' r/r_a)}{\xi} - \frac{X_0(nr/r_a) X_1(\xi' r_o/r_a)}{\xi n X_1(nr_o/r_a)} \right]$$

for the constant power case and

$$\frac{\bar{u}}{u_N} = \frac{1}{(1 - \alpha_U/\kappa)} \left[ \frac{K_0(\xi' r/r_a)}{(\xi'^2 + d)} - \frac{\xi' K_0(nr/r_a) E_1(\xi' r_a/r_a)}{n K_1(n r_a/r_a)(\xi'^2 + d)} \right]$$

for the declining power source.

#### 6.10 Stress.

Stresses for all the cases studied here may be obtained once pore pressure, temperature and displacement increases are known.

Stresses will be most meaningful when obtained in cylindrical form as found previously the only non-zero components of displacement are:

$$\epsilon_{rr} = -\frac{\partial u_r}{\partial r} \text{ and } \epsilon_{rr} = \frac{-u_r}{r}$$

thus  $\epsilon_v = -\left(\frac{\partial u_r}{\partial r} + \frac{u_r}{r}\right)$  where  $u_r$  = radial displacement.

$$\text{Now } \sigma_{rr} = 2G\epsilon_{rr} + \lambda\epsilon_v + u + b'\theta$$

$$\sigma_{vv} = 2G\epsilon_{vv} + \lambda\epsilon_v + u + b'\theta$$

$$\sigma_{rz} = \lambda\epsilon_v + u + b'\theta$$

$$\sigma_{rv} = G\gamma_{rv}$$

$$\sigma_{rz} = G\gamma_{rz}$$

$$\sigma_{ra} = G\gamma_{ra}$$

From equation 6.4a  $u + b'\theta = -(\lambda + 2G)\epsilon_v$

This results in

$$\sigma_{rr} = 2G \frac{U_r}{r} \quad 6.10a$$

$$\sigma_{rv} = 2G \frac{\partial U_r}{\partial r} \quad 6.10b$$

$$\sigma_{rz} = 2G \left( \frac{\partial U_r}{\partial r} + \frac{U_r}{r} \right) \quad 6.10c$$

Additionally  $\gamma_{ry} = 0$     $\gamma_{rz} = 0$     $\gamma_{rz} = 0$  due to symmetry and the infinite length of the cylinder.

Thus the expressions for displacements derived previously readily lead to the expressions for stress in all cases studied.

## 7. Study of the Interior of a Cylindrical Source

The case now examined is that of the interior of a heat source. This is studied as it may have relevance to laboratory studies of the effect of heat on a soil where an external heat source is applied to body of soil. Such heat sources may be modelled by sources in laboratory studies. Experiments of this sort may lead to a greater understanding of the behaviour of heated soils in the field. The source in this case is a cylindrical shell and various types of heat sources are examined. The model developed for the soil behaviour in the previous examination is again relevant, and the solution to these problems depends only upon a modification of the boundary conditions.

### 7.1. The Constant Power.

This case is considered as it may be easily simulated in the laboratory. In considering the interior of the source from  $0 \leq r \leq r_0$ , where  $r_0$  is the radius of the source, the function  $K_0(\xi' r/r_0)$  must be ignored as this function has a discontinuity at  $r = 0$ . Thus the solution is

$$\bar{\theta} = A I_0(\xi' r/r_0) \quad (7.1a)$$

The boundary condition for a constant power source becomes

$$\frac{d\bar{\theta}}{dr} = \frac{\bar{q}}{(2\pi r_0 K)} \quad (7.1b) \quad r = r_0$$

Note: Unlike the previous case of  $r \geq r_0$  the right hand side of the equation is positive as the radius is

measured in the reverse direction to previously.

The derivative of the function  $I_0(z)$  is  $I_1(z)$  thus

$$KI_1(\xi') - \frac{\xi'}{r_0} = \frac{\bar{q}}{2\pi r_0 K} \quad \text{at } r = r_0$$

$$A = \frac{\bar{q}}{2\pi \xi' K I_1(\xi')}$$

$$\bar{\theta} = \frac{\bar{q}}{2\pi K \xi'} \cdot \frac{I_0(\xi' r/r_0)}{I_1(\xi')} \quad (7.1c)$$

For the case of the constant power source  $\bar{q} = \frac{q_0}{s}$

and if  $\theta_H = \frac{q_0}{2\pi K}$

$$\frac{\bar{\theta}}{\theta_H} = \frac{I_0(\xi' r/r_0)}{\xi' I_1(\xi')} \quad (7.1d)$$

## 7.2 The Constant Temperature Source.

A constant surface temperature source is examined as it is easily produced under laboratory conditions and is a natural choice in terms of a basic type of heat source. The solution here follows that of section 7.1 with the exception that now:

$$\bar{\theta} = \frac{\theta_H}{s} \quad \text{at } r = r_0$$

leading to  $\bar{\theta} = \frac{\theta_H \ln(\xi' r/r_0)}{\xi' I_0(\xi')} \quad (7.2a)$

### 7.3 The Linearly Increasing Temperature Source.

This source is studied as it may be combined in various ways with the constant heat source to approximate laboratory conditions such as rapid heating to a plateau, of the source. Different cases may be achieved by adding or subtraction the results of 7.2 and 7.3.

Let the temperature of the source follow

$\theta = MT$  where  $M$  is a constant for the source with units of temp/dimensionless time.

then  $\bar{\theta} = \frac{M}{\pi^2} r^2$  at  $r = r_0$

From 7.1a  $\bar{\theta} = A I_0 \left[ \frac{\xi' r}{r_0} \right]$  then in this case  $\frac{M}{\pi^2} = A I_0(\xi')$

thus

$$\bar{\theta} = \frac{M I_0(\xi' r/r_0)}{\pi^2 I_0(\xi')} = \frac{M I_0(\xi' r/r_0)}{\xi'^2 I_0(\xi')} \quad (7.3b)$$

$M$  could be expressed as  $\alpha_M/T_M$  where  $\alpha_M$  and  $T_M$  are both constants. Then

$$\bar{\theta} = \frac{\alpha_M(\xi' r/r_0)}{\xi'^2 I_0(\xi') T_M}$$

### 7.4 Pore Pressure for the Interior

#### Case -Preliminary Work.

This case a permeable soil and permeable source is examined as this is likely to be encountered in a laboratory examination. An impermeable source or soil means the pore pressure response follows that of

temperature and no new understanding is gained. Equation 6.1a is considered

$$\bar{u} = -f(\lambda + 2G)\bar{\epsilon}_v + b'\bar{\epsilon}_l + \bar{T}$$

In a case such as this the constant function  $f$  is not zero as the region is bounded thus

$$\bar{u} = -f(\lambda + 2G)\bar{\epsilon}_v + b'\bar{\epsilon}_l + \bar{T} \dots (7.4a)$$

Following a method similar to that in section 6.4 it is found for the interior case

$$\nabla^2(\bar{u} - \bar{T}) = s(\bar{u} - \bar{T} - x\bar{\theta})\frac{\kappa}{r_0^2} \dots (7.4b)$$

where  $X = (\lambda + 2G)a_{ll} - b'$

The complete solution becomes

$$\bar{u} = \bar{T} + A I_0(n r / r_0) + \frac{x\bar{\theta}}{(1 - c_v/\kappa)} \dots (7.4c)$$

where  $A$  is a constant and  $n = \sqrt{\frac{8K}{c_v}}$

Two boundary conditions are required to solve  $\bar{T}$  and  $A$ . For the permeable source  $\bar{u} = 0$  at  $r = r_0$  then

$$0 = \bar{T} + A I_0(n) + \frac{x\bar{\theta}_{r=r_0}}{(1 - c_v/\kappa)} \dots (7.4d)$$

### 7.5 The Displacements to the Interior.

In order to solve the pore pressures a boundary condition for the displacements, corresponding to a rigid heat source, is incorporated. The constant

function  $f$  does not appear in the expressions for displacements. Naturally the displacements are presented in the cylindrical coordinate system.

$$\text{From equation 6.4a } -\bar{\epsilon}_v = \frac{(\bar{u} + b'v) - \bar{f}}{(\lambda + 2G)}$$

$$-\bar{\epsilon}_v = \frac{\partial U_r}{\partial r} + \frac{U_r}{r}$$

a) For the constant power source this leads to

$$\frac{\partial U_r}{\partial r} + \frac{U_r}{r} =$$

$$\left[ A I_0(n r / r_0) + \frac{\chi \bar{q} I_0(\xi' r / r_0)}{2\pi K \xi I_1(\xi)(1 - c_v/\kappa)} + \frac{b' \bar{q} I_0(\xi' r / r_0)}{2\pi K \xi I_1(\xi)} \right] / (\lambda + 2G)$$

or

$$\frac{\partial U_r}{\partial r} + \frac{U_r}{r} = \frac{\bar{q}}{2\pi K} \bar{m}_*$$

$$\text{where } \bar{m}_* = Y \left[ \frac{I_0(\xi' r / r_0)}{I_1(\xi)} \right] + Z \left[ \frac{I_0(n r / r_0)}{n I_1(n)} \right]$$

$$\text{and } Y = (b' + \chi / (1 - c_v/\kappa)) / (\lambda + 2G)$$

$$Z = \frac{2\pi K A I_1(n)}{q(\lambda + 2G)}$$

As in the formulation of displacements for the exterior case a solution is obtained.

The complete solution is

$$\frac{\bar{U}_r}{r} = \frac{\bar{q}Y}{2\pi K \xi} \left[ \frac{I_1(\xi' r/r_o) r_o}{I_1(\xi') r} \right] + \frac{AI_1(n)}{(\lambda + 2G)} \left[ \frac{I_1(nr/r_o) r_o}{n I_1(n) r} \right] + \frac{M}{r^2}$$

where M is a constant

The  $K_0$  and  $K_1$  Bessel Functions are not included in this expression as they each have a discontinuity at  $r = 0$ . In addition, the constant M must be zero to prevent a discontinuity at  $r = 0$ .

In order to find the constant A a rigid heat source is assumed where  $\bar{U}_r/r = 0$  at  $r = r_o$ .

$$\text{thus } A = \frac{-\bar{q}Y(\lambda + 2G)n}{\xi^2 I_1(n) 2\pi K} \quad \dots 7.5a$$

leading to the final solution

$$\frac{\bar{U}_r}{r} = \frac{\bar{q}Y}{2\pi K \xi^2} \left[ \frac{I_1(\xi r/r_o) r_o}{I_1(\xi) r} - \frac{I_1(nr/r_o) r_o}{I_1(n) r} \right] \quad (7.5b)$$

For the constant power source  $\bar{q} = \frac{q_{av}}{\xi}$

b) For the constant temperature source

$$\begin{aligned} \frac{\partial \bar{U}_r}{\partial r} + \frac{\bar{U}_r}{r} &= \left[ AI_0(nr/r_o) + \frac{\lambda \rho q I_0(\xi' r/r_o)}{(1-\rho \nu/\kappa) \xi^2 I_0(\xi')} + \right. \\ &\quad \left. \frac{b' \rho q I_0(\xi' r/r_o)}{\xi^2 I_0(\xi')} \right] / (\lambda + 2G) \end{aligned}$$

or

$$\frac{\xi \bar{U}_r}{\partial r} + \frac{\bar{U}_r}{r} = \rho q n^2$$

where

$$n^+ = Y \left[ \frac{I_0(\xi' r/r_0)}{\xi' I_0(\xi')} \right] + Z \left[ \frac{I_0(nr/r_0)}{n^2 I_0(n)} \right]$$

and

$$Y = [b' + x/(1 - c_0/\kappa)]/(\lambda + 2G)$$

$$Z = \frac{AI_0(n)n^2}{(\lambda + 2G)\theta_0}$$

The Solution, not including functions with discontinuities at  $r = r_0$  is:

$$\frac{\theta_r}{r} = \left[ \frac{\theta_0 Y}{\xi'} \left[ \frac{I_1(\xi' r/r_0)}{I_0(\xi')} \right] + \frac{n^2 AI_0(n)}{(\lambda + 2G)} \left[ \frac{I_1(nr/r_0)}{n^2 I_0(n)} \right] \right] r^2$$

Again  $\frac{\theta_r}{r} = 0$  at  $r = r_0$  for the rigid source.

$$\text{then } A = \frac{-\theta_0 Y (\lambda + 2G) n}{\xi'^2 I_0(n)} \quad \dots \quad (7.5c)$$

$$\text{thus } \frac{\theta_r}{r} = \frac{\theta_0 Y}{\xi'} \left[ \frac{I_1(\xi' r/r_0) r_0}{I_0(\xi') r} - \frac{I_1(nr/r_0) r_0}{I_0(n) r} \right] \quad \dots \quad (7.5d)$$

(c) The linearly increasing temperature produces a similar solution where:

$$\frac{\theta_r}{r} = \left[ \frac{\theta_M Y}{T_M \xi'} \left[ \frac{I_1(\xi' r/r_0)}{I_0(\xi')} \right] + \frac{n^2 AI_0(n)}{(\lambda + 2G)} \left[ \frac{I_1(nr/r_0)}{n^2 I_0(n)} \right] \right] r^2$$

$$\text{where } Y = b' + x/(1 - c_0/\kappa)/(N + 2G)$$

Again for a rigid source  $\frac{\theta_r}{r} = 0$  at  $r = r_0$  then

$$A = \frac{-\theta_M}{T_M} \frac{Y (\lambda + 2G) n}{\xi'^2 I_0(n)} \quad \dots \quad (7.5e)$$

thus

$$\frac{U_r}{r} = \frac{\rho_M}{T_H} \frac{Y}{\epsilon} \cdot S \left[ \frac{I_1(\xi' r/r_0) r_0}{I_0(\xi')} - \frac{I_1(nr/r_0) r_0}{I_0(n/r)} \right] \quad (7.5f)$$

### 7.6 Final Solution of Pore Pressures.

Having applied the boundary condition of the source being rigid, in section 7.5 the value of the constant A is now known. Thus the complete pore pressure solutions are known.

In order to obtain the full solution for pore pressure the value of A from section 7.5 is used in conjunction with equations 7.4c and d.

From equation 7.4c and d

$$\bar{u} = A(I_0(nr/r_0) - I_0(n)) + \frac{Y}{(1 - c_v/\kappa)} [\bar{e} - \bar{e}_{r=r_0}] \quad (7.6a)$$

a) For the constant power case  $A = -\frac{q_0 Y (\lambda + 2G)}{\epsilon^2 I_1(n) 2\pi K}$

and  $Y = \frac{b'(1 - c_v/\kappa) + x}{(\lambda + 2G)(1 - c_v/\kappa)}$

This gives the solution:

$$\bar{u} = \left[ \frac{q_0 x}{2\pi K} \right] \cdot \frac{1}{(1 - c_v/\kappa)} \cdot \frac{1}{\xi^2} \left[ \bar{p}^* - \bar{q}^* \right] \quad (7.6(b))$$

where  $\bar{q}^* = \frac{b'(1 - c_v/\kappa) + x}{Y} \left[ \frac{n I_0(nr/r_0) - n I_0(n)}{I_1(n)} \right]$

$$\bar{p}^* = \frac{\xi' I_0(\xi' r/r_0) - \xi' I_0(\xi)}{I_1(\xi)}$$

b) The solution for the pore pressure increase using the results from 7.5 and 7.6 becomes:

$$\bar{u} = \frac{\theta_0 X}{(1 - c_v/\kappa) \xi' s} \left[ \bar{r}_* - \bar{s}_* \right] \quad (7.6c)$$

where  $\bar{r}_* = \left[ \frac{\xi' I_0(\xi') r/r_0}{I_0(\xi)} - \frac{\xi' I_0(\xi')}{I_0(\xi)} \right]$

$$\bar{s}_* = \left[ \frac{b'(1 - c_v/\kappa) + 1}{X} \right] \left[ \frac{n I_0(nr/r_0)}{I_0(n)} - \frac{n I_0(n)}{I_0(n)} \right]$$

c) For the source with temperature linearly increasing with time, using equations from sections 7.5 and 7.6

$$\bar{u} = \frac{\theta_0 X}{T_m(1 - c_v/\kappa) \xi' s} \left[ \bar{r}_* - \bar{s}_* \right] \quad (7.6d)$$

where  $\bar{r}_*$  and  $\bar{s}_*$  are as in b)

In solving these pore pressures numerically only the case of  $c_v/\kappa$  equal to 0.5 was considered. This is because it has been adequately shown in the case of  $r=r_0$ , that a lower value of  $c_v/\kappa$  ratio corresponds to low permeability. A high permeability results in a greater mitigating effect on pore pressure due to the flow of pore water.

In addition a value of  $\frac{b'}{X}$  is required.

$X = a_u(\lambda + 2G) - b'$ . For numerical results the case of  $a_u(\lambda + 2G) = 2b'$  was considered, thus  $b'/X = 1$ .

Pore pressures were calculated using a suitable form of LTFORM. Results are in Appendix 3.

### 7.7 Stress For Interior Case.

In this case the effect of the constant function on stress is additive thus following section 6.10 the stresses become

$$\tilde{\sigma}_{rr} = \bar{f} + \frac{2G\bar{U}_r}{r} \quad (7.7(a))$$

$$\tilde{\sigma}_{rr} = \bar{f} + \frac{2G\delta\bar{U}_r}{\delta r} \quad (7.7(b))$$

$$\tilde{\sigma}_{zz} = \bar{f} + 2G\left[\frac{\bar{U}_r}{r} + \frac{\delta\bar{U}_r}{\delta r}\right] \quad (7.7(c))$$

All other components of stress are zero.

### 7.8 Interior Study.

The program used previously in the evaluation of the functions for the exterior case can be used again. However this time a new subroutine to evaluate I functions of various order was obtained. This time LTFORM was modified to call the subroutine evaluating the I Bessel functions. Thus the dimensionless temperature increases were evaluated for various r values less than 1 (i.e. the interior of the source) and the same dimensionless time values as used for the exterior case.

8. The examination of the Response Between  
Two Coaxial Cylindrical Sources.

In extending the modelling of possible laboratory examinations of the effect of heat on soil the behaviour of an annular region of soil between two heat sources is considered. Here two different heat sources affect the soil and thus a picture of the combined effect of heat sources can be found. The heat sources are of the form of coaxial cylinders and again could be modelled by sources in an experiment. It is hoped the various cases studied could be combined to produce a more complete picture of the reaction of soil to heating. Once again the modelling in previous sections remains valid and the problem becomes one of boundary conditions.

Thus

$$\bar{\theta} = AI_0 \left( \frac{k' r}{r_o} \right) + BK_0 \left( \frac{k' r}{r_o} \right)$$

is the relevant equation.

The inner source is assumed to have a radius of  $r_o$  and the outer source a radius of  $r_i$ .

8.1 The Case of the Interior Source of Constant Power and the Outer Source Insulated.

In this case neither  $I_0$  or  $K_0$  are to be discounted as the range of  $r$  values are limited to those between  $r_o$  and  $r_i$ . Here there are 2 boundary conditions, one for each source.

For the inner source of constant power the boundary

condition becomes

$$K \frac{\partial \theta}{\partial r} = -\frac{\bar{q}}{2\pi K \xi}, \text{ at } r = r_0 \quad (8.1a)$$

which produces the equation

$$AI_1(\xi') - BK_1(\xi') = -\frac{\bar{q}}{2\pi K \xi} \quad (8.1b)$$

For the outer source which is insulated the boundary condition becomes

$$\frac{\partial \theta}{\partial r} = 0 \text{ at } r = r_1 \quad (8.1c)$$

which produces the equation

$$AI_1(\xi' r_1/r_0) - BK_1(\xi' r_1/r_0) = 0 \quad (8.1d)$$

Equations 8.1b and 8.1d may be solved simultaneously to obtain the full solution

$$A = \frac{BK_1(\xi' r_1/r_0)}{I_1(\xi' r_1/r_0)} \quad \dots \quad 8.1d$$

then upon substitution into equation 8.1b the final solution becomes

$$\bar{\theta} = \frac{\bar{q}}{2\pi K \xi} \left[ \frac{K_1(\xi' r_1/r_0) I_0(\xi' r/r_0) + I_1(\xi' r_1/r_0) K_0(\xi' r/r_0)}{(K_1(\xi') I_1(\xi' r/r_0) - I_1(\xi') K_1(\xi' r_1/r_0))} \right]$$

or non-dimensionally

$$\bar{\theta}_n = \frac{1}{\xi'^2} \left[ \frac{K_1(\xi' r/r_0) I_0(\xi' r/r_0) + I_1(\xi' r_1/r_0) K_0(\xi' r/r_0)}{(K_1(\xi') I_1(\xi' r/r_0) - I_1(\xi') K_1(\xi' r_1/r_0))} \right]$$

For the case of constant power source. As previously the program may be run with the calling routine LTFORM

calling routines to evaluate I functions in addition to those to evaluate K functions. In addition there must be an inclusion of  $r_i < r < r_o$ ; thus  $1 < r/r_o < r_i/r_o$ . In this case the previous values of the ratio  $r/r_o$  are replaced with values between 1 and  $r_i/r_o$  with the same time constants used as previously. In addition the value of  $r_i/r_o$  may vary and the program is run for various values of this parameter. The results are presented in Appendix 3.

### 8.2 The Case of the Interior Source of Constant Temperature and the Outer Source Insulated

Here the solution follows 8.1 but the inner boundary condition

$$\bar{\theta} = \frac{\theta_{in}}{n} \text{ at } r = r_o \quad (8.2)$$

$$\text{thus } AI_0(\xi') + BK_0(\xi') = \frac{\theta_{in}}{n} \quad (8.2b)$$

and for the second boundary condition as before

$$AI_1(\xi' r_i/r_o) - BK_1(\xi' r_i/r_o) = 0 \quad (8.2c)$$

Upon solving the simultaneous equations produced by the boundary conditions:

$$\frac{\theta}{\theta_{in}} = \frac{1}{\xi'^2} \left[ \frac{K_1(\xi' r_i/r_o) I_0(\xi' r/r_o) + I_1(\xi' r/r_o) K_0(\xi' r/r_o)}{K_0(\xi') I_1(\xi' r_i/r_o) - K_1(\xi' r_i/r_o) I_0(\xi')} \right]$$

Again the results are evaluated using the computer program with the same values of  $r/r_o$ ,  $r_i/r_o$  and the dimensionless time value. The results are presented in Appendix 3.

### 8.3 The Constant Power and Zero Temperature Sources.

Here the case of a constant power interior source and a constant zero temperature outer source is examined.

The boundary conditions are  $K\frac{\partial \theta}{\partial r} = -\bar{q}$  at  $r = r_o$  (8.3a)

$$AI_i(\xi') - BK(\xi') = -\frac{\bar{q}}{2\pi K\xi}, \quad (8.3b)$$

and  $\bar{\theta} = 0$  at  $r = r_i$  (8.3c)

$$\text{then } AI_o(\xi' r_i/r_o) + BK_o(\xi' r_i/r_o) = 0$$

this leads to the solution

$$\frac{\bar{\theta}}{\bar{\theta}_N} = \frac{1}{\xi'^2} \left[ \frac{I_0(\xi' r_i/r_o)K_o(\xi' r/r_o) - K_o(\xi' r_i/r_o)I_0(\xi' r/r_o)}{I_i(\xi')K_o(\xi' r_i/r_o) + I_o(\xi' r_i/r_o)K_i(\xi')} \right]$$

Which can be solved such as in cases 8.1 and 8.2 with results in Appendix 3.

### 8.4 The Case of a Narrow Strip Between two Electrodes.

The case of a narrow strip in soil between two heat sources may be approximated by using the general theory for the two sources with the difference between  $r_o$  and  $r_i$  very small. This is examined for the 3 cases looked at in 8.1, 8.2 and 8.3. In order that the accuracy of this approximation can be assessed the exact solution may also be obtained. This is presented for the case of the constant temperature source and the insulating outer source.

In this case the corresponding equations, based on a

dimensionless time  $T = \kappa t/d^2$  becomes

$$\frac{d^2\bar{\theta}}{dz^2} = \pi/d^2\bar{\theta} \quad \dots \quad (8.4a)$$

This differential equation may be solved by the operator method giving

$$\bar{\theta} = A \sinh\left[\frac{i\pi z}{d}\right] + B \cosh\left[\frac{i\pi z}{d}\right] \dots \quad (8.4b)$$

There are two boundary condition that enable the full solution to be determined.

In the case of the constant temperature inner source at  $z = 0$  and the insulation source at  $z = d$  may be studied. The boundary conditions for this situation are:

$$\bar{\theta} = \frac{\theta_{in}}{s} \quad \text{at } z = 0$$

$$\frac{d\bar{\theta}}{dz} = 0 \quad \text{at } z = d$$

This leads to the solution:

$$\bar{\theta} = -\frac{\theta_{in}}{s} \frac{\sinh[i\pi s]}{\cosh[i\pi s]} \sinh\left[\frac{i\pi z}{d}\right] + \frac{\theta_{in}}{s} \cosh\left[\frac{i\pi z}{d}\right] \dots \quad (c)$$

This result may be computed numerically using an appropriate version of LTFORM and compared to the result where  $r_o$  and  $r_i$  are close together for the inner constant temperature source and the outer insulated source.

In comparing the results it should be remembered that the results are dependent on the time constant  $T$ . For the annular approximation  $T = \frac{\kappa t}{r_o^2}$  and for the exact

solution  $T = \frac{kt}{d^2}$ . Now to compare the results at a similar time we must consider  $r_o^2$  is very large and  $d^2$  is relatively small. As a result the temperature increase should be examined at much smaller values of  $T$  for the annular approximation compared to the exact solution. As this is a verification of the annular approximation, studying the single case of the interior source at constant temperature and the exterior electrode insulated, is sufficient. Pore Pressures for the strip are not studied as trends can be predicted from the results of the annular region.

#### 8.5 Pore Pressure for the Double Electrode Examination

For an impermeable soil pore pressure increase is directly proportional to the temperature increase and found in previous studies. The pore pressures can be found by a process similar to that used to evaluate pore pressures for  $r > r_o$  and  $r < r_o$  examinations. The results are complicated expressions involving  $K$  and  $I$  Bessel functions of degree 0 and 1 and related to temperature in the same way as previous cases. Due to their complexity these calculations are not presented but similar trends to those in previous examples are expected.

## Discussion of Results.

### 9.1 The Temperature and Pore Pressures for the Cylindrical Sources.

#### Temperature Effects.

As discussed previously primarily 3 cases were studied, the constant power source, the exponentially declining power source and the constant temperature source. Of these cases the constant power source input an infinite amount of energy into the soil over time, with the other cases inputting finite energy. The temperature rise was compared to  $O_n$ , a reference temperature and results were obtained for a dimensionless time parameter and the radial distance compared to the radius of the source. Results were plotted primarily for various values of  $r/r_0$  and with respect to the logarithm of the dimensionless time parameter.

In accordance with the infinite input of power for the case of a constant power source (Figure 3.1) the temperature continued to rise indefinitely with the curves for various values of  $r/r_0$  becoming parallel on the log plot indicating a fairly constant rate of increase in temperatures throughout the soil as the time became large.

The data can also be examined as temperature increase divided by the reference temperature verses  $r/r_0$  with curves plotted for various time values (Figure 3.1a). This tended to show that the decline in temperatures with increasing radius was much more rapid near the source than further away.

For the exponential source the exponent was  $-dT$  where  $T$  is dimensionless time and  $d$  is a constant. A representative value of 0.1 was

used for d. A very low value of d meant the response was very close to that of a constant power source, with a value of zero being the constant power source. Higher values of d meant the response was almost completely damped. The various trends in behaviour were though generally the same for various values of d. The value 0.1 was used for all subsequent exponentially declining power sources.

For the exponentially declining power source a peak in temperature occurred relatively quickly after which the temperature increase declined to zero (Figure 3.5) with lower peak temperatures occurring further away from the source and the peak occurring at a slightly later time. This is to be expected as the heat effect takes time to travel to areas further away from the source but the response is still quite rapid.

As would be expected the case of the constant temperature source, (Figure 3.9) falls between those of the constant power source and the exponentially declining power source. Here the soil approaches the temperature of the source, with the rate of increase of temperature slowing considerably with time.

#### Pore Pressure Effects.

As mentioned previously the excess pore pressures developed are examined in two categories. Regardless of the type of source the increase in pore pressure for an impermeable soil is directly proportional to the rise in temperature. There is no mitigating effect as drainage of the pore water from areas of high to low pressure is impossible. This is the critical case in terms of the integrity of the barrier against the migration of nuclear waste particularly in the case of the constant power source see figure where the continued rise in pore pressures would

almost certainly cause cracking. The soil barrier may perhaps be preserved in the case of the exponentially decaying power source, which most closely models the behaviour of nuclear waste, if the peak pore pressure reached is not too great.

For the case of permeable soils it is clear the mitigating effect of pore water flow is significant. Several cases were studied with  $Cv/K=0.5, 1$ , and  $2.0$  being considered. The increase in pore pressure was compared to a reference pore pressure  $U_w$  or  $U_w'$  and the behaviour of the pore pressure was examined over the logarithm of the dimensionless time parameter with curves examined for different values of  $r/r_o$ . In the case of the constant power source, (Figures 3.2 to 3.4) the mitigating effect meant a limiting pore pressure was reached instead of pore pressure continuing to rise. For lower values of the ratio  $Cv/K$  the final pore pressure reached was higher than in the case of larger  $Cv/K$  values. This can be explained by the fact a higher  $Cv$  means a lower permeability and thus higher values of  $Cv/K$  mean that the mitigating effect of pore water flow is limited. The same trend was observed in the results for the constant temperature and exponentially declining power sources. (Figures 3.6-3.8 and 3.10-3.11).

For the exponentially declining power source peaks were observed in the pore pressure response for the permeable soil. The peaks occurred at slightly later times for lower values of  $Cv/K$  indicating the permeability of the soil had a small effect on the response time; the mobility of the pore water aided the passage of heat. For this case the peak in the pore pressure response occurred before the peak in temperature response confirming the findings of Wickens (1982.)

For the constant temperature source, (Figures 3.10 and 3.11); the mitigating response was again observed. Instead of rising to a constant value the pore pressures were observed to decline from an initial maximum very close to the source, decline after peaking at intermediate distances away from the source and rise to a constant value far away from the source. Near the source the maximum pore pressure is reached immediately and declines due to pore water flow. However further away from the source the heating does not occur immediately and pore pressures build up with time. A peak is reached in the response at reasonable distances away from the source as the effect of the flow of pore water begins to take effect lowering the pore pressures. The final value of pore pressure reached in all of these cases is very close indicating an equilibrium pore pressure is reached throughout the region. The final value reached is much lower for the case of the permeable soil compared to the impermeable soil and the overall maximum is also reduced.

This indicates the permeability of the soil is significant in determining the susceptibility of the soil to cracking over a long period of time after the hot source is placed.

For both temperature and pore pressure response the case of a constant temperature source is intermediate to the constant and exponentially declining power sources. For a finite constant power cylinder due to the real behaviour may be gained by realising the effects will be tempered compared to the infinite cylinder. The constant surface temperature source of Booker & Savvidou (1984) spherical source can provide information as to the nature of this effect.

Another feature of importance to be delineated by this solution is that the effect of the hot source becomes negligible before  $r/r_0$  reaches

50 for the exponentially declining power source and after  $r/r_0$  reaches 50 for the constant power and constant temperature sources. Thus the effects of the heat source remain important at significant distances away and this

should be considered when assessing the suitability of deposits for the burial of nuclear waste.

#### Conclusion.

In conclusion it was found the results of this study confirmed the results of other researchers outlined previously. Temperature drops were quite steep close to the source, permeability was found to be significant and temperature and pore pressure effects were observed at large distances from the source. Additionally the pore pressure response to heat was found to be extremely rapid, peaking even before the temperature response. The inclusion of these results provides an improved picture of the response of clay to specific types of heat sources.

#### 10.2 Temperature Response for the Line Sources.

Line sources of infinite length were studied for the cases of constant power and exponentially declining power. The results were presented in the same form as for the cylindrical case with the exception that the radial distance is compared to a reference radius  $r_*$  instead of the radius of the cylindrical source. The results of the cylindrical source and the line source may be compared if the reference radius for the line source is assumed to equal the radius of the cylindrical source. If this is the case not only should values of  $r/r_* > 1$  be considered but also values less than 1. The solution follows the form of that for the cylindrical source. As time values are dependent on  $r_*$  or  $r_0$ .

examining the responses as if  $r_a$  equals  $r_c$  means they are compared in equal time frames.

#### The Constant Power Line Source.

In comparing the constant power case for the cylindrical source and the line source the major difference at radial distances greater than one occur at early times. (Figures 3.12 and 3.13). The response to the heat source at equal values of the radial distance ratio is much lower for the line source at early times but becomes almost identical to that of the cylindrical source at greater times. This is likely to be because the heat response takes longer to reach a particular position (for the ratio values greater than one) in the case of the line source as it is further away. However at later times when the response steadies, the response to the line source is able to 'catch up' to the cylindrical source response. This response is observed at all values of the radial distance ratio greater than one.

As mentioned it was relevant to consider a radial distance ratios less than 1 for the line source. At a value of 0 for this ratio there is a discontinuity (where the temperature reaches infinity) which is consistent with being at the centre of the line source. As would be expected closer to the constant power line source the temperature rises more rapidly than further from the source. In all cases, for the dimensionless radial distance ratio both less and greater than one the temperature continues to rise which is consistent with an infinite amount of power being input over time from the constant power source.

#### The Exponential Power Line Source.

For the exponentially declining power cylindrical and line sources the same trend is observed for the radial distance ratio values greater than

one. (Figures 3.14 and 3.15). Here the rise in temperature for the line source almost matches that of the cylindrical source by the time the peak response is reached but the gap is greater for greater values of the distance ratio. For the constant power case the growing gap does not manifest. This is because for the exponentially declining source the power input is limited and the extent over which the response extends is limited and the further distance of the source in the line case is more significant. When the radial

distance ratio is less than one as would be expected greater peaks are observed closer to the source but the time at which the peak occurs very gradually becomes later further away from the source.

The main difference a line source shows compared to the cylindrical sources is lower initial response at comparable radial distances to the line source being effectively further away. Similar trends are observed in the pore pressure responses.

### 10.3 The Temperature and Pore Pressure Response for $r < r_*$ .

Temperature.

Here the major difference to the examination of  $r > r_*$  is that the system is limited in extent. The increase in temperature was compared to a reference temperature and plotted against the logarithm of the dimensionless time parameter. This was done for various values of  $r/r_*$  with  $r/r_*$  less than 1.

For the case of the constant power source (Figure 13.6) there was little variation in the response for various  $r/r_*$  values particularly after a long time. That is after a reasonable time the temperature

throughout the area is approximately the same and continued to rise approximately linearly with time. Again this non-abating response is due to the infinite energy input over time and the uniformity of the response a result of the contained area.

As would be expected in the case of the constant temperature source (Figure 3.18) the temperature of the soil approaches that of the source. This occurs relatively quickly taking slightly longer further from the source. Again this case can be considered intermediate to the two previously discussed areas.

As discussed previously the case of a linearly increasing temperature source was studied in order that it could be combined with the constant temperature source to simulate conditions of non constant heating. It was found that the linearly increasing temperature source produced results of similar form to those of the constant power source; (Figure 3.20). The advantage is that steepness could be adjusted so that at lower slopes the behaviour of the linearly increasing temperature source becomes closer to that of the constant temperature source. The numeric results were produced for a single case that produced results similar to the constant power source where temperature throughout the region rose approximately linearly with time. There was only a slight delay in response for areas further from the source.

Generally the case of the interior behaviour compared to the exterior behaviour the response is more uniform due to the confined space and also more extreme for the same reason but the same trends are observed.

#### Pore Pressures.

In this case the pore pressure response is studied for  $Cv/K$  value of 0.5. The results are presented as the pore pressure increase compared to

a reference pore pressure and plotted against the logarithm of the dimensionless time. The plots are presented for various values of  $r/r_0$  less than 1.

The case of a permeable soil and a permeable heat source was considered numerically. The impermeable soil was of little practical interest, as without a means by which pore water can escape the pore pressure response follows that of temperature. For the same reason the impermeable source was not considered.

As would be expected for a permeable soil and a permeable source the mitigating effect of pore water flow is evident. For the constant power source, (Figure 3.17) at each position a limiting pore pressure was reached. Throughout the region the response was very rapid, quickly becoming within less than a percent of the maximum value. As would be expected the delay was slightly greater further away from the source. The maximum reached at each position, continued to increase towards a maximum at the centre of the region. In developing pore pressures in this contained region there are two opposing effects. At early times the heat has not reached areas remote from the source and thus the increase in pore pressure is greatest near the source. However at later times when the heat has reached areas further from the source we find the pore pressures closest to the source are less than those further away from the source. This is because the source is permeable and water close to it escapes readily while water further away from the source cannot escape easily. It was observed for the constant power source at early times the pore pressure response was greatest near the source but a limiting pore pressure was reached at each position, the value being greatest at the furthest point from the source, as the flow of water became the dominant force in limiting pore pressures.

The linearly increasing temperature source, (Figure 3.21) produced pore pressures corresponding to those of the constant power source, following the trend established for temperatures.

In the case of the constant temperature source again the early response was most extreme near the source and a later times a maximum at the further point away from the source for the same reasons as discussed above; (Figure 3.19). However in this case the far more limited energy input meant that a maximum response was established initially, due to heating before pore water began to flow, with pore pressures eventually declining to zero. The final equilibrium situation was achieved gradually as the pore water drained away.

#### Conclusion

The temperature responses for the interior case are of similar form to those observed in the case for  $r$  greater than  $r_e$ , for responding sources but the confined region meant the temperatures were very much greater. However the pore pressure response was far more limited in this interior case. This is because the finite region and permeable source provided much more favourable conditions for drainage of pore water than in the case of  $r$  greater than  $r_e$  where the region was infinite.

#### 10.4 The Two Source Case Temperature Increase.

##### Temperature.

Pairs of heat sources with differing boundary conditions were examined in this case. It was the response of the soil in between two sources that was under consideration. The behaviour in cases not specifically considered here may, in some cases, be predicted by combining cases

presented in this study. In this analysis the case of an inner source of constant power and an outer insulating source was studied in addition to those of an inner constant temperature source and an outer insulated source and finally an inner constant power source and an outer source held at a constant zero temperature. In addition, from this analysis, the case of the behaviour of the soil between two source strips could be examined by allowing the radius of both sources to become very large.

The inner source was assumed to have a radius of  $r_i$ , while the outer source had a radius of  $r_o$ . Thus the values of the dimensions ratio  $r_i/r_o$  varied between 1 and the value of the ratio  $r_o/r_i$ . The temperature increase was compared to a reference temperature and plotted against the logarithm of dimensionless time with various  $r_i/r_o$  values examined for each  $r_o/r_i$  value. The values of  $r_i/r_o$  considered were 1.5 and 5.

Firstly the constant power interior source and insulated outer source was examined (Figure 3.22 and 3.23). The insulating source prevented the energy from the interior source from escaping into the outer parts of the soil. As for the study of the interior cases the confinement of the region led to a response that was approximately uniform regardless of position with only a small time lag in response further away from the constant power source. As would be expected the temperature of the soil continued to rise indefinitely due to the infinite amount of power input, that could not escape, and the rise was approximately linear with time. Though pore pressures were not calculated it would be expected that they follow the nature of the temperature rise as was found in the study of the interior. The temperatures established at a particular time are greater for lower values of  $r_i/r_o$  as would be expected as the power input is concentrated in a smaller area.

Secondly the inner source of constant temperature was combined with an outer insulating source (Figure 3.26 - 3.28). The observations for the previous case are generally relevant here. As would be expected the soil reached the temperature of the inner source throughout the region. Due to the confined region this occurred almost immediately with only slight delays further from the constant temperature source. Naturally the constant temperature throughout the region is established more quickly for smaller cross sectional areas where  $r_o/r_i$  is small.

The third case studied was that of an interior constant power source combined with an exterior constant surface temperature source held at zero temperature (Figure 3.24 and 3.25). This is analogous to heat being removed here in order to prevent a rise of temperature there. As a result temperatures are greatest near the inner source. The temperature distribution changes little after a short initial time period. This shows an equilibrium between the input power at the inner source and the removal of heat at the outer source is quickly established. Larger values of the ratio of the radius of the outer source to the inner source result in a longer time before equilibrium is established as would be expected as the heat response has further to travel. The temperatures established at equilibrium are greater throughout the region for greater values of  $r_o/r_i$  and the rate of decline of temperature as the zero temperature source is approached is steeper for lower values of  $r_o/r_i$ , as would be expected.

#### The Strip

The case of a strip of soil between the two heat sources was studied numerically for the case of an interior source of constant temperature an

an outer insulation. Both an exact solution and an approximate solution obtained from the coaxial cylindrical sources were examined (Figure 3.29). In the exact solution showed that throughout the region the temperature reached the temperature of the inner source with some delay in response at the insulated end. In the approximation the trend was very similar when equivalent dimensional times were compared.

To achieve this approximation the radii of the two sources were very close together. Generally if similar dimensional time frames are used the response in the annular region is much more rapid than for the strip. This is expected as the annular region is bounded while the strip is not.

#### Pore Pressures

The complexity of the functions involved meant that pore pressures were not evaluated for the two source case. For permeable sources and soil the mitigating effect of pore water flow would once again be expected to be significant. For the cases with the insulated source with both sources impermeable the pore pressure response would follow that of temperature as there would nowhere for the water to flow to. However for the case with the zero temperature source the temperature response does not approach uniformity. This means even if the sources were impermeable water under high pressure near the source could flow towards the zero temperature source where pore pressure are lower. As a result for the case with the zero temperature source and impermeable sources the pore pressure responses would be more uniform than the temperature response.

## Conclusion

Studying the case of two concentric sources has led to a greater understanding of the interaction of sources but generally reinforces the behaviour of a confined body of soil subject to heat as examined in the interior case. Again equations for a situation such as this may be relevant for laboratory examinations with various heat conditions applied to the soil simultaneously. The cases studied here may be combined to produce various combinations of conditions. The line source showed that these results may also have relevance for geometries other than coaxial cylindrical sources.

## General Conclusions.

The trends established in all cases followed intuitive predictions of the behaviour of soil exposed to heating. Perhaps the most important trend established was the significance of the flow of pore water from areas of high pressure to low pressure, which resulted in a limitation upon the excess pore water pressures generated. The pore pressure response in the soil tended to precede noticeable temperature increases but there was a delay in the mitigating flow of pore water as time was required for passage of the water.

Comparisons could also be made between the cases of a heat source interior to the soil body, and an exterior heat source. Temperatures produced as a result of an external heat source were much greater due to the confined region but for the same reason excess pore pressures were more limited in this case, as pore water could readily escape from the confined region. The case of two sources of heat in soil confirmed previous results.

For the source of heat contained within the soil body the temperature and pore pressure responses were highly dependent upon position particularly at earlier times while the confined soil region for the external heat source produced much more uniform results.

As discussed previously solutions to a finite cylindrical source may be predicted by comparing the results of the infinite source with Booker & Savvidous' (1984) spherical source. The results for the spherical source of constant power follow very closely the trends established for the infinitely long cylindrical source of constant surface temperature. A

reasonable prediction can thus be made, that for a finite cylindrical heat source of constant power the results fall somewhere between those for an infinite cylindrical constant power source and an infinite cylinder of constant temperature; the assumption being the effect of a finite source is to have a reduced power output, compared to the infinite case. This is to be expected as an infinite source naturally inputs much more energy to the soil than a finite source.

The results of this thesis confirmed much of what other researchers in this field have found, particularly in the consideration of the mitigating effect of the flow of pore water. Various cases considered may be combined to further broaden the picture, of the response of soil to various types of heat sources.

## References.

- Booker, J.R. and Savvidou, C (1984) Consolidation around a point heat source, International Journal for Numerical and Analytical Methods in Geomechanics (in press)
- Barsetto, M. Carradori, G. and Ribacchi, R. (1981). Coupled seepage heat transfer and stress analysis with application to geothermal problems, Numerical Methods in Heat Transfer, Editors Lewis, R.W. Morgan, K. Zienkiewicz, O.C., John Wiley and Sons Ltd., Chapter 12, pps. 233-259.
- Brown, B.F., McCallum, P.A., Laplace Transform Tables and Theorems, 1965. Holt, Rinehart and Winston Inc.
- Campanella, R.G. (1965) The effect of temperature and stress on time - deformation behaviour of saturated clay, Phd. Thesis, University of California, Berkeley.
- Campanella, R.G. and Mitchell, J.K. (1968) Influence of temperature variations on soil behaviour, Journal of the Soil Mechanics and Foundation Division ASCE, 94 No.-SM3, May, 1969, pps. 709-734.
- Dawson, P.R. and Chavez, P.F. (1982) Thermomechanically coupled creeping flow of saturated cohesive porous media. Finite Elements in Fluids, 4, pps. 213-231.

- HICKOX, C.E. (1982) Thermal convection at low Rayleigh number from concentrated sources in porous media, Sandia National Laboratories, Subseabed Disposal Program, Annual Report 1980 (Published 1982), Part 1 pps. 336-373.
- HICKOX, C.E. Gartling, DK, McVey, DF, Russo, AS and Nutall, HE (1980) Analysis of heat and mass transfer in subseabed disposal of nuclear waste, Marine Technology, October 1980.
- HICKOX, C.E., Watts, H.A. (1980) Steady thermal convection from a concentrated source in a porous medium, Journal of Heat Transfer, ASME, 102, May 1980 pps. 248-253.
- LUIKOV, A.V. (1975) Systems of differential equations of heat and mass transfer in capillary porous bodies, International Journal of Heat and Mass Transfer, 18, pps. 1-14.
- McTIGUE, D.F. (1985) A Linear Theory for Porous Thermaelastic Materials Prepared by Sandia National Laboratories, New Mexico, USA, SAND 85-1149.
- PERIVAL, C.M. (1982) Laboratory simulation of a deep ocean insitu heat transfer experiment, Oceans 1982, pps. 18-22 October, Washington, DC.

plum, R.L. (1968) The effect of temperature on soil compressibility and pore pressure, MSc Dissertation, Cornell University, Ithaca, New York, USA.

Savvidou, C. (1984) Effects of a Heat Source in Saturated Clay Phd, University of Cambridge.

Wickens, L.M. (1982) The pore water and effective stress response of clay sediments to a heat source, Theoretical Physics Division - AERE Harwell Oxon TP966, November 1982.

# **APPENDIX 1**

FIGURE 1.1: BURIAL OF WASTE IN SEA BED.

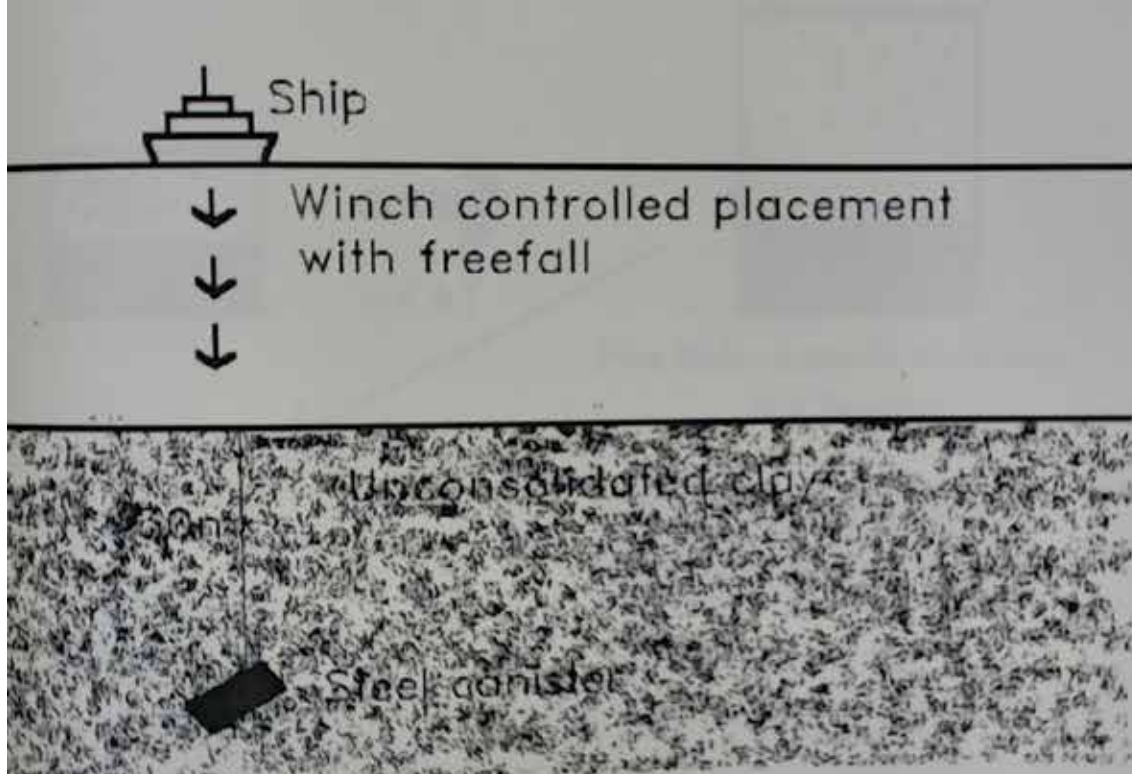
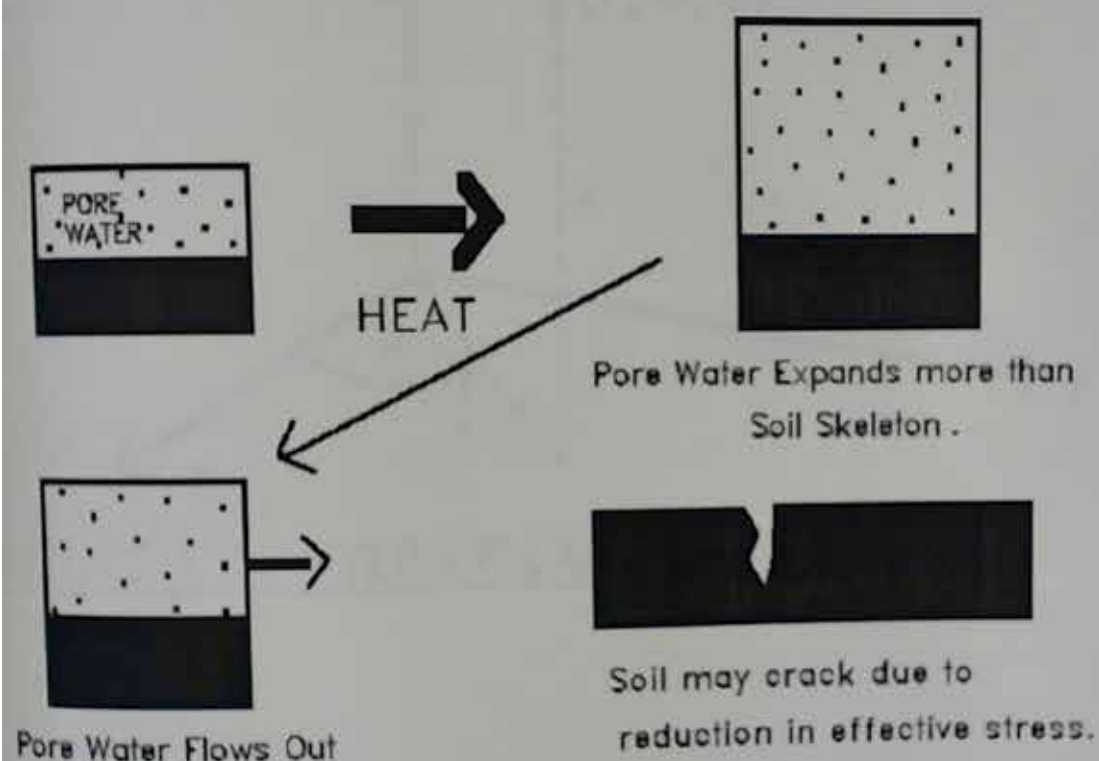


FIGURE 1.2: THE EFFECT OF HEAT ON SOIL



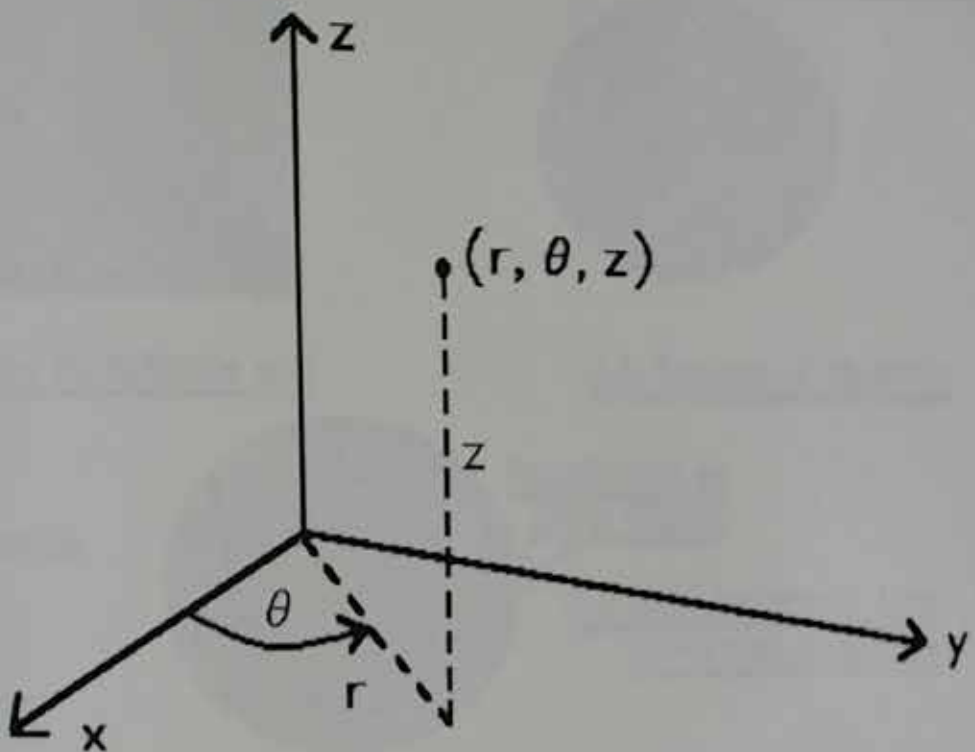
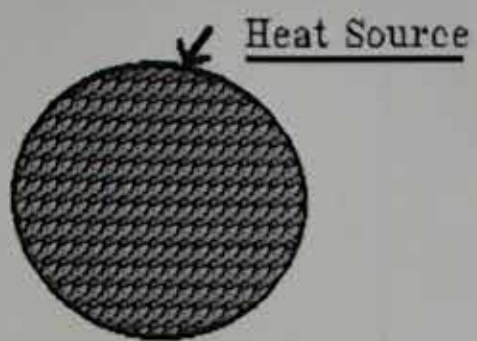


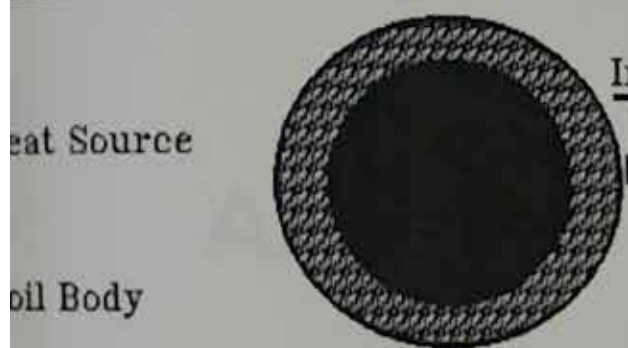
FIGURE 1.3: CYLINDRICAL CO-ORDINATES



a Source in infinite soil



4.b External Source



Heat Source  
oil Body  
Insulated or  
zero temp.

4.c Soil between two co-axial sources

FIGURE 1.4: CROSS-SECTION OF SOURCES

## **APPENDIX 2**

PROGRAM TALTEST

THE PURPOSE OF THIS PROGRAM IS TO ENSURE THAT THE INVERSION OF  
A BESSEL FUNCTION GIVES THE CORRECT RESULT FOR A KNOWN CASE.

THE CASE IS  $K_0(\sqrt{S}) \rightarrow 1/(2*T) * \exp(-1/(4*T))$

DECLARE VARIABLES.

RNUMBER : THE NUMBER OF R VALUES  
RARRAY : THE ARRAY WHICH STORES THESE PARAMETERS.  
TNUMBER : THE NUMBER OF TIME VALUES.  
TARRAY : THE ARRAY IN WHICH THESE VALUES ARE STORED.  
R : THE RATIO OF THE FUNCTION.  
FUNCRES : IS THE RESULT OF THE CALCULATION  
I,J : OVER USED COUNTER VARIABLES.

```
INTEGER RNUMBER, TNUMBER
PARAMETER (RNUMBER = 5)
PARAMETER (TNUMBER = 8)
DOUBLE PRECISION R, RARRAY(RNUMBER), TARRAY(TNUMBER)
DOUBLE PRECISION FUNCRES
COMMON /RATIO/R
```

SET UP THE ARRAYS

THE TIMES.

TARRAY(1)	=	0.0001
TARRAY(2)	=	0.0005
TARRAY(3)	=	0.001
TARRAY(4)	=	0.005
TARRAY(5)	=	0.01

```

TARRAY(5) =      0.1
TARRAY(7) =      1.0
TARRAY(8) =     10.0
TARRAY(1) =      0.1
TARRAY(2) =      0.5
TARRAY(3) =      1.0
TARRAY(4) =      5.0
TARRAY(5) =     10.0
TARRAY(6) =    100.0
TARRAY(7) =   1000.0
TARRAY(8) =  10000.0

```

### SET UP THE RATIO NUMBERS

```

BARRAY(1) = 1.00
BARRAY(2) = 2.0
BARRAY(3) = 5.0
BARRAY(4) = 10.00
BARRAY(5) = 50.0

```

## PRINT OUT THE HEADING

```
PRINT *, 'PROGRAM TO TEST THE INVERSION OF A BESSEL FUNCTION.'  
PRINT *, 'BESSEL FUNCTION INVERSION TEST PROGRAM'  
PRINT *, 'BY JEFFREY M. HARRIS'
```

WE ARE NOW GOING TO LOOP THROUGH THE DIFFERENT RATIOS AND CALCULATE  
THE FUNCTION FOR EACH TIME AT THE GIVEN RATIO.

```
DO 10, I = 1, RNUMBER  
PRINT *, *
```

```
1 ASSIGN R TO THE ARRAY VALUE.  
2  
3 R = RARRAY(I)  
4  
5 PRINT OUT A HEADER  
6  
7 PRINT *, 'FOR THE RATIO VALUE ', RARRAY(I)  
8 PRINT *, 'XXXXXXXXXXXXXXXXXXXXXXXXXXXX'  
9 PRINT *, ''  
10  
11 LOOP THROUGH EACH OF THE TIMES.  
12  
13 DO 20, J = 1, TNUMBER  
14  
15 CALL THE PROGRAM.  
16  
17 CALL TALBOT( FUNCRES, TARRAY(J) )  
18  
19 PRINT OUT THE RESULT.  
20  
21  
22 PRINT *, 'THE RESULT FOR THE TIME ', TARRAY(J), ' IS ', FUNCRES  
23 CONTINUE  
24 CONTINUE  
25  
26 EXIT  
27  
28 END  
29  
30 SUBROUTINE TALBOT( FUNT, TIME )  
31 IMPLICIT DOUBLE PRECISION (A,B,D-H,O-Z)  
32 COMMON /CONSTS/PI  
33  
34 NUMERICAL INVERSION OF A LAPLACE TRANSFORM USING
```

THE COMPLEX INVERSION THEOREM. METHOD DUE TO :

A. TALBOT - J. Inst. Maths Applies (1979) 23, 97-120.

METHOD REPUTED TO WORK FOR ALL LAPLACE TRANSFORMS EXCEPT THOSE WITH AN INFINITE NUMBER OF SINGULARITIES WHOSE IMAGINARY PARTS EXTEND TO INFINITY.

MAJOR VARIABLES :

TIME = VALUE OF TIME (SUPPLIED TO ROUTINE)

FUNT = VALUE OF FUNCTION (RETURNED TO CALLING PROG)

THE LAPLACE TRANSFORM MUST BE EXPRESSIBLE IN THE FORM

$$F(X + iY) = G + iH$$

THE TRANSFORM F MUST BE PROVIDED BY A USER SUBROUTINE LTFORM

I.E. X AND Y ARE INPUT TO SUBROUTINE LTFORM WHICH THEN RETURNS VALUES FOR G AND H

```
DATA TAU,SIG,RNU,NSUM/6.,0.,1.,20/
      WRITE(0,1001)
1001 FORMAT(2X,'ENTERING TALBOT')
PI=4. DO=DATA(1,DO)
I01 = 0
IF(DABS(TIME).LT.1.E-10) GO TO 200
RL = TAU/TIME
SUM = 0.
DO 11 K = 1,NSUM
TH = (X-1)*RL/NSUM
A = 1.
B = 0.
```

```

IF (K .EQ. 1) GO TO 100
A = TH^DCOS( TH ) / DSIN( TH )
B = TH + A^(A-1, D+O) / TH
100 X = A*RL + SIG
Y = RNU*TH*RL
TNT = TH*RNU*TAU
CALL LTPORM( X, Y, G, H )
SUM = SUM + DEXP( A*TAU ) * ((RNU*G-B*H)^DCOS( TNT ) -
(RNU*H+B*G)^DSIN( TNT ))
IF (K.EQ.1) SUM = 0.5*SUM
50 WRITE(0,1002) A, B, X, Y, G, H, SUM
1002 FORMAT( 2X, 7F12.4 )
51 CONTINUE
PUNT = SUM*RL^DEXP( SIG*TIME ) / NSUM
52 WRITE(0,1002) PUNT
53 WRITE(0,1003)
1003 FORMAT( 2X, 'LEAVING TALBOT' )
RETURN
200 WRITE(101,201)
201 FORMAT( 1X, 'ZERO TIME NOT PERMITTED IN TALBOT INVERSION' )
STOP
END

```

SUBROUTINE K2EONE(X, Y, RE0, IM0, RE1, IM1)

THE VARIABLES X AND Y ARE THE REAL AND IMAGINARY PARTS OF  
 THE ARGUMENT OF THE FIRST TWO MODIFIED BESSEL FUNCTIONS  
 OF THE SECOND KIND, K0 AND K1. RE0, IM0, RE1, IM1 GIVE  
 THE REAL AND IMAGINARY PARTS OF EXP(X)^K0 AND EXP(X)^K1,  
 RESPECTIVELY. ALTHOUGH THE REAL NOTATION USED IN THIS  
 SUBROUTINE MAY SEEM INELEGANT WHEN COMPARED WITH THE

COMPLEX NOTATION THAT FORTRAN ALLOWS. THIS VERSION RUNS  
ABOUT 30 PERCENT FASTER THAN ONE WRITTEN USING COMPLEX  
VARIABLES.

```
DOUBLE PRECISION X, Y, X2, Y2, RE0, IMO, RE1, IM1,  
* R1, R2, T1, T2, P1, P2, RTERM, ITERM, EXSQ(8), TSQ(8)  
DATA TSQ(1) /0.0D0/, TSQ(2) /3.19303633920635D-1/,  
* TSQ(3) /1.29075862295915D0/, TSQ(4)  
* /2.95837445869665D0/, TSQ(5) /5.4090315972444D0/,  
* TSQ(6) /8.80407957805676D0/, TSQ(7)  
* /1.34685357432515D1/, TSQ(8) /2.02499163658709D1/,  
* EXSQ(1) /0.5641003087264D0/, EXSQ(2)  
* /0.4120286874989D0/, EXSQ(3) /0.1584889157959D0/,  
* EXSQ(4) /0.3078003387255D-1/, EXSQ(5)  
* /0.2778068842913D-2/, EXSQ(6) /0.1000044412325D-3/,  
* EXSQ(7) /0.1059115547711D-5/, EXSQ(8)  
* /0.1522475804254D-6/
```

THE ARRAY TSQ AND EXSQ CONTAIN THE SQUARE OF THE  
ABSCISSAS AND WEIGHT FACTORS USED IN THE GAUSS-  
HERMITE QUADRATURE.

```
R2 = X*X + Y*Y  
RR = DBLE(R2)  
IF(X.GT.0.0D0 .OR. RR.GT.1.0D-9) GO TO 10  
WRITE(*,99999)  
RETURN  
10 IF(R2.GE.1.96D2) GO TO 50  
IF(R2.GE.1.849D1) GO TO 30
```

THIS SECTION CALCULATES THE FUNCTIONS USING THE SERIES  
EXPANSION.

```
T2 = L/2.0D0
```

```
T2 = Y/2.0D0
P1 = X2*X2
P2 = Y2*Y2
T1 = -(DLOG( P1+P2 ) / 2.0D0+0.5772156649015329D0)
```

```
THE CONSTANT IN THE PRECEDING STATEMENT IS EULER'S  
CONSTANT
```

```
T2 = -DATAN2( Y, X )
X2 = P1 - P2
Y2 = X*Y2
RTERM = 1.0D0
ITERM = 0.0D0
RE0 = T1
IHO = T2
T1 = T1 + 0.5D0
RE1 = T1
IHO = T2
P2 = DSQRT( R2 )
L = 2.106D0*P2 + 4.4D0
IF ( P2 .LT. 8.0D-1 ) L = 2.129D0*P2 + 4.0D0
DO 20 N = 1, L
  P1 = N
  P2 = NAN
  R1 = RTERM
  RTERM = ( R1*X2 - ITERM*Y2 ) / P2
  ITERM = ( R1*Y2 + ITERM*X2 ) / P2
  T1 = T1 + 0.5D0/P1
  RE0 = RE0 + T1*RTERM - T2*ITERM
  IHO = IHO + T1*ITERM + T2*RTERM
  P1 = P1 + 1.0D0
  T1 = T1 + 0.5D0/P1
  RE1 = RE1 + ( T1*RTERM - T2*ITERM ) / P1
  IHO = IHO + ( T1*ITERM + T2*RTERM ) / P1
 20 CONTINUE
```

```

      WRITE(0,1001) RE0, IM0, RE1, IM1
1001 FORMAT(2X,'SERIES', 4F12.6)
10 CONTINUE
      R1 = X/R2 - 0.5D0*(X*RE1 - Y*IM1)
      R2 = -Y/R2 - 0.5D0*(X*IM1 + Y*RE1)
      P1 = DEXP(X)
      RE0 = P1*RE0
      IM0 = P1*IM0
      RE1 = P1*R1
      IM1 = P1*R2
      WRITE(0,1001) RE0, IM0, RE1, IM1
      RETURN

1 THIS SECTION CALCULATES THE FUNCTIONS USING THE INTEGRAL
2 REPRESENTATION, EVALUATED WITH 15 POINT GAUSS-
3 HERMITE QUADRATURE
4
5
10 X2 = 2.0D0*X
      T2 = 2.0D0*Y
      R1 = T2*T2
      P1 = DSQRT(X2*X2+R1)
      P2 = DSQRT(P1+X2)
      T1 = EXSQ(1)/(2.0D0*P1)
      RE0 = T1*P2
      IM0 = T1/P2
      RE1 = 0.0D0
      IM1 = 0.0D0
      DO 40 N = 2, 8
      T2 = X2 + TSQ(N)
      P1 = DSQRT(T2*T2+R1)
      P2 = DSQRT(P1+T2)
      T1 = EXSQ(N)/P1
      RE0 = RE0 + T1*P2
      IM0 = IM0 + T1/P2

```

```
T1 = EXSQ(N)*TSQ(N)
RE1 = RE1 + T1*P2
IM1 = IM1 + T1/P2
WRITE(0,1002) RE0, IM0, RE1, IM1
1002 FORMAT(2X,'QUAD',4F12.6)
10 CONTINUE
T2 = -Y2*IM0
RE1 = RE1/R2
R2 = Y2*IM1/R2
RTERM = 1.41421356237309D0*DCOS(Y)
ITERM = -1.41421356237309D0*DSIN(Y)
```

THE CONSTANT IN THE PREVIOUS STATEMENTS IS SQRT(2)

```
IM0 = RE0*ITERM + T2*RTERM
RE0 = RE0*RTERM - T2*ITERM
T1 = RE1*RTERM - R2*ITERM
T2 = RE1*ITERM + R2*RTERM
RE1 = T1*X + T2*Y
IM1 = -T1*Y + T2*X
WRITE(0,1002) RE0, IM0, RE1, IM1
RETURN
```

THIS SECTION CALCULATES THE FUNCTIONS USING THE ASYMPTOTIC EXPANSIONS

```
20 ITERM = 1.0D0
ITERM = 0.0D0
RE0 = 1.0D0
IM0 = 0.0D0
RE1 = 1.0D0
IM1 = 0.0D0
P1 = 8.0D0*R2
P2 = DSQRT(R2)
```

```

L = 3.9100+8.12D1/P2
R1 = 1.000
R2 = 1.000
K = -8
E = 3
DO 60 N = 1, L
  H = H + B
  K = K - M
  R1 = FLOAT(K-4)*R1
  R2 = FLOAT(E)*R2
  T1 = FLOAT(N)*P1
  T2 = RTERM
  RTERM = (T2*X+ITERM*Y)/T1
  ITERM = 1-T2*Y+ITERM*X)/T1
  RE0 = RE0 + R1*RTERM
  IM0 = IM0 + R1*ITERM
  RE1 = RE1 + R2*RTERM
  IM1 = IM1 + R2*ITERM
  WRITE(0,1003) RE0, IM0, RE1, IM1
1003 FORMAT(2X,'ASS.', 4F12.6)
60 CONTINUE
T1 = DSQRT(P2+X)
T2 = -Y/T1
P1 = 8.86226925452758D-1/P2

```

THIS CONSTANT IS SQRT(PI)/2.0, WITH PI=3.14159...

```

RTERM = P1*DCOS(Y)
ITERM = -P1*DSIN(Y)
R1 = RE0*RTERM - IM0*ITERM
R2 = RE0*ITERM + IM0*RTERM
RE0 = T1*R1 - T2*R2
IM0 = T1*R2 + T2*R1
R1 = RE1*RTERM - IM1*ITERM

```

```
R2 = RE1*ITERM + IM1*TERM  
IM1 = T1*R1 - T2*R2  
IM1 = T1*R2 + T2*R1  
WRITE(0,1003) RE0, IM0, RE1, IM1  
RETURN  
1003 FORMAT(1X,'ARGUMENT OF THE BESSSEL FUNCTIONS IS ZERO,  
* OR LIES IN LEFT HALF COMPLEX PLANE')  
END  
SUBROUTINE KOK1K2(CARG, CK0, CK1, CK2, CDK0, CDK1, CDK2)
```

MODIFIED BESSEL FUNCTIONS OF THE SECOND KIND ORDERS 0, 1, 2  
AND THEIR DERIVATIVES.

IMPLICIT COMPLEX (C)

DOUBLE PRECISION X, Y, RE0, IM0, RE1, IM1

```
XX = REAL(CARG)  
YY = AIMAG(CARG)  
X = XX  
Y = YY  
CALL KEEONE(X, Y, RE0, IM0, RE1, IM1)  
1001 WRITE(0,1001) X, Y  
1001 FORMAT(2X,'KOK1K2', 2F12.6)  
WRITE(0,*1) RE0, IM0  
WRITE(0,*1) RE1, IM1  
X0 = EXP(-XX)  
R0 = XX*RE0  
S0 = XX*IM0  
CK0 = CMPLX(R0, S0)  
K1 = XX*RE1  
I1 = XX*IM1  
CK1 = CMPLX(R1, I1)
```

FORM K2 AND ITS DERIVATIVE BY RECURRENCE RELATIONS

```
CK2 = CK0 + 2.*CK1/CARG
CDK2 = -CK1 - 2.*CK2/CARG
CDK0 = -CK1
CDK1 = 0.5*(CK0+CK2)
      WRITE(0,1004) CK0, CDK0
      WRITE(0,1004) CK1, CDK1
      WRITE(0,1004) CK2, CDK2
1004 FORMAT(2X,'K0K1K2',4F12.6)
      RETURN
      END
```

THIS IS THE SECTION OF THE PROGRAM TO CALCULATE I BESSSEL  
FUNCTIONS.

SUBROUTINE IGUTS(N, X, Y, E, F)

Modified Bessel function of the first kind and of integer order  
with arbitrary complex argument.

This routine computes function value by either ascending series  
or asymptotic expansion. The calling routine INUI determines in which  
part of the complex plane the argument lies.

```
IMPLICIT INTEGER*4 (I-N)
IMPLICIT DOUBLE PRECISION (A-H,O-Z)
```

Compute modulus and argument of X + iY

```
R = DSQRT(X*X + Y*Y)
```

```
TH = THETA(X, Y)
NN = N
IF (N LT. 0) NN = -N

check for degenerate conditions

IF (DABS(R), LT. 1, D-10, AND , NN, EQ. 0) THEN
  E = 1. DO
  F = 0. DO
  RETURN
END IF

IF (DABS(R), LT. 1, D-10, AND , NN, GT. 0) THEN
  E = 0. DO
  F = 0. DO
  RETURN
END IF

Compute (X+1Y)*(X+1Y)

Z2R = X*X - Y*Y
Z2I = 2. DO*X*Y
RN = R**NN
ARG = NN*TH
TNR = RN*DCOS(ARG)
TNI = RN*DSIN(ARG)

RN is modulus value which determines if ascending series
or asymptotic expansion is used

RM = 18. DO + 3. DO*NN/7. DO
IF (R, LE, RM) THEN

  Ascending series
```

```

CR = ZZR/4. DO
CI = ZZI/4. DO
FAC = 1. DO/2. DO**NN
C1R = ZNR*FAC
C1I = ZNI*FAC
D = NFAC(NN)
TMR = C1R/D
TMI = C1I/D
E = TMR
F = TMI
TEST = 0. DO

DO 100 K = 1, 100
  FAC = 1. DO/K/(K+NN)
  TKR = (CR*TMR - CI*TMI)*FAC
  TEI = (CR*TMI + CI*TMR)*FAC
  E = E + TKR
  F = F + TEI
  DEN = DSQRT(E*E + F*F)
  IF (DEN.GT.1. D-10) TEST = DSQRT(TKR*TKR + TEI*TEI)/DEN
  IF (DEN.GT.1. D-10, AND TEST.LT.1. D-10) GO TO 110
    TMR = TKR
    TMI = TEI
100 CONTINUE
110 CONTINUE

ELSE

ASymptotic expansion

PI = 4. DO*DATAN(1. DO)
ROOTR = DSQRT(PI)
ROOTI = ROOTR*DCOS(TH/2. DO)
ROOTII = ROOTR*DSIN(TH/2. DO)

```

```
RR = ROOTZR^ROOTZR + ROOTZI^ROOTZI  
  
GAM = 1.772453850905516027D0  
ISTOP = NN + NN - 1  
IPROD = 1  
IF (NN.GE.1) THEN  
    DO 200 I = 1,ISTOP,2  
        IPROD = IPROD*I  
    CONTINUE  
100 END IF  
GAM = GAM^IPROD/2^NN  
POW = NN + NN + 0.5D0  
FAC = NFAC(NN+NN)/GAM/NFAC(NN)/2**POW  
FR = FAC^ROOTZR/RR  
FI = -FAC^ROOTZI/RR  
EX = DEXP(X)  
EZR = EX^DCOS(Y)  
E2I = EX^DSIN(Y)  
A = (NN+0.5D0)*PI - Y  
EZR = DCOS(A)/EX  
E2I = DSIN(A)/EX  
  
TMR = 1,DO  
TMI = 0,DO  
TNR = TMR  
TNI = TMI  
CR = 0.5D0*X/R/R  
CI = -0.5D0*Y/R/R  
S1R = TMR  
S1I = TMI  
S2R = TNR  
S2I = TNI  
XSTOP = 10  
XTEST = 0
```

```

LTEST = 0
DO 210 K = 1, KSTOP
  AA = (NN*K-0, 5D0)*(-NN+K-0, 5D0)/K
  IF (KTEST, EQ, 0) THEN
    TKR = -AA*(TMR*CR-TNI*CI)
    TKI = -AA*(TMR*CI+TNI*CR)
    S1R = S1R + TKR
    S1I = S1I + TKI
    RATIO1 = DSQRT( TKR*TKR+TEI*TKI ) / DSQRT( TMR*TMR+TNI*TNI )
    IF (RATIO1, LT, 1, D-10, OR, RATIO1, GT, 1, 0) KTEST = 1
    TMR = TKR
    TNI = TKI
  END IF
  IF (LTEST, EQ, 0) THEN
    TLR = AA*(TNR*CR-TNI*CI)
    TLI = AA*(TNR*CI+TNI*CR)
    S2R = S2R + TLR
    S2I = S2I + TLI
    RATIO2 = DSQRT( TLR*TLR+TLI*TLI ) / DSQRT( TNR*TNR+TNI*TNI )
    IF (RATIO2, LE, 1, D-10, OR, RATIO2, GT, 1, 0) LTEST = 1
    TNR = TLR
    TNI = TLI
  END IF
CONTINUE
SUMR = E1R*S1R + E1I*S1I + E2R*S2R + E2I*S2I
SUMI = E1R*S1I + E1I*S1R + E2R*S2I + E2I*S2R
E = PR*SUMR - PI*SUMI
F = PR*SUMI + PI*SUMR
END IF
RETURN
END
FUNCTION NFAC(I)

```

Routine computes factorial I

```

INTEGER*4 I, NFAC, K
NFAC = 1
IF (I.GT.0) THEN
  DO 100 K = 1, I
    NFAC = NFAC*K
  CONTINUE
END IF
RETURN
END
SUBROUTINE TH0Z(N, X, Y, G, H)

```

Modified Bessel function of the first kind and of integer order with arbitrary complex argument :  $I_n(x+iy)$

```

IMPLICIT INTEGER*4 (I-N)
IMPLICIT DOUBLE PRECISION (A-H,O-Z)

PI = 3.141592653589793D0
TH = THETA(X,Y)
IF (TH.GT. -PI .AND .TH.LT. 0.D0) THEN

```

Argument lies in third or fourth quadrants of the complex plane or on negative imaginary axis.

Use the following relation :

```

IN(X+Y) = EXP(-I*PI)*IN(X+Y)*EXP(I*PI))

U = -1.D0
S = 0.D0
XI = C*X - S*Y
YY = C*Y + S*X
CALL THUT0(N, XX, YY, E, F)

```

```
C = DCOS(-N*PI)
S = DSIN(-N*PI)
G = C*E - S*F
H = C*F + S*E
ELSE
```

Argument lies in first or second quadrant of complex plane  
or on real axis or positive imaginary axis.

```
CALL IGUTS(N, X, Y, G, H)
END IF
RETURN
END
```

```
FUNCTION THETA(X, Y)
```

Argument of a complex number  $x + iy$

Computations entirely in double precision

```
IMPLICIT DOUBLE PRECISION (A-H, O-Z)
PI = 4. DO^DATAN(1. DO)
IF (DABS(X). GT. 1. D-10) THEN
  THETA = DATAN2(Y, X)
  IF (DABS(THETA). LT. 1. D-6) THETA = 0. DO
ELSE
  THETA = 0. DO
  IF (Y. GT. 0. DO) THETA = PI/2. DO
  IF (Y. LT. 0. DO) THETA = -PI/2. DO
END IF
RETURN
END
```

-----PAH-15/8/89-----

```
SUBROUTINE LTFORM(X, Y, G, H)
```

UFORM IS A SUBROUTINE TO CALCULATE THE FUNCTION TO BE INVERTED  
BY TALBOT.

#### DECLARE VARIABLES:

#### **READER VARIABLES:**

: THE REAL PART OF S.  
: THE IMAGINARY PART OF S.  
: REAL PART OF THE FUNCTION RETURNED.  
: THE IMAGINARY PART OF THE FUNCTION RETURNED.

## LOCAL VARIABLES.

REAL PART OF THE SQUARE ROOT OF S (U)  
IMAGINARY PART " "

## IMPLICIT DOUBLE PRECISION (A,B,P=1,Q=1)

## IMPLICIT COMPLEXA16 (CI)

## DOUBLE PRECISION B

COMMON PASTURES

COMMON /CONSTANTS/

© 1987 THE PROGRAM

$$H = \text{SQUAREROOT}(S) = A + iB$$

READ IN AN INTEGER N FROM THE KEYBOARD.

147 ■ 4

A = DBLE(CU)  
B = DIMAG(CU)

1 AND 2 ARE THE REAL AND IMAGINARY PARTS OF S^0.5

AR = R\*A  
BR = R\*B

3 AND 4 ARE THE REAL AND IMAGINARY PARTS OF S^0.5 + R/Ro

ARAT = RAT \* A  
BRAT = RAT \* B

5 AND 6 ARE THE REAL AND IMAGINARY PARTS OF S^0.5 + R1/Ro

CALL E2EONE(A, B, RK0, IK0, RK1, IK1)  
CR1 = DCMPLX(RK1, IK1) / DEXP(A)

CALL E2EONE(AR, BR, RK0R, IK0R, RK1R, IK1R)  
CR0R = DCMPLX(RK0R, IK0R) / DEXP(AR)

CALL E2EONE(ARAT, BRAT, RK0RAT, IK0RAT, RK1RAT, IK1RAT)  
CR1RAT = DCMPLX(RK1RAT, IK1RAT) / DEXP(ARAT)

7 = 0  
CALL INUT(N, AR, BR, RI0R, II0R)  
CR0R = DCMPLX( RI0R, II0R)

7 = 1  
CALL INUT(N, A, B, RI1, II1)  
CR1 = DCMPLX( RI1, II1)  
  
CALL INUT(N, ARAT, BRAT, RI0RAT, II0RAT)  
CR0R = DCMPLX( RI0RAT, II0RAT)

```
CA = CK1RAT/((CK1RAT^CI1)-(CK1*CI1RAT))
CB = CI1RAT/((CI1RAT^CK1)-(CI1*CK1RAT))
CC = CU*CU*CU

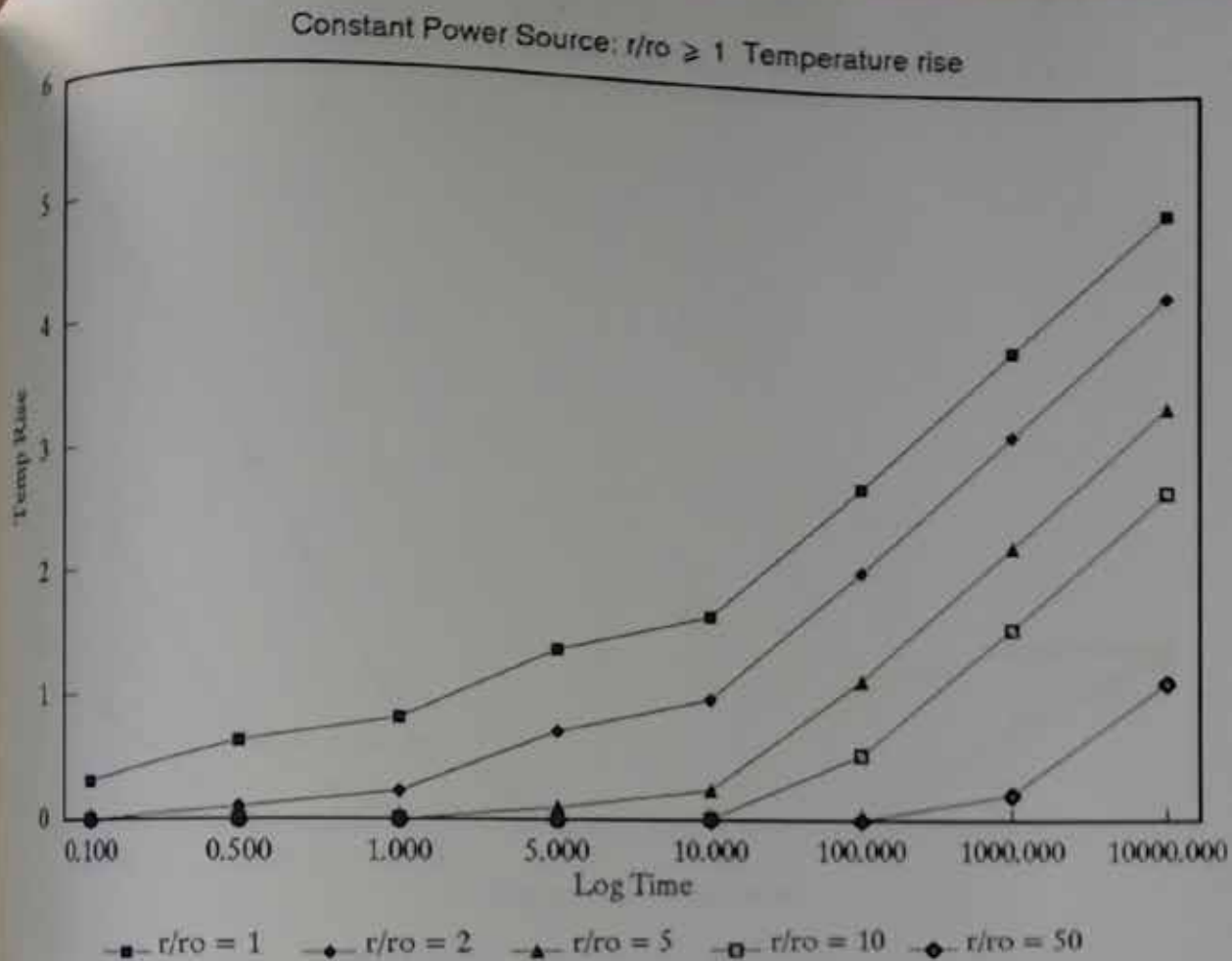
CF = ((CA^CIOR)+(CB*CKOR))/CC

G = DBLE(CF)
H = DIMAG(CF)

EXIT OUT OF LTFORM.

RETURN
END
```

## **APPENDIX 3**

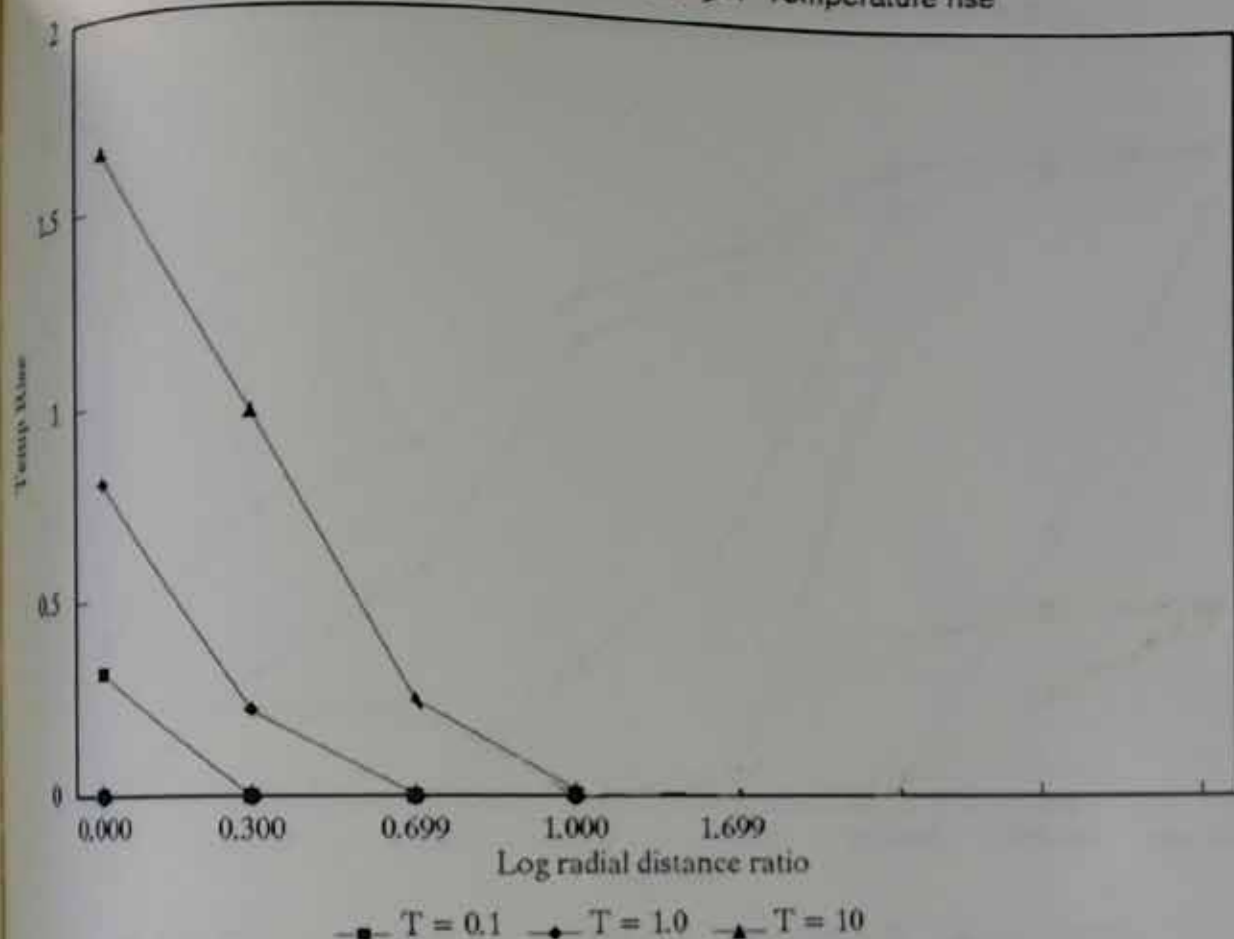


Constant Power Source:  $r/r_o \geq 1$  Temperature rise

$r/r_o = 1$	$r/r_o = 2$	$r/r_o = 5$	$r/r_o = 10$	$r/r_o = 50$
0.100	0.314	2.630E-03	0.000	0.000
0.500	0.617	9.940E-02	5.900E-05	0.000
1.000	0.802	0.220	7.640E-04	1.230E-11
5.000	1.362	0.701	9.610E-02	1.010E-03
10.000	1.651	0.975	0.244	1.580E-02
100.000	2.723	2.032	1.138	0.529
1000.000	3.861	3.168	2.254	1.570
10000.000	5.010	4.317	3.401	2.709

Figure 3.1a. Constant Power Source:  $r/r_o \geq 1$  Temperature rise

Constant Power Source:  $r/r_0 \geq 1$  Temperature rise

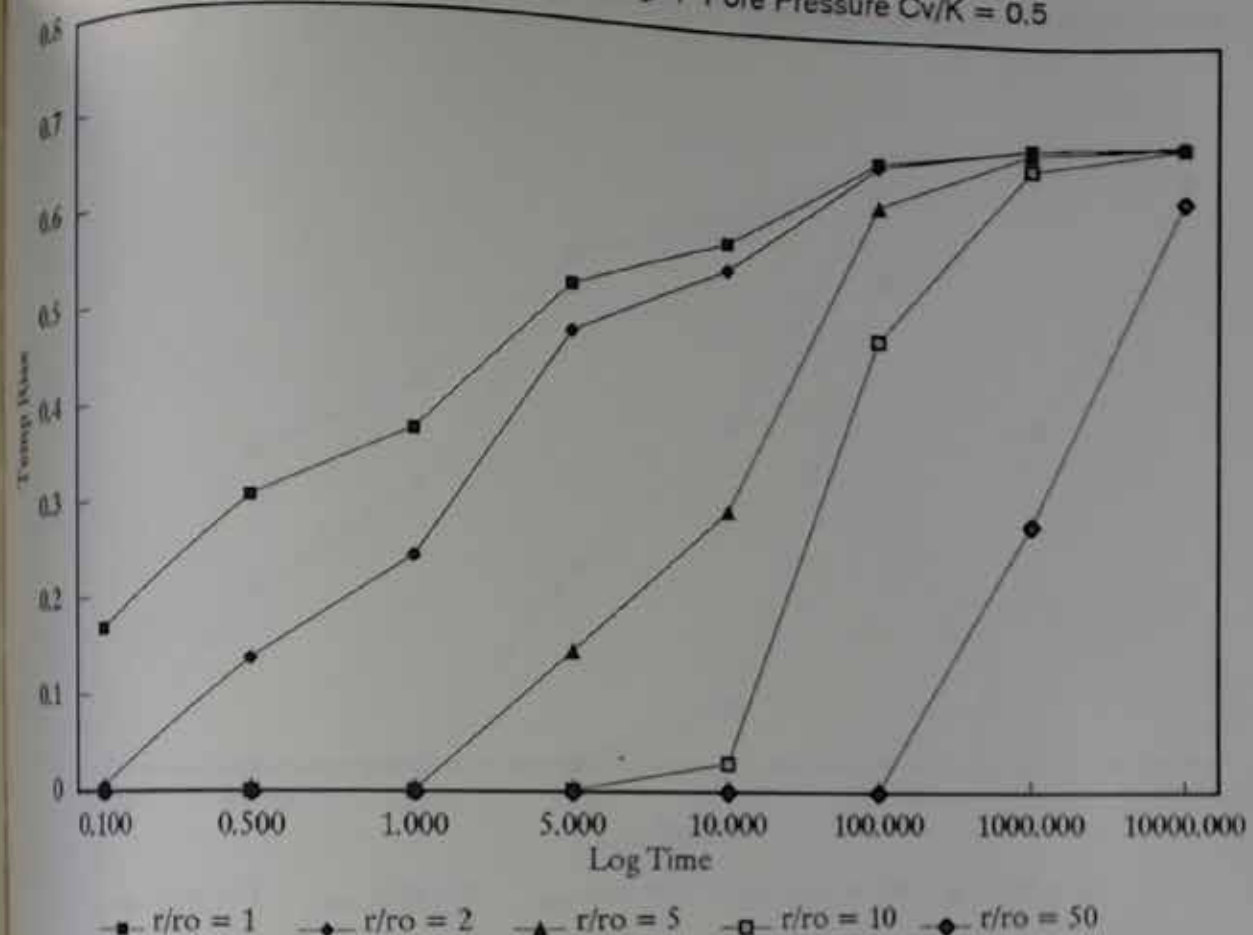


Constant Power Source:  $r/r_0 > 1$  Temperature rise

radial distance $r/r_0$	$T = 0.1$	$T = 1.0$	$T = 10$
0.000	0.314	0.802	1.651
0.300	2.630E-03	0.220	0.975
0.699	0.000	2.200E-01	0.244
1.000	0.000	0.000	1.580E-02
1.699	0.000	0.000	0.000

Figure 3.1b. Constant Power Source:  $r/r_0 > 1$  Temperature rise

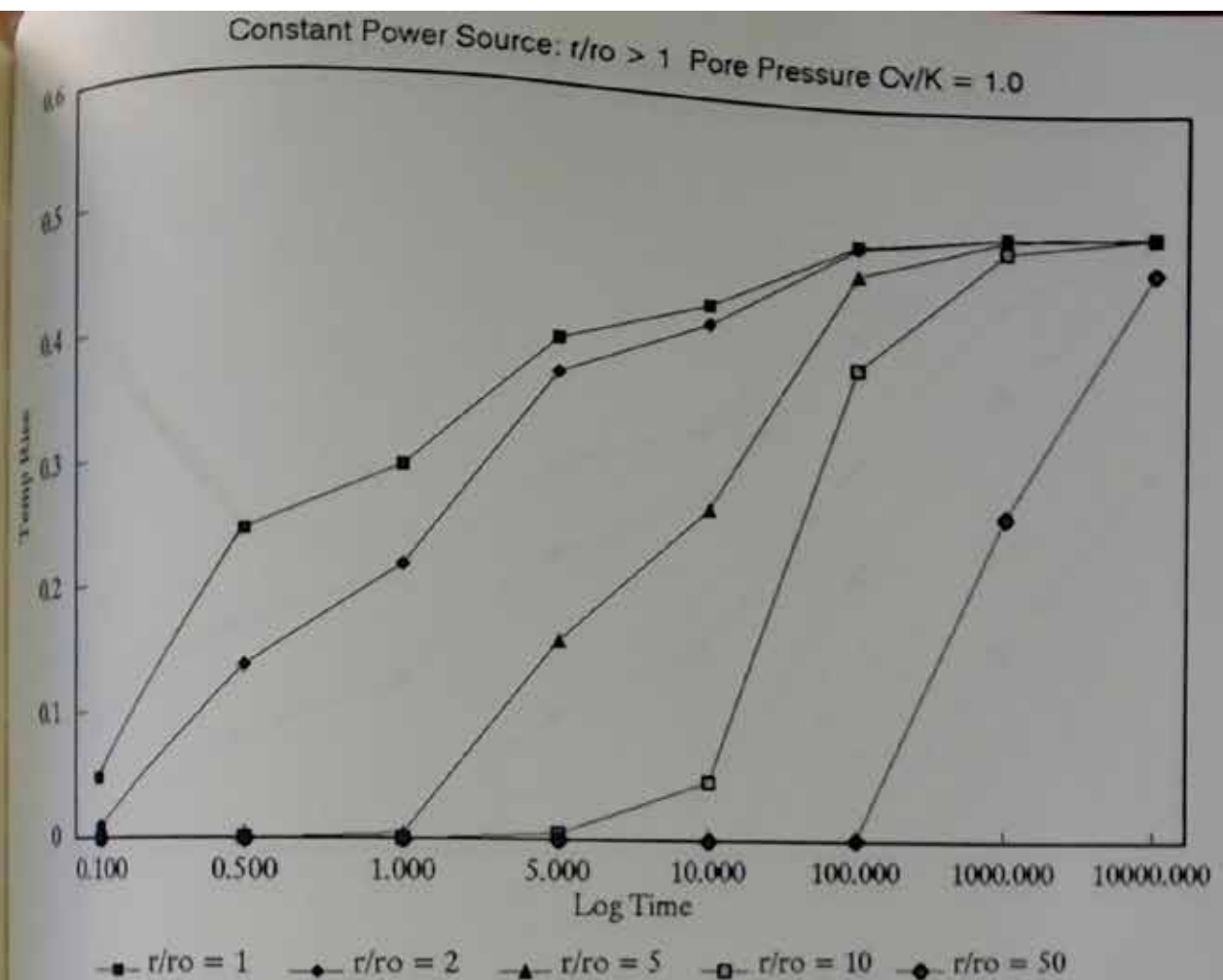
Constant Power Source:  $r/r_o \geq 1$  Pore Pressure  $Cv/K = 0.5$



Constant Power Source:  $r/r_o \geq 1$  Pore Pressure  $Cv/K = 0.5$

	$r/r_o = 1$	$r/r_o = 2$	$r/r_o = 5$	$r/r_o = 10$	$r/r_o = 50$
time	Temp rise	Temp rise	Temp rise	Temp rise	Temp rise
0.100	0.168	5.070E-03	0.000	0.000	0.000
0.500	0.302	0.135	1.181E-05	3.519E-17	0.000
1.000	0.371	0.242	1.516E-03	2.453E-11	0.000
5.000	0.525	0.476	0.146	2.006E-03	0.000
10.000	0.577	0.548	0.296	2.958E-02	0.000
20.000	0.669	0.665	0.622	4.807E-01	2.909E-04
50.000	0.689	0.689	0.684	6.665E-01	0.286
100.000	0.692	0.693	0.692	6.903E-01	0.633

Figure 3.2. Constant Power Source:  $r/r_o \geq 1$  Pore Pressure  $Cv/K = 0.5$

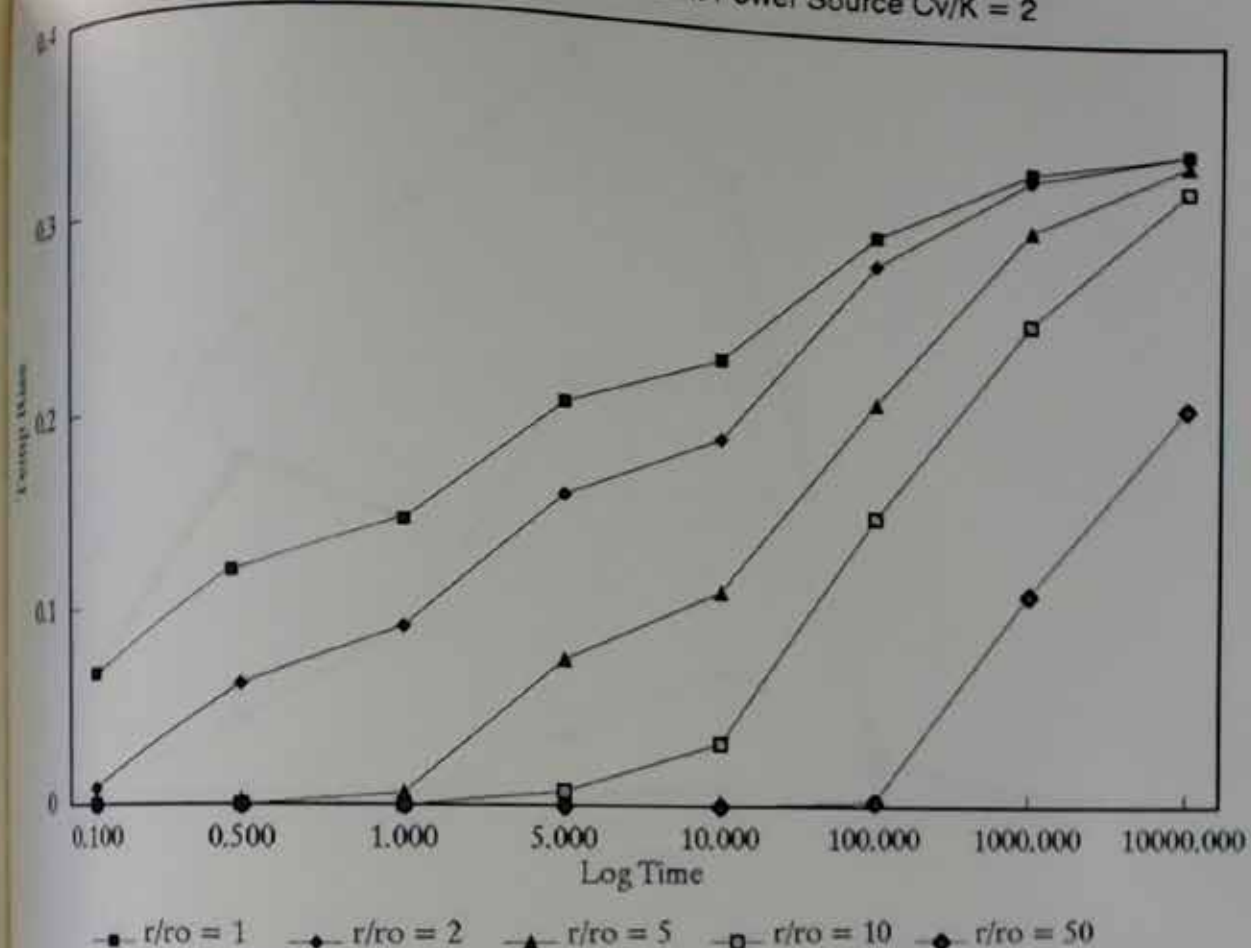


Constant Power Source:  $r/r_o > 1$  Pore Pressure  $Cv/K = 1$

	$r/r_o = 1$	$r/r_o = 2$	$r/r_o = 5$	$r/r_o = 10$	$r/r_o = 50$
time	Temp rise	Temp rise	Temp rise	Temp rise	Temp rise
0.100	0.038	9.645E-03	0.000	0.000	0.000
0.500	0.242	0.135	5.451E-05	0.000	0.000
1.000	0.293	0.215	3.961E-03	2.652E-10	0.000
5.000	0.399	0.372	0.158	5.220E-03	0.000
10.000	0.432	0.417	0.268	4.732E-02	1.501E-17
100.000	0.487	0.485	0.463	0.386	1.024E-03
1000.000	0.498	0.498	0.496	0.486	0.268
10000.000	0.500	0.500	0.499	0.499	0.470

Figure 3.3. Constant Power Source:  $r/r_o > 1$  Pore Pressure  $Cv/K = 1$

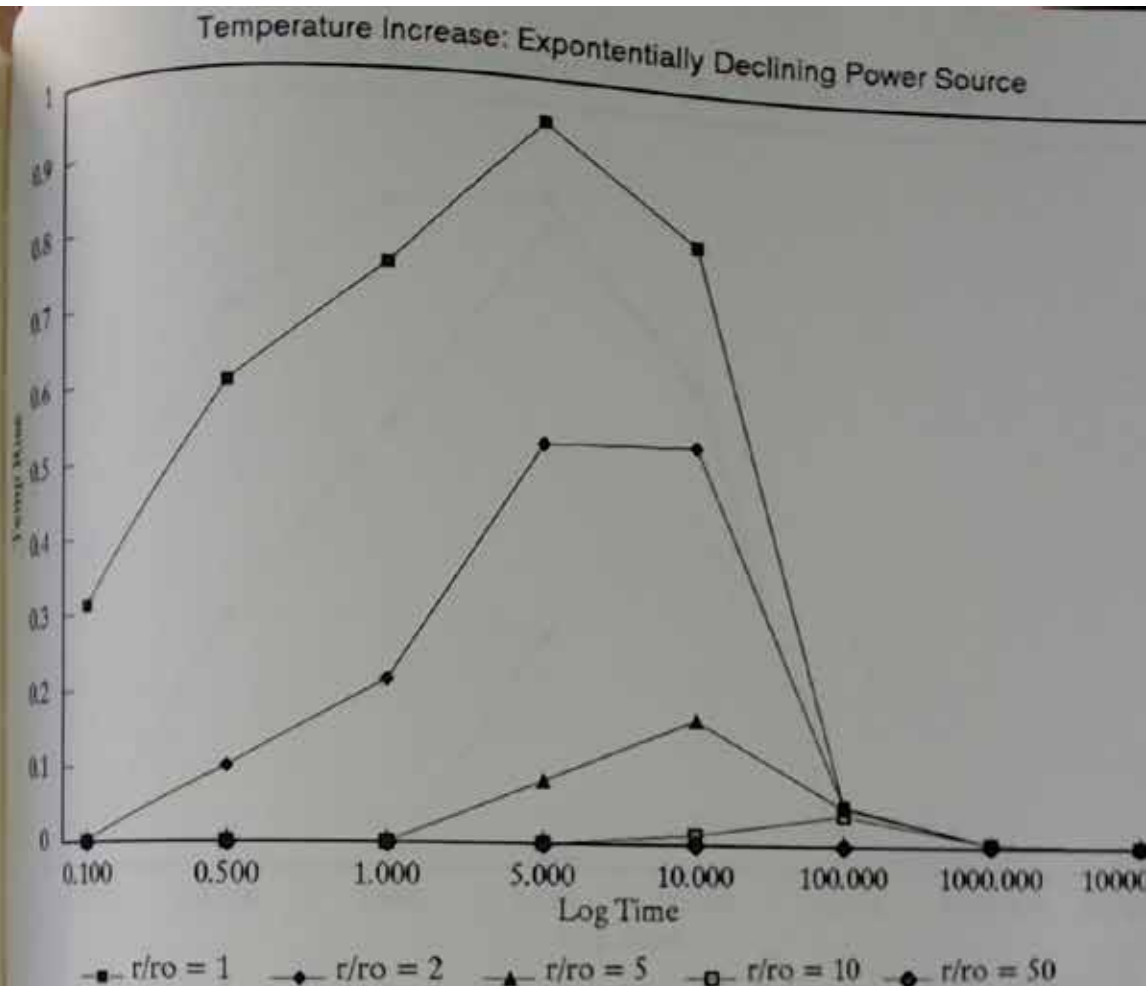
Pore Pressure Increase: Constant Power Source  $Cv/K = 2$



Pore Pressure Increase: Constant Power Source  $Cv/K = 2$

	$r/ro = 1$	$r/ro = 2$	$r/ro = 5$	$r/ro = 10$	$r/ro = 50$
time	Temp rise	Temp rise	Temp rise	Temp rise	Temp rise
0.100	6.686E-02	8.552E-03	0.000	0.000	0.000
0.500	0.132	6.063E-02	3.791E-04	0.000	0.000
1.000	0.143	8.913E-02	5.730E-03	3.851E-07	0.000
3.000	0.205	0.158	7.400E-02	7.394E-03	0.000
10.000	0.229	0.189	0.110	3.251E-02	0.000
30.000	0.296	0.261	0.210	0.150	2.787E-03
100.000	0.332	0.328	0.301	0.252	0.111
300.000	0.343	0.343	0.337	0.323	0.209

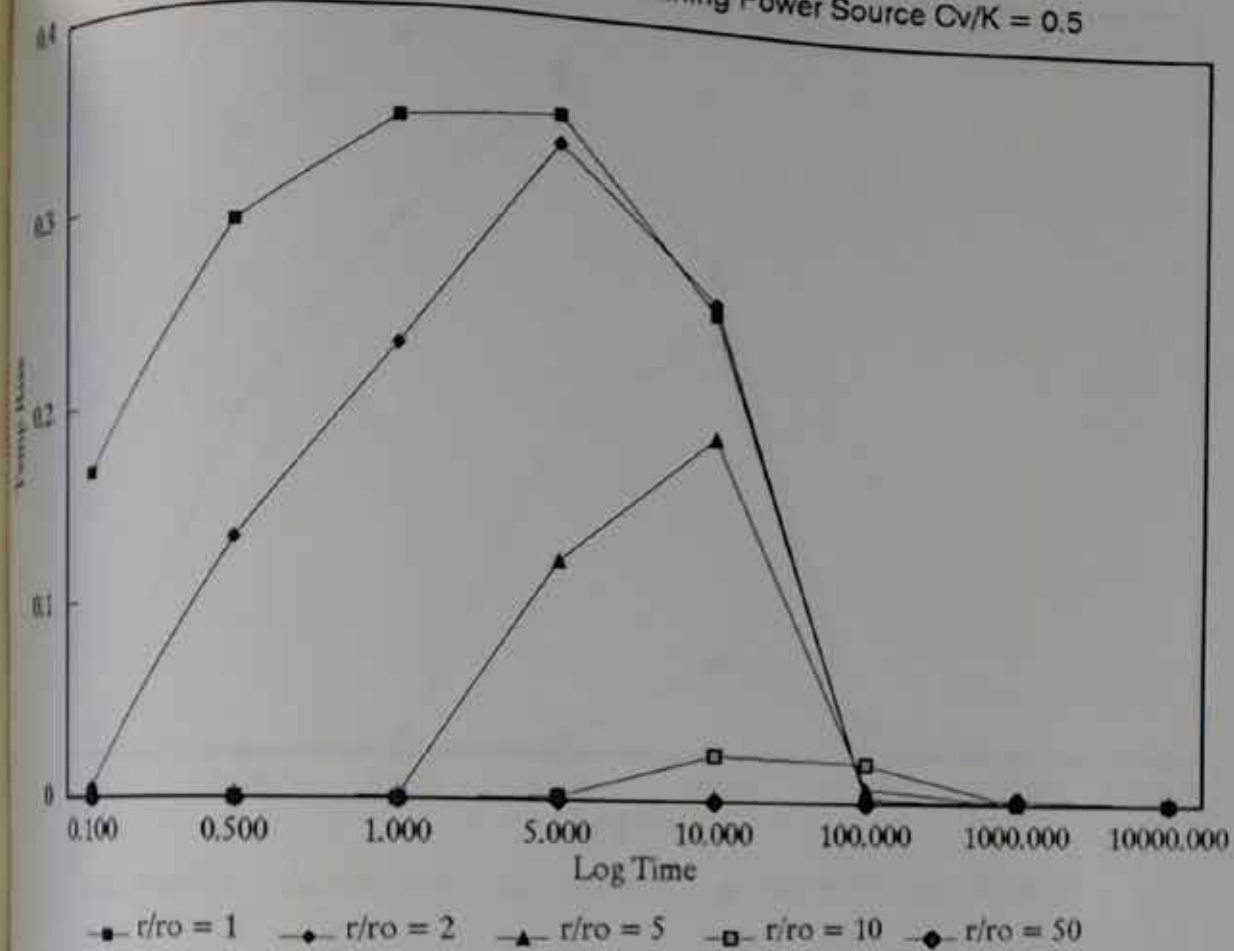
Figure 3.4. Pore Pressure Increase: Constant Power Source  $Cv/K = 2$



Temperature Increase: Exponentially Declining Power Source					
	$r/ro = 1$	$r/ro = 2$	$r/ro = 5$	$r/ro = 10$	$r/ro = 50$
time	Temp rise	Temp rise	Temp rise	Temp rise	Temp rise
0.100	0.312	2.623E-03	0.000	0.000	0.000
0.500	0.595	0.098	5.877E-06	0.000	0.000
1.000	0.747	0.211	7.529E-04	1.221E-11	0.000
5.000	0.944	0.524	0.082	9.407E-04	0.000
10.000	0.794	0.528	0.165	1.282E-02	0.000
50.000	5.496E-02	5.468E-02	5.174E-02	4.199E-02	6.411E-05
100.000	5.031E-03	5.029E-03	5.005E-03	4.913E-03	2.686E-03
1000.000	5.003E-04	5.002E-04	5.000E-04	4.991E-04	4.700E-04

Figure 3.5  
Temperature Increase: Exponentially Declining Power Source

Pore Pressure: Exponentially Declining Power Source Cv/K = 0.5

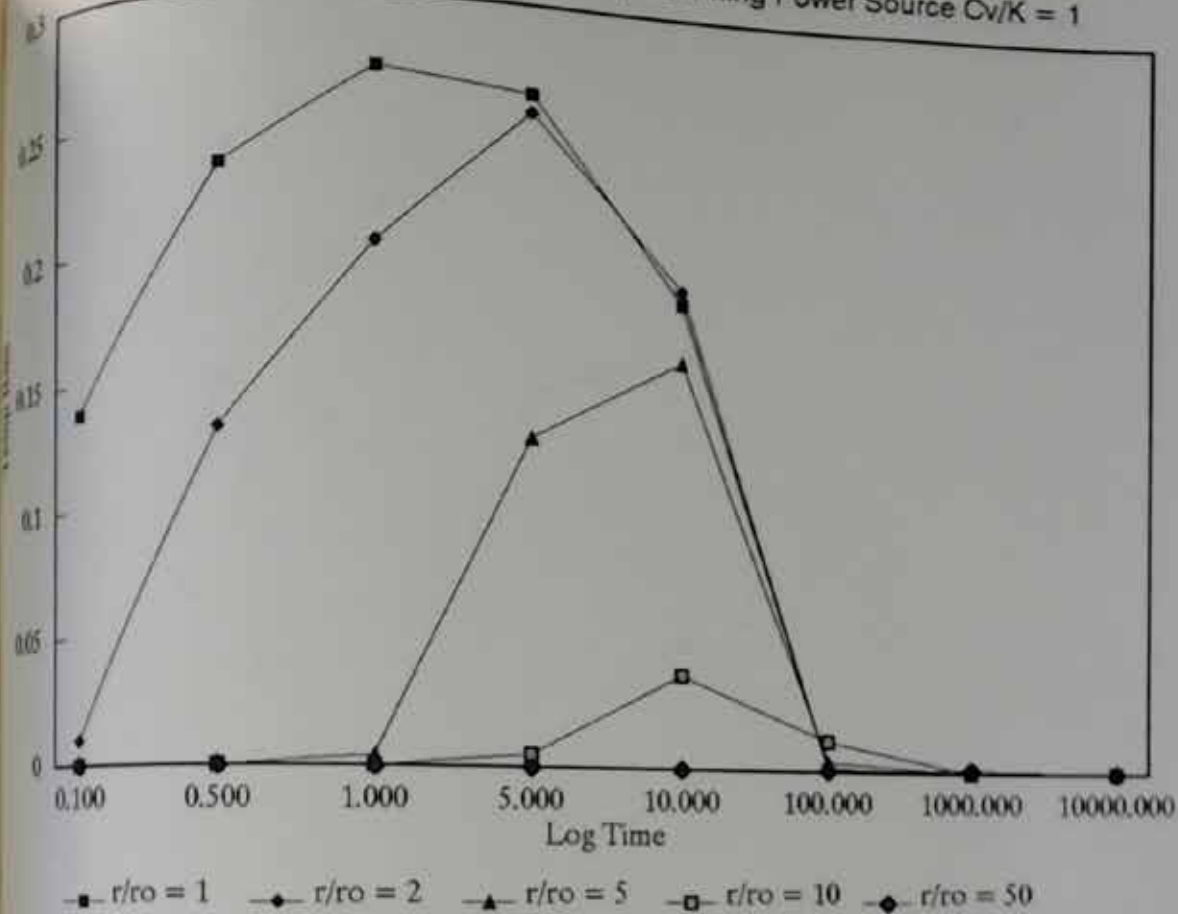


Pore Pressure: Exponentially Declining Power Source Cv/K = 0.5

	$r/r_o = 1$	$r/r_o = 2$	$r/r_o = 5$	$r/r_o = 10$	$r/r_o = 50$
time	Temp rise	Temp rise	Temp rise	Temp rise	Temp rise
1.100	0.167	5.062E-03	0.000	0.000	0.000
1.500	0.291	0.132	1.175E-05	0.000	0.000
1.000	0.344	0.230	1.494E-03	2.443E-11	0.000
5.000	0.350	0.335	0.123	1.867E-03	0.000
10.000	0.252	0.258	0.189	2.389E-02	0.000
20.000	2.349E-03	2.812E-03	7.838E-03	2.051E-02	1.280E-04
50.000	3.181E-05	3.584E-05	8.346E-05	2.602E-04	2.508E-03
100.000	4.316E-07	4.719E-07	9.505E-07	2.782E-06	5.715E-07

Figure 3.6. Pore Pressure: Exponentially Declining Power Source Cv=0.5

Pore Pressure Increase: Exponentially Declining Power Source  $Cv/K = 1$

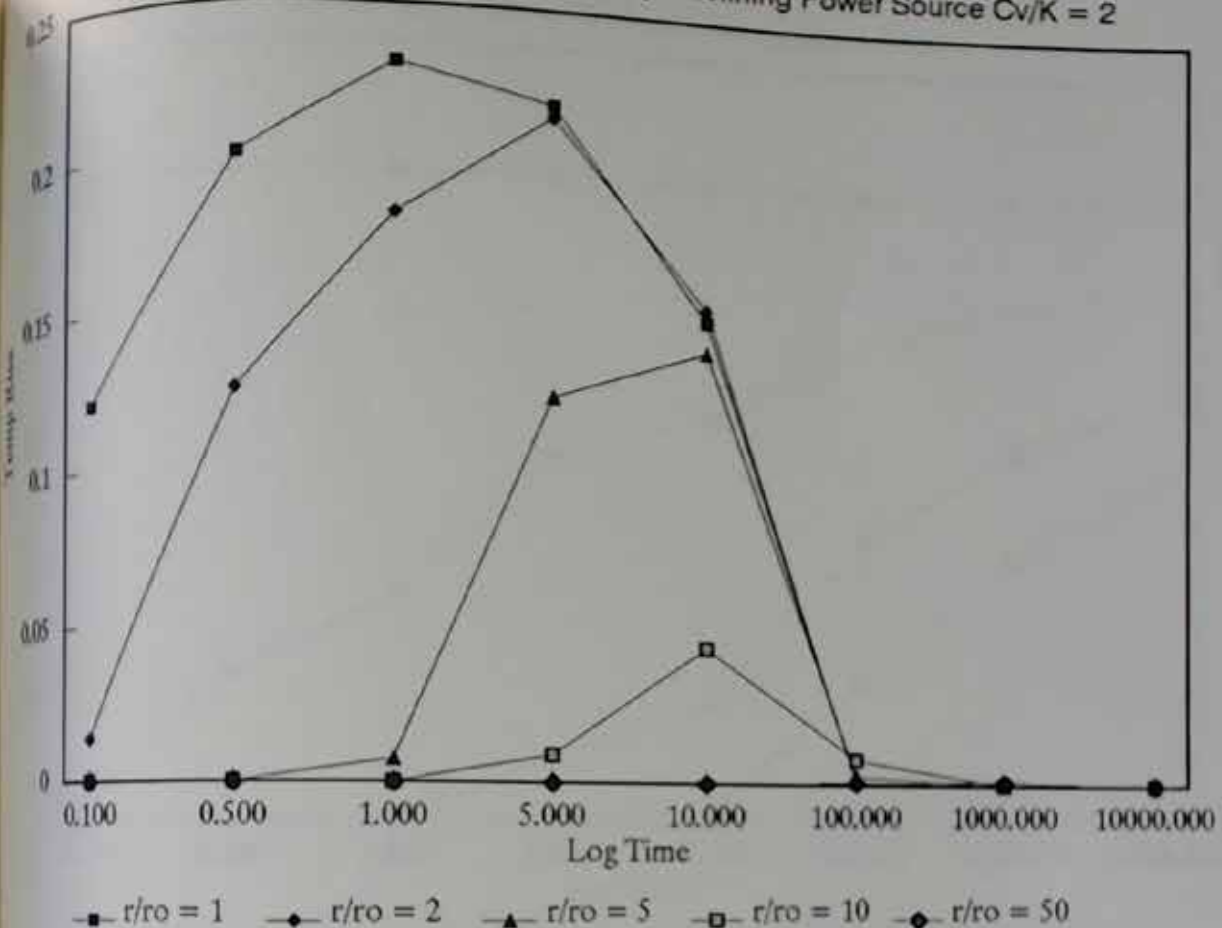


Pore Pressure: Exponentially Declining Power Source  $Cv/K = 1$

	$r/ro = 1$	$r/ro = 2$	$r/ro = 5$	$r/ro = 10$	$r/ro = 50$
Time	Temp rise	Temp rise	Temp rise	Temp rise	Temp rise
1.00	0.138	9.613E-03	0.000	0.000	0.000
1.500	0.233	0.131	5.456E-05	0.000	0.000
1.000	0.271	0.203	3.891E-03	2.635E-10	0.000
1.000	0.264	0.257	0.129	4.813E-03	0.000
1.000	0.185	0.190	0.162	3.697E-02	0.000
1.000	1.324E-03	1.564E-03	4.241E-03	1.199E-02	4.201E-04
1.000	1.692E-05	1.895E-05	4.293E-05	1.329E-04	1.691E-03
1.000	2.254E-07	2.455E-07	4.848E-07	1.402E-06	2.947E-05

14.3.7. Pore Pressure: Exponentially Declining Power Source  $Cv/K = 1$   
Increase

Pore Pressure Increase: Exponentially Declining Power Source Cv/K = 2

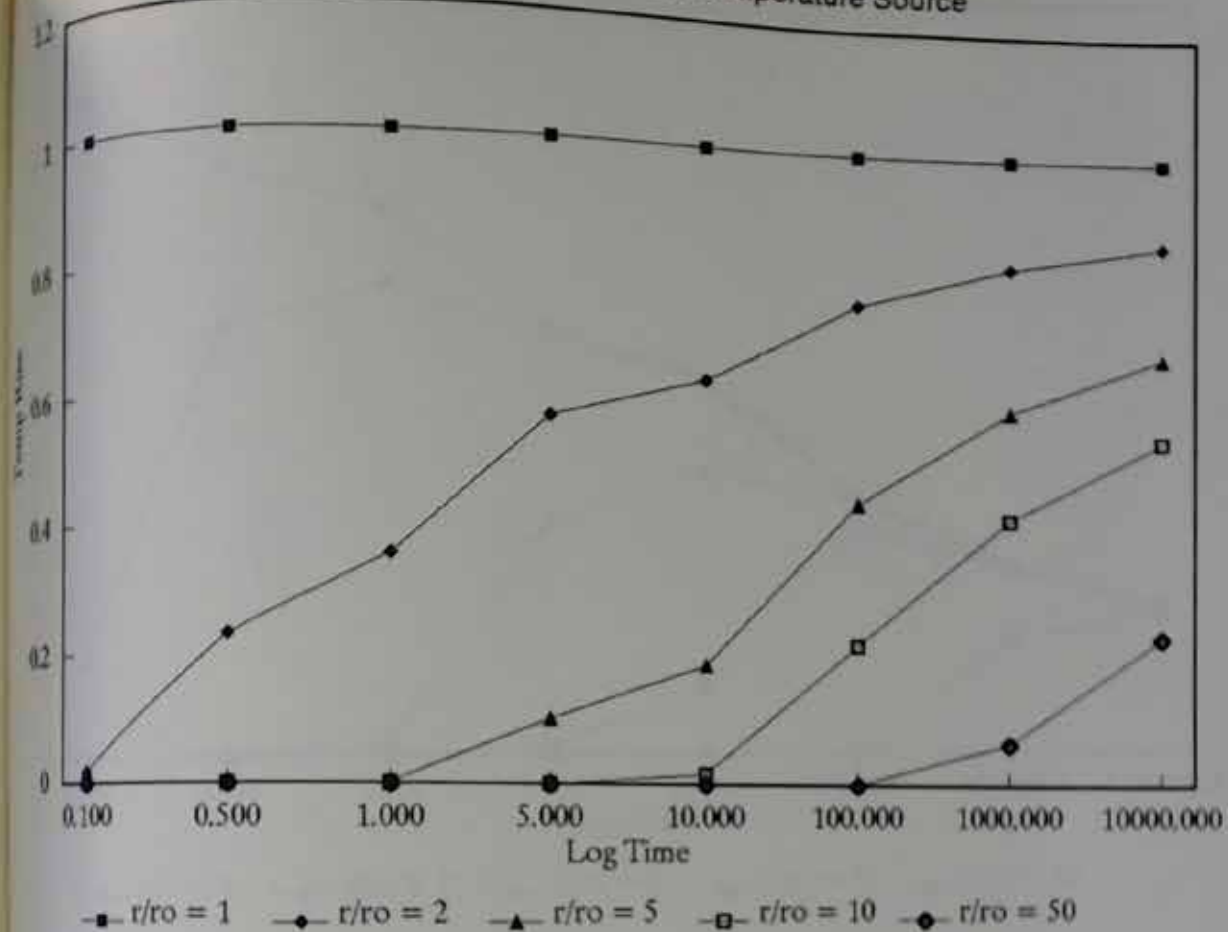


Pore Pressure: Exponentially Declining Power Source Cv/K = 2

	$r/r_o = 1$	$r/r_o = 2$	$r/r_o = 5$	$r/r_o = 10$	$r/r_o = 50$
Time	Temp rise	Temp rise	Temp rise	Temp rise	Temp rise
0.100	0.121	1.385E-02	0.000	0.000	0.000
0.500	0.201	0.125	2.708E-04	0.000	0.000
1.000	0.231	0.182	7.543E-03	3.597E-08	0.000
5.000	0.219	0.215	0.124	9.123E-03	0.000
10.000	0.151	0.155	0.141	4.439E-02	0.000
20.000	9.335E-04	1.096E-03	2.926E-03	8.484E-03	1.032E-03
40.000	1.163E-05	1.299E-05	2.903E-05	8.949E-05	1.256E-03
80.000	1.536E-07	1.670E-07	3.268E-07	9.391E-07	1.988E-05

Part 3.8. Pore Pressure: Exponentially Declining Power Source Cv/K= 2

Temperature Rise = Constant Temperature Source

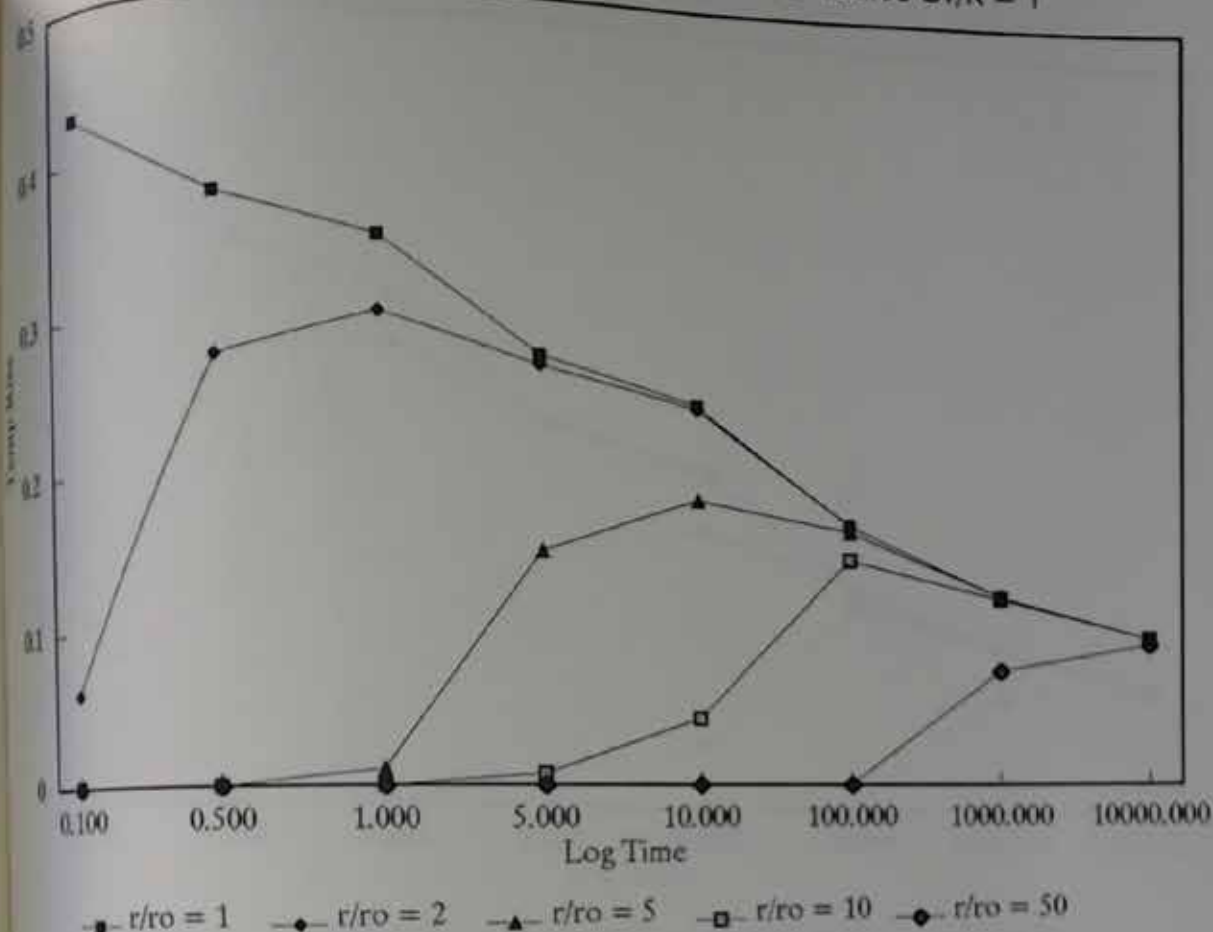


Temperature Rise = Constant Temperature Source

	r/ro = 1	r/ro = 2	r/ro = 5	r/ro = 10	r/ro = 50
time	Temp rise				
1.100	1.000	1.808E-02	0.000	0.000	0.000
1.500	1.000	0.230	2.890E-05	0.000	0.000
1.000	1.000	0.351	2.166E-03	6.353E-11	0.000
1.000	1.000	0.568	0.101	1.510E-03	0.000
1.500	1.000	0.631	0.188	1.567E-02	0.000
1.000	1.000	0.761	0.446	0.222	9.293E-05
1.000	1.000	0.826	0.596	0.423	6.571E-02
1.500	1.000	0.864	0.684	0.549	0.237

Figure 3.9. Temperature Rise = Constant Temperature Source

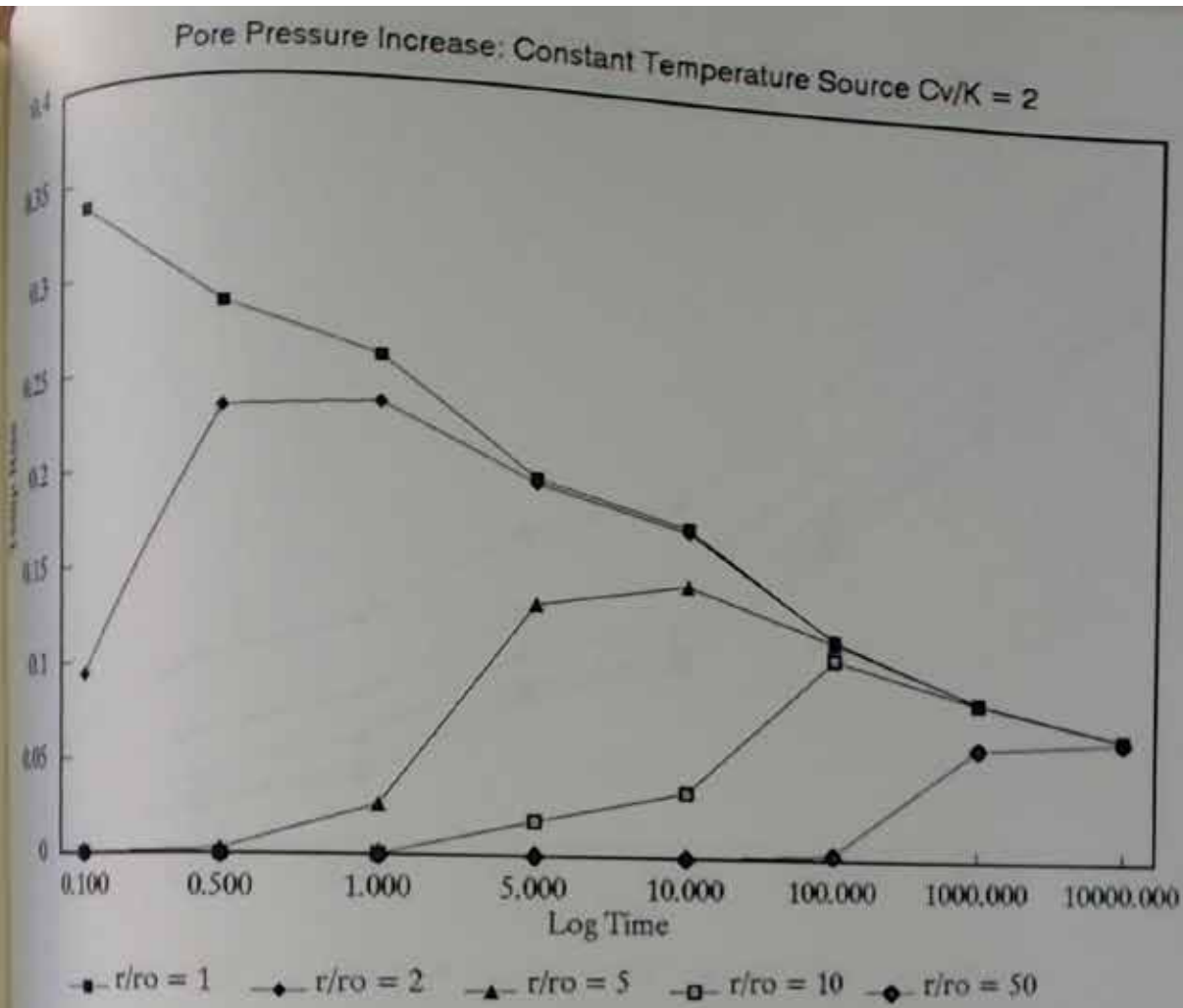
Pore Pressure Increase: Constant Temperature Source  $Cv/K = 1$



Pore Pressure Increase: Constant Temperature Source  $Cv/K = 1$

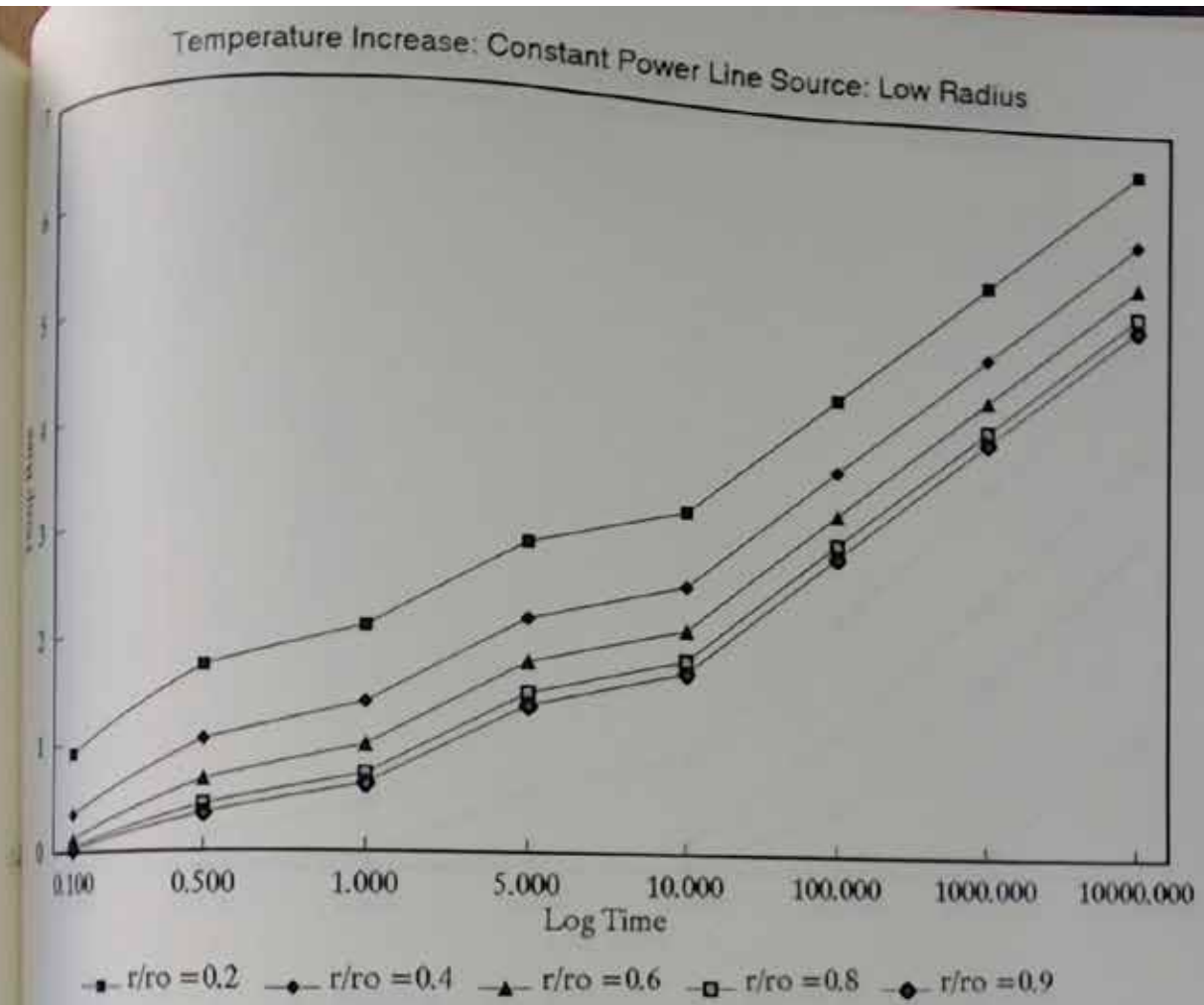
$r/ro = 1$	$r/ro = 2$	$r/ro = 5$	$r/ro = 10$	$r/ro = 50$
Time	Temp rise	Temp rise	Temp rise	Temp rise
1.100	0.430	6.078E-02	0.000	0.000
1.300	0.375	0.272	2.579E-04	0.000
1.900	0.346	0.298	1.054E-02	1.347E-09
1.000	0.274	0.267	0.149	7.378E-03
1.000	0.245	0.242	0.184	4.362E-02
1.000	0.170	0.170	0.166	0.148
1.000	0.125	0.125	0.125	0.124
1.000	9.794E-02	9.794E-02	9.793E-02	9.766E-02

Fig. 3.10. Pore Pressure Increase: Constant Temperature Source  $Cv/K = 1$



Pore Pressure Increase: Constant Temperature Source $Cv/K = 2$					
	$r/ro = 1$	$r/ro = 2$	$r/ro = 5$	$r/ro = 10$	$r/ro = 50$
Time	Temp rise	Temp rise	Temp rise	Temp rise	Temp rise
0.100	0.337	9.367E-02	1.600E-10	0.000	0.000
0.300	0.283	0.229	2.894E-03	8.753E-11	0.000
1.000	0.256	0.232	2.616E-02	3.018E-06	0.000
3.000	0.196	0.193	0.131	1.826E-02	0.000
10.000	0.174	0.172	0.144	3.465E-02	1.945E-15
30.000	0.118	0.118	0.117	0.108	3.101E-03
100.000	8.686E-02	8.685E-02	8.676E-02	8.623E-02	6.197E-02
300.000	6.789E-02	6.789E-02	6.789E-02	6.786E-02	6.602E-02

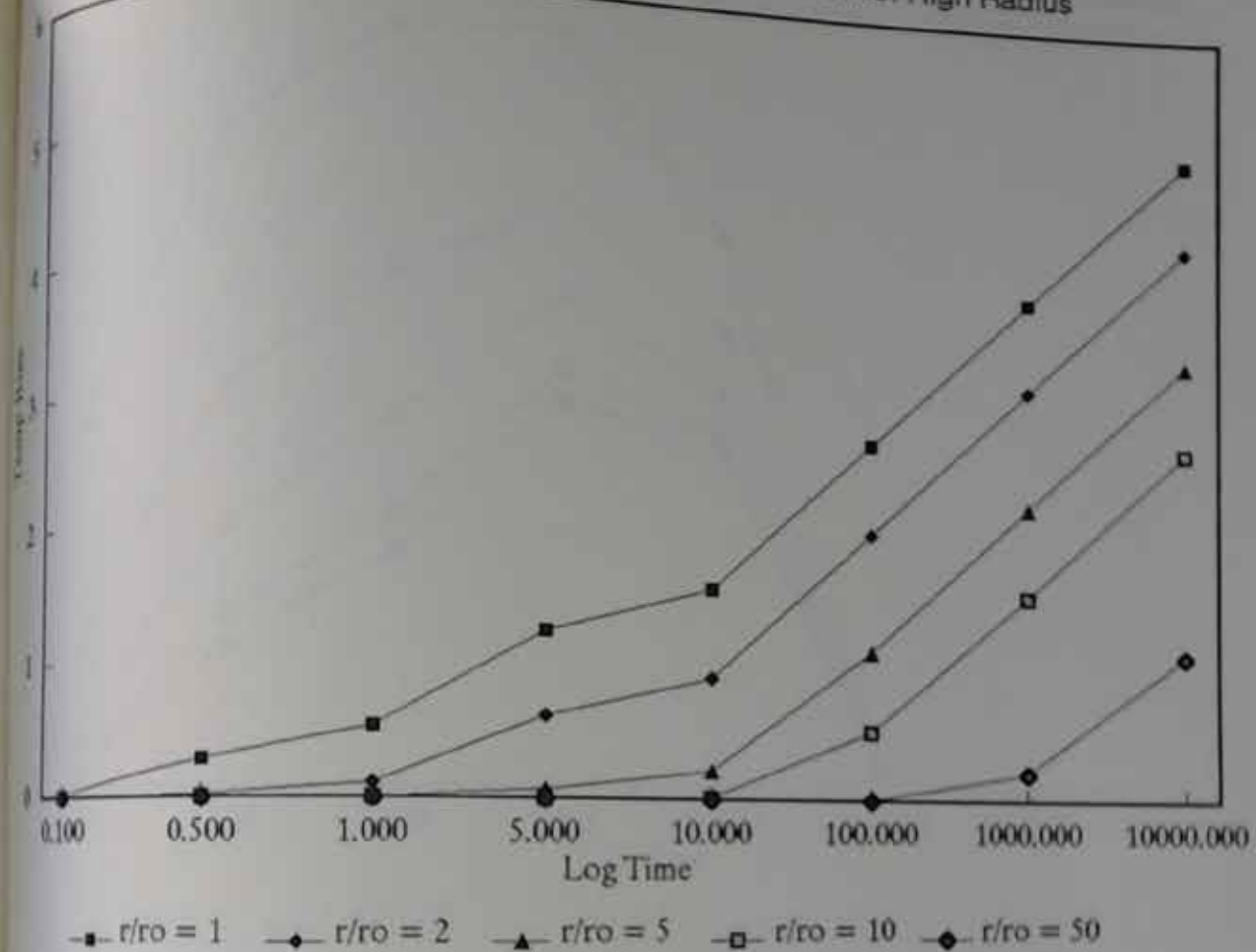
Fig. 3.11. Pore Pressure Increase: Constant Temperature Source  $Cv/K = 2$



Temperature Increase: Constant Power Line Source: Low Radius					
	$r/ro = 0.2$	$r/ro = 0.4$	$r/ro = 0.6$	$r/ro = 0.8$	$r/ro = 0.9$
time	Temp rise				
1.100	0.911	0.352	0.130	4.315E-02	2.362E-02
1.500	1.677	1.013	0.655	0.429	0.347
1.000	2.019	1.341	0.959	0.705	0.606
1.000	2.819	2.130	1.729	1.448	1.335
1.000	3.166	2.474	2.071	1.787	1.671
1.000	4.316	3.624	3.218	2.931	2.813
1.000	5.468	4.775	4.369	4.081	3.964
1.000	6.619	5.926	5.520	5.232	5.115

9.1.12 Temperature Increase: Constant Power Line Source: Low Radius

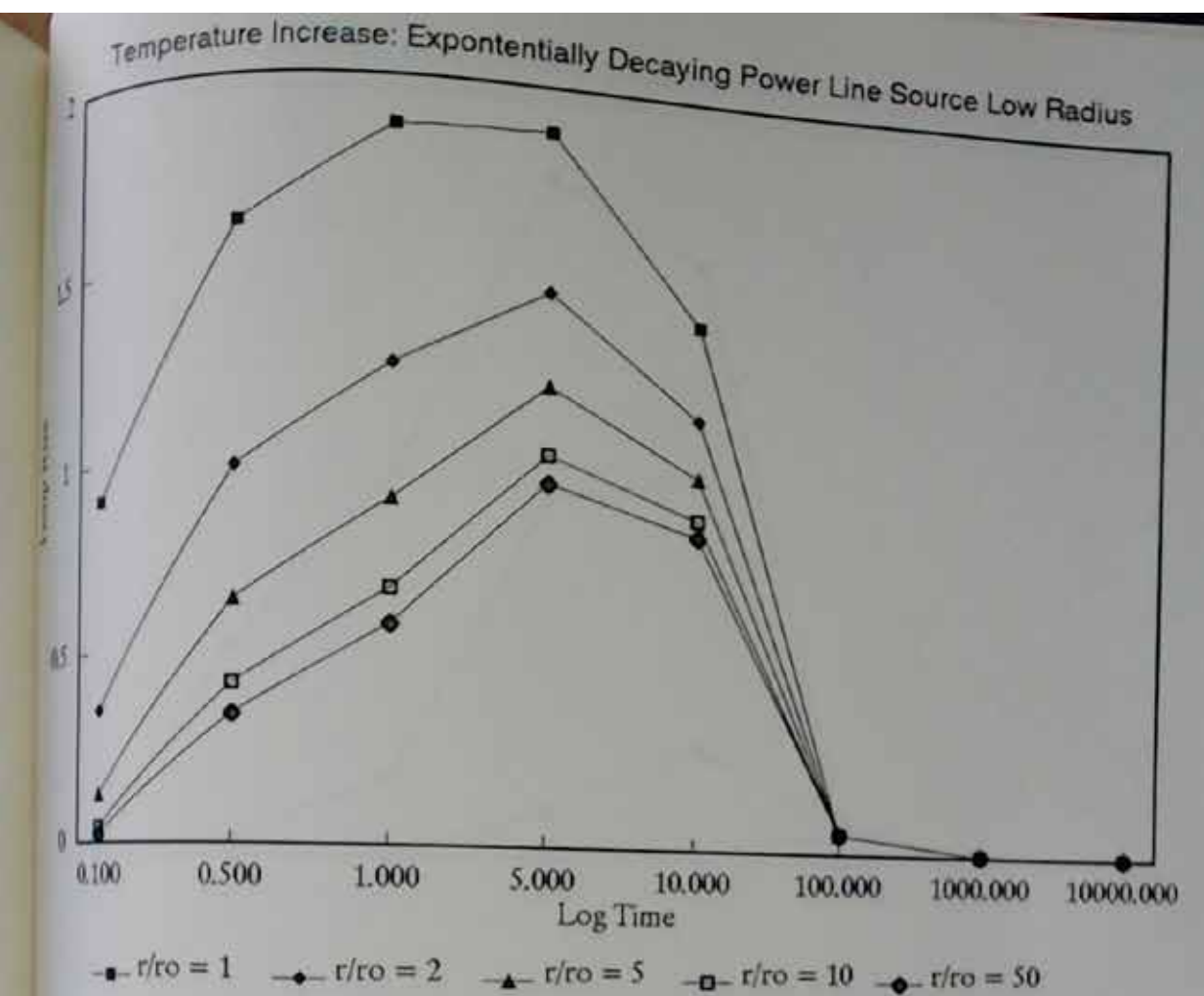
Temperature Increase: Constant Power Line Source: High Radius



Temperature Increase: Constant Power Line Source: High Radius

	$r/ro = 1$	$r/ro = 2$	$r/ro = 5$	$r/ro = 10$	$r/ro = 50$
Time	Temp rise	Temp rise	Temp rise	Temp rise	Temp rise
0.100	1.246E-02	2.078E-06	0.000	0.000	0.000
0.500	0.279	2.445E-02	1.387E-07	0.000	0.000
1.000	0.522	0.110	1.352E-04	0.000	0.000
5.000	1.234	0.611	7.321E-02	5.741E-04	0.000
10.000	1.568	0.911	0.216	1.246E-02	0.000
50.000	2.708	2.019	1.128	0.522	1.352E-04
100.000	3.859	3.166	2.252	1.568	0.216
1000.000	5.010	4.317	3.401	2.708	1.128

Constant Power Line Source: High Rad.

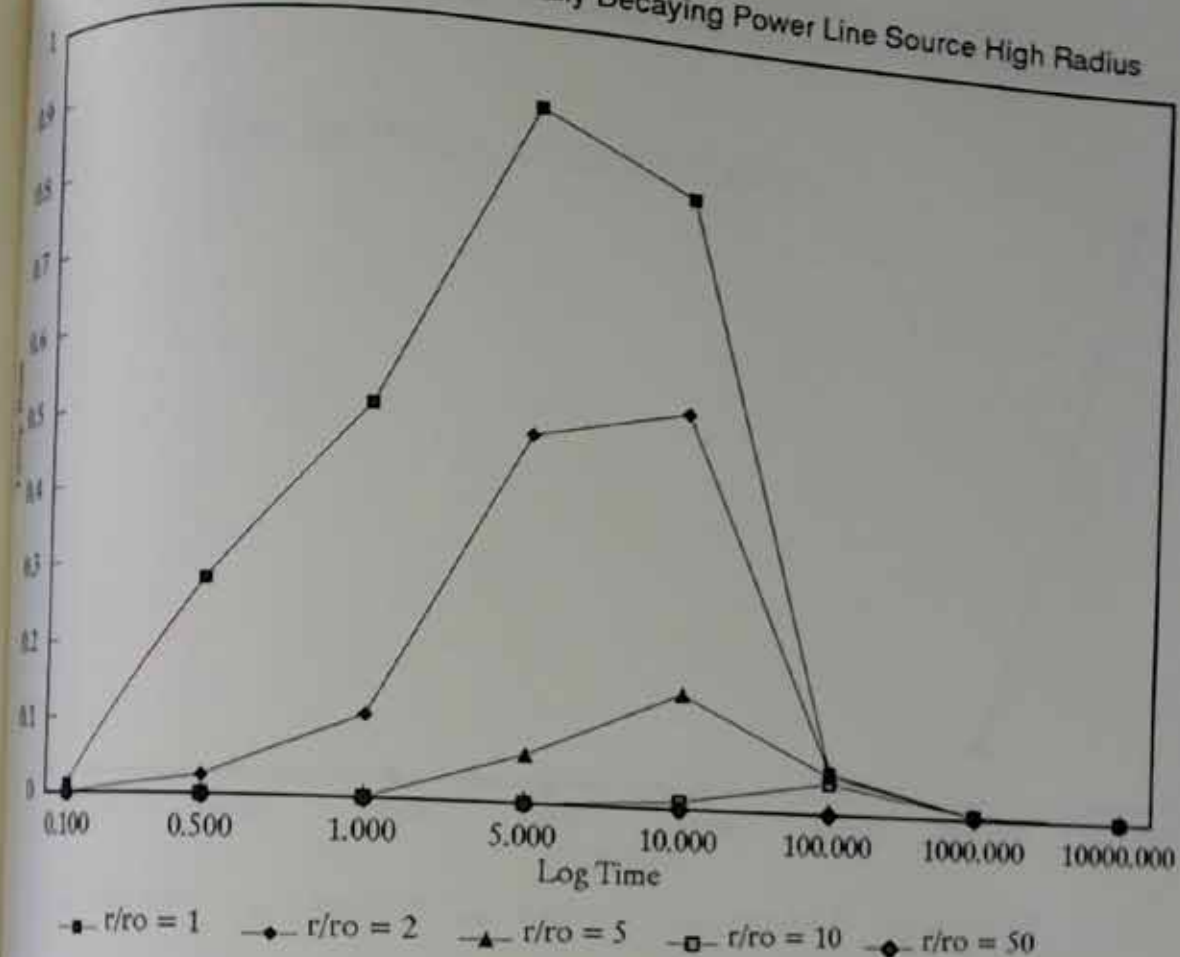


Temperature Increase: Exponentially Decaying Power Line Source Low Rad

r/ro	r/ro = 0.2	r/ro = 0.4	r/ro = 0.6	r/ro = 0.8	r/ro = 0.9
Temp rise	0.906	0.350	0.130	4.304E-02	2.357E-02
Temp rise	1.618	0.982	0.637	0.419	0.339
Temp rise	1.871	1.253	0.903	0.667	0.575
Temp rise	1.881	1.458	1.209	1.031	0.958
Temp rise	1.400	1.148	0.995	0.884	0.839
Temp rise	5.670E-02	5.665E-02	5.659E-02	5.653E-02	5.650E-02
Temp rise	5.051E-03	5.051E-03	5.051E-03	5.050E-03	5.050E-03
Temp rise	5.005E-04	5.005E-04	5.005E-04	5.005E-04	5.005E-04

Figure 3.14. Temperature Increase: Exponentially Decaying Power Line  
Source Low Radius

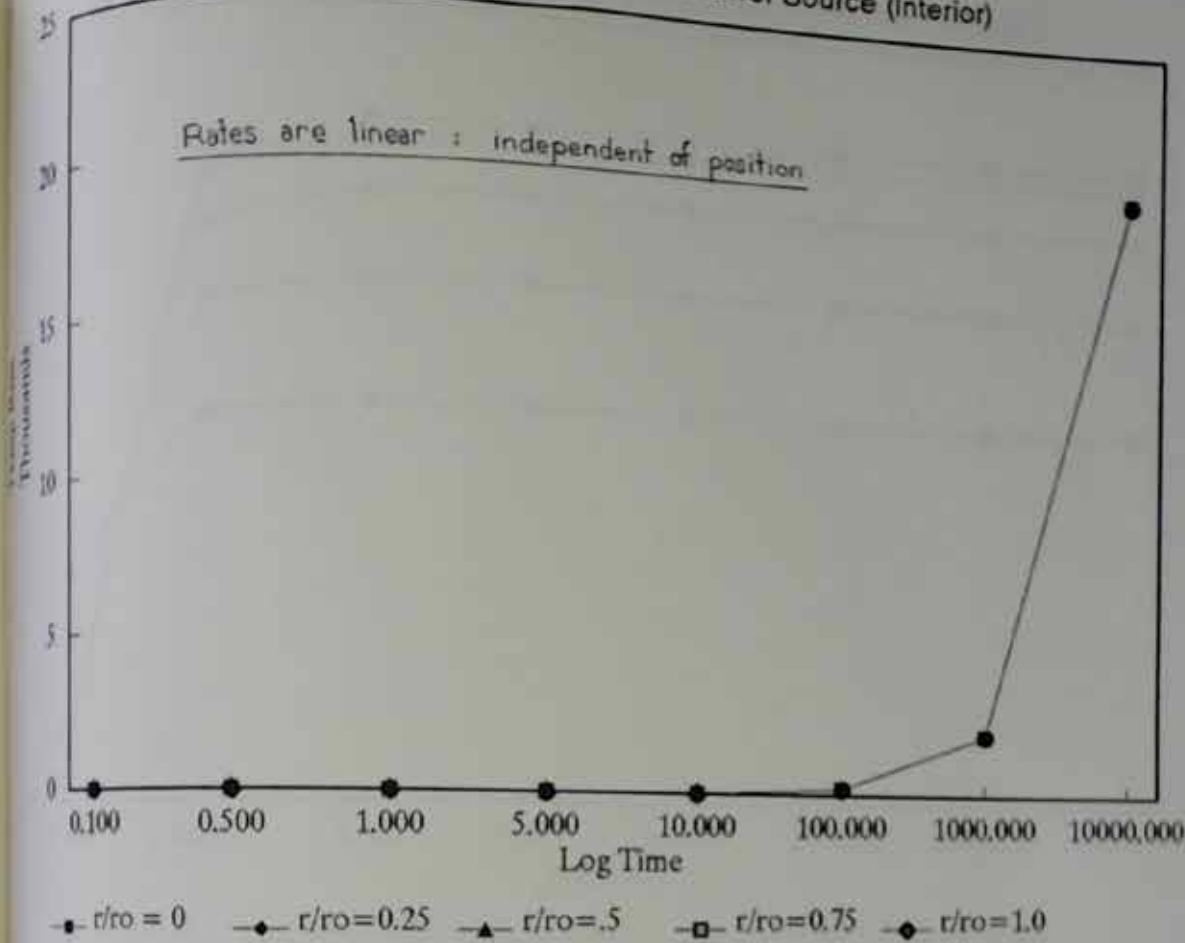
Temperature Increase: Exponentially Decaying Power Line Source High Radius



Temperature Increase: Exponentially Decaying Power Line Source High Radius					
	$r/r_o = 1$	$r/r_o = 2$	$r/r_o = 5$	$r/r_o = 10$	$r/r_o = 50$
Time	Temp rise	Temp rise	Temp rise	Temp rise	Temp rise
1.00	1.234E-02	2.077E-06	0.000	0.000	0.000
5.00	0.274	2.417E-02	1.382E-07	0.000	0.000
10.00	0.500	0.106	1.337E-04	0.000	0.000
20.00	0.893	0.473	6.351E-02	5.382E-04	0.000
40.00	0.798	0.517	0.151	1.026E-02	0.000
80.00	5.646E-02	5.594E-02	5.259E-02	4.234E-02	6.003E-05
160.00	5.050E-03	5.046E-03	5.019E-03	4.925E-03	2.686E-03
320.00	5.005E-04	5.005E-04	5.002E-04	4.993E-04	4.701E-04

Figure 3.15. Temperature Increase: Exponentially Decaying Power Line Source High Radius

**Temperature Increase: Constant Power Source (Interior)**

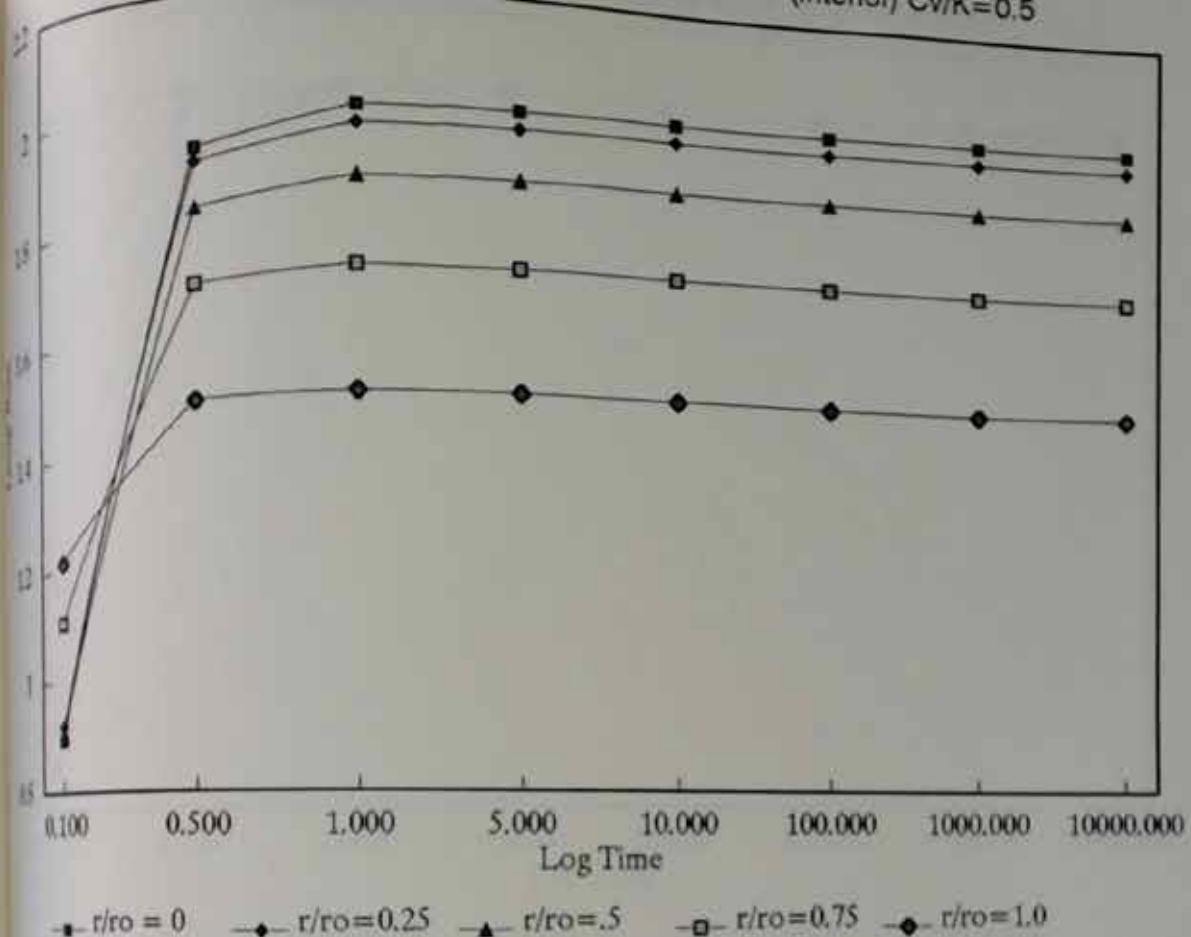


**Temperature Increase: Constant Power Source (Interior)**

	$r/ro = 0$	$r/ro = 0.25$	$r/ro = 0.5$	$r/ro = 0.75$	$r/ro = 1.0$
Time	Temp rise	Temp rise	Temp rise	Temp rise	Temp rise
1.100	2.692E-02	4.192E-02	9.661E-02	2.146E-01	0.418
1.500	0.750	0.781	0.875	1.031	1.250
1.000	1.750	1.781	1.875	2.031	2.250
1.000	9.750	9.781	9.875	10.031	10.250
1.000	19.750	19.781	19.875	20.031	20.250
1.000	199.750	199.781	199.875	200.031	200.250
1.000	1999.750	1999.781	1999.875	2000.031	2000.250
1.000	19999.750	19999.781	19999.875	20000.031	20000.250

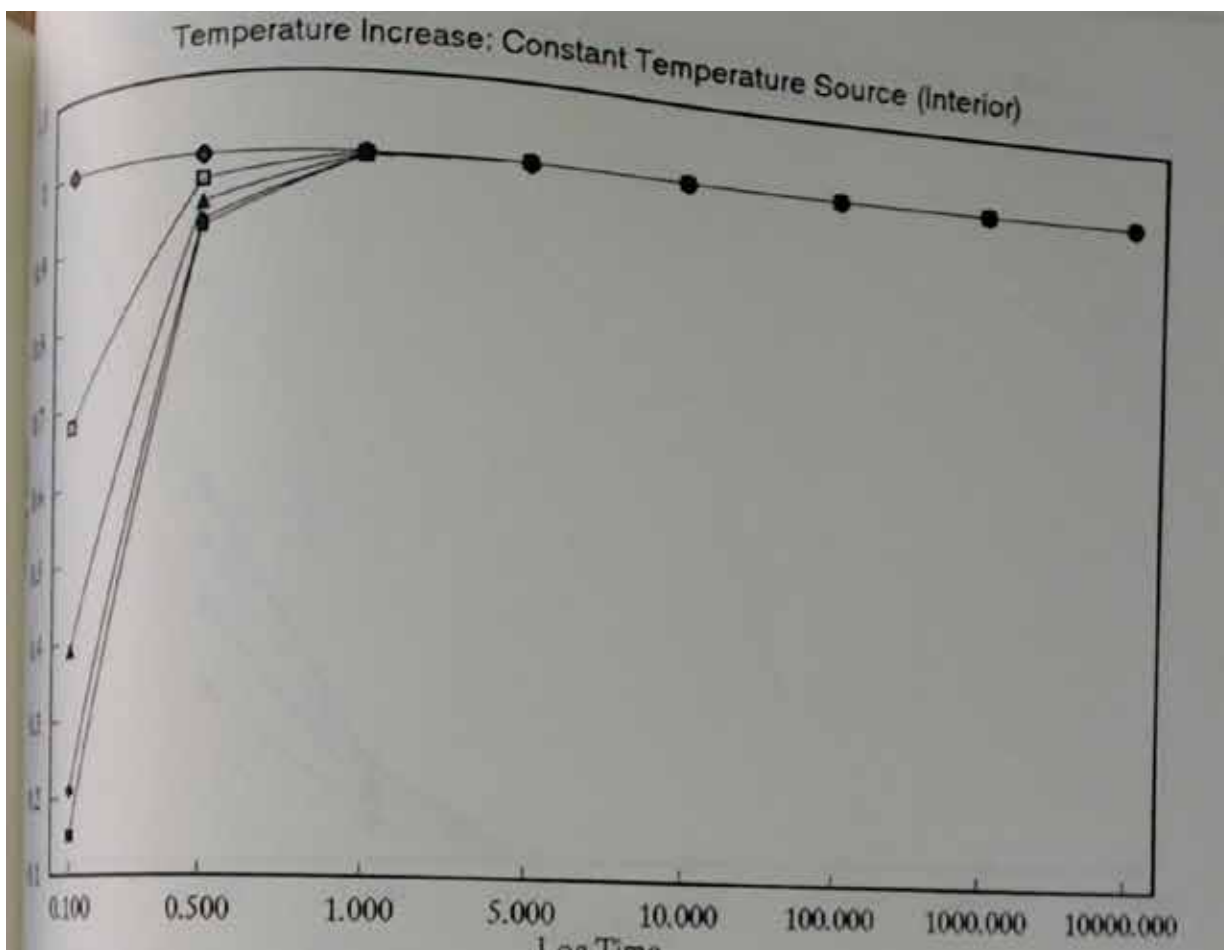
Case 3.16, Temperature Increase: Constant Power Source (Interior)

Pore Pressure

Increase: Constant Power Source (Interior)  $Cv/K=0.5$ Temperature Increase: Constant Power Source (Interior)  $Cv/K=0.5$ 

$r/ro$	$r/ro = 0$	$r/ro = 0.25$	$r/ro = .5$	$r/ro = 0.75$	$r/ro = 1.0$
1.100	0.896	0.919	0.903	1.107	1.215
1.500	1.928	1.902	1.823	1.687	1.486
2.000	1.998	1.966	1.873	1.718	1.500
2.500	1.999	1.968	1.875	1.718	1.500
3.000	2.000	1.968	1.875	1.718	1.500
3.500	2.000	1.968	1.875	1.718	1.500
4.000	2.000	1.968	1.875	1.718	1.500
4.500	2.000	1.968	1.875	1.718	1.500

Pore Pressure Increase: Constant Power Source (Interior)  $Cv/K=0.5$

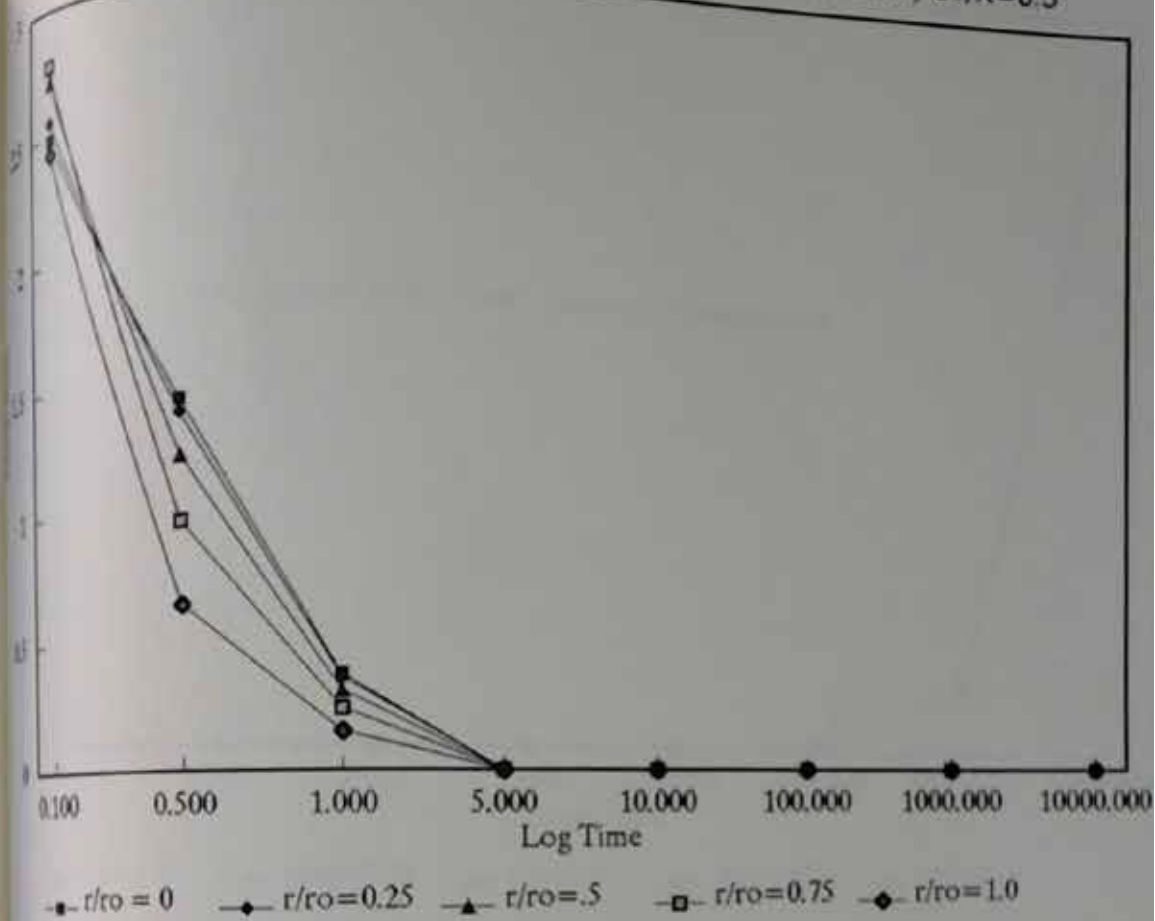


■  $r/ro = 0$    ■  $r/ro = 0.25$    ▲  $r/ro = .5$    □  $r/ro = 0.75$    ●  $r/ro = 1.0$

Temperature Increase: Constant Temperature Source (Interior)					
	$r/ro = 0$	$r/ro = 0.25$	$r/ro = .5$	$r/ro = 0.75$	$r/ro = 1.0$
1.00	0.152	0.210	0.390	0.677	1.000
1.00	0.911	0.919	0.940	0.970	1.000
1.00	0.995	0.995	0.997	0.998	1.000
1.00	1.000	1.000	1.000	1.000	1.000
1.00	1.000	1.000	1.000	1.000	1.000
1.00	1.000	1.000	1.000	1.000	1.000
1.00	1.000	1.000	1.000	1.000	1.000
1.00	1.000	1.000	1.000	1.000	1.000

3.18. Temperature Increase: Constant Temperature Source (Interior)

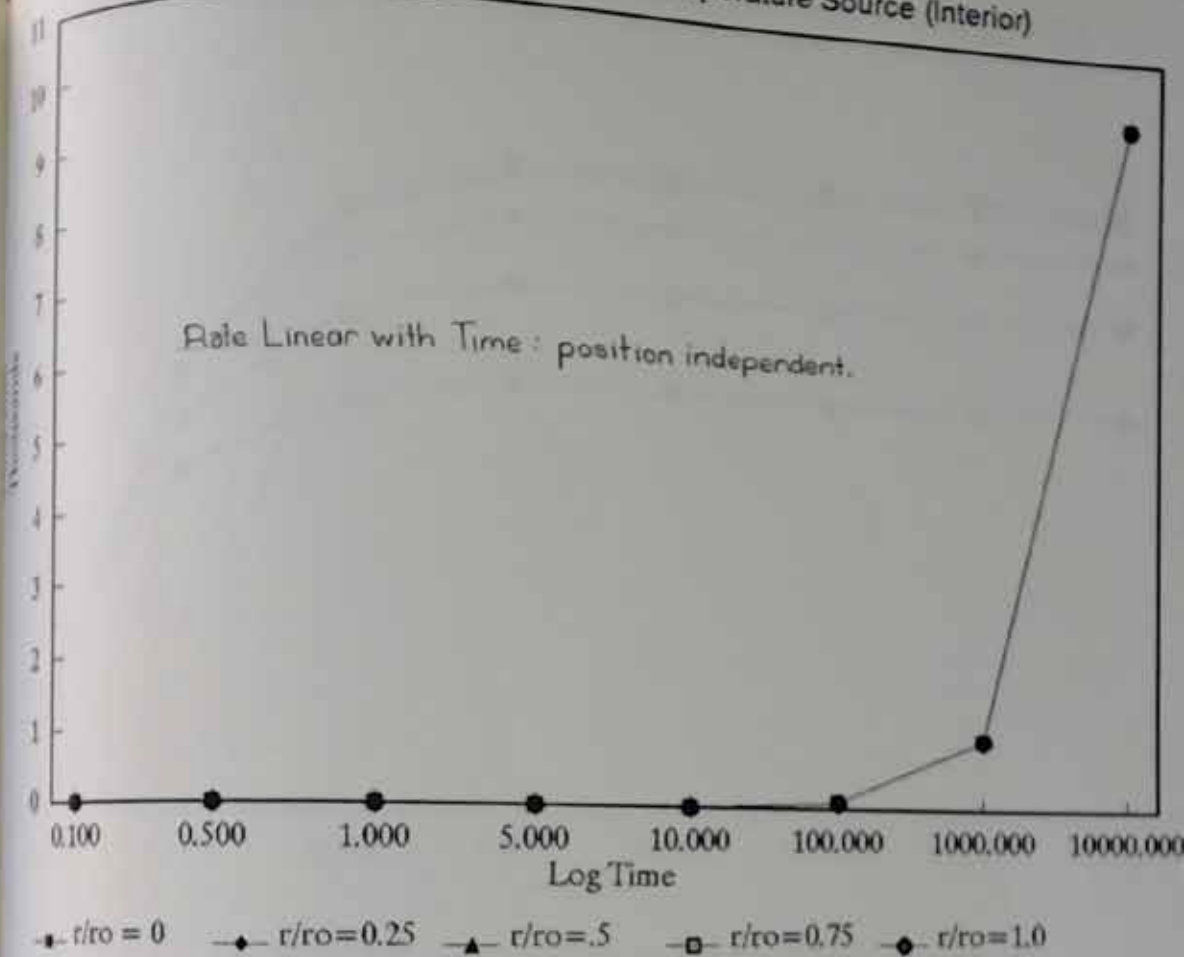
Pore Pressure Increase: Constant Temperature Source (Interior)  $C_v/K=0.5$



Pore Pressure Increase: Constant Temperature Source (Interior) $C_v/K=0.5$					
$r/r_o = 0$	$r/r_o = 0.25$	$r/r_o = .5$	$r/r_o = 0.75$	$r/r_o = 1.0$	
Time	Temp rise	Temp rise	Temp rise	Temp rise	Temp rise
100	2.491	2.561	2.720	2.780	2.435
300	1.421	1.366	1.205	0.954	0.638
1000	0.367	0.353	0.305	0.235	0.150
10000	3.574E-06	3.414E-06	2.957E-06	2.262E-06	1.421E-06
100000	0.000	0.000	0.000	0.000	0.000
1000000	0.000	0.000	0.000	0.000	0.000
10000000	0.000	0.000	0.000	0.000	0.000
100000000	0.000	0.000	0.000	0.000	0.000

Figure 3.19. Pore Pressure Increase: Constant Temperature Source (Interior)  $C_v/K=0.5$

Temperature Increase: Constant Temperature Source (Interior)

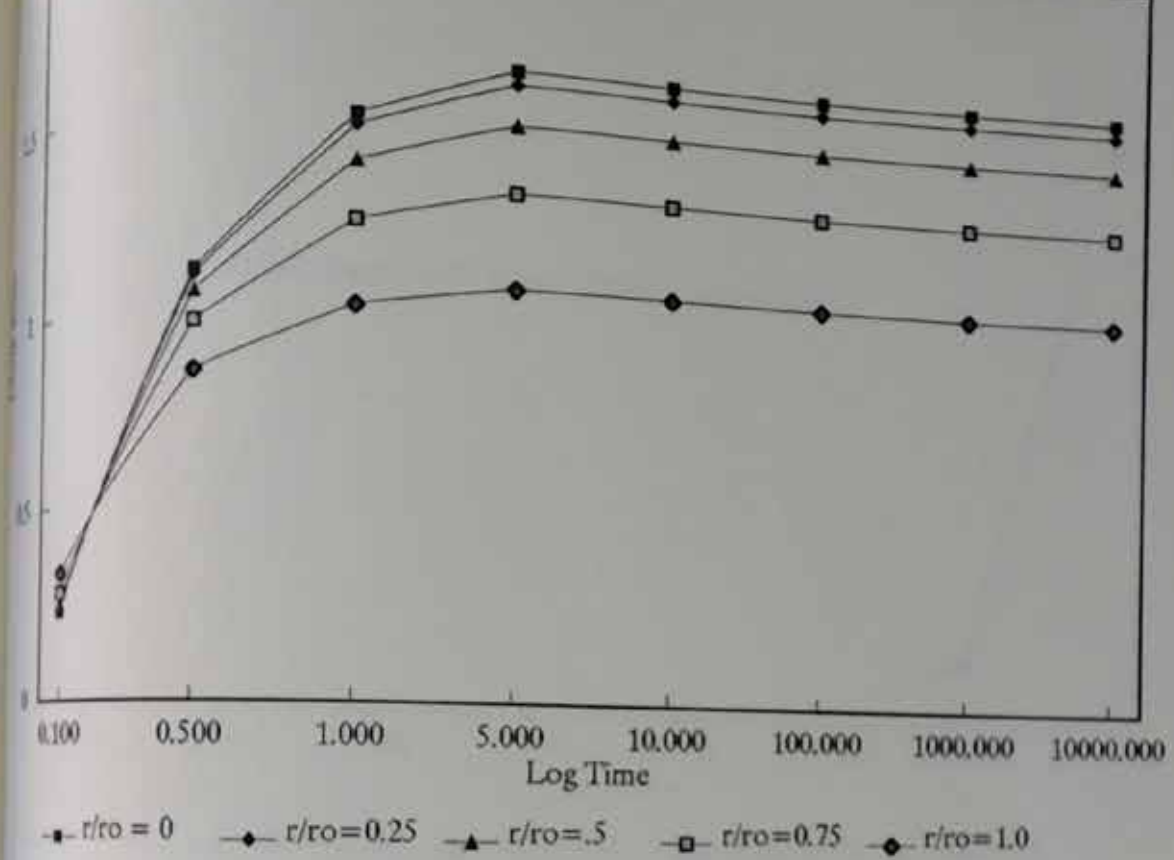


Temperature Increase: Constant Temperature Source (Interior)

$r/r_o$	0	0.25	.5	0.75	1.0
0.100	3.703E-03	6.300E-03	1.685E-02	4.376E-02	0.100
0.500	0.265	0.280	0.323	0.396	0.500
1.000	0.751	0.766	0.813	0.891	1.000
5.000	4.750	4.766	4.813	4.891	5.000
10.000	9.750	9.766	9.813	9.891	10.000
100.000	99.750	99.766	99.813	99.891	100.000
1000.000	999.750	999.766	999.813	999.891	1000.000
10000.000	9999.750	9999.766	9999.813	9999.891	10000.000

1.10. Temperature Increase: Constant Temperature Source (Interior)

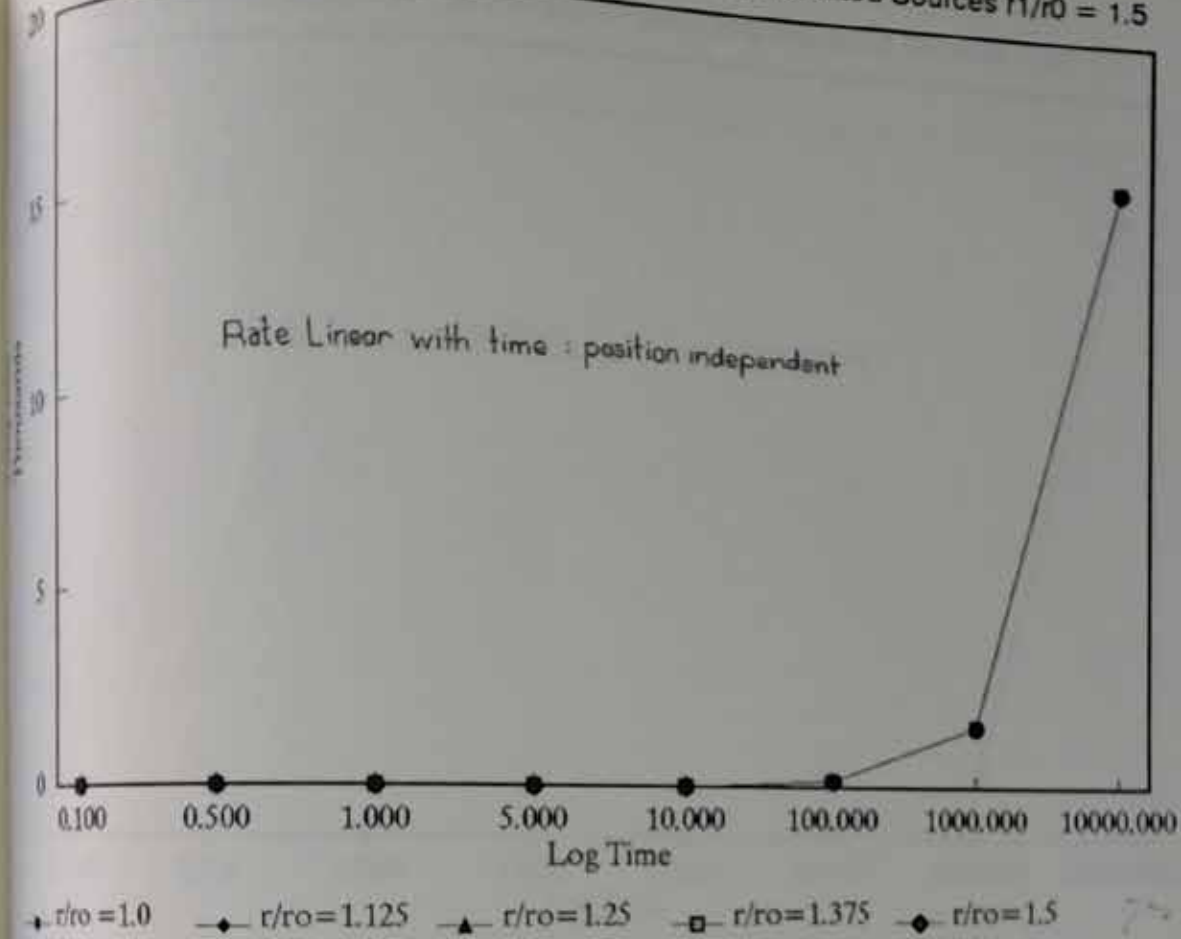
Pore Pressure: Linearly Increasing Temperature Source (Interior)  $Cv/K = 0.5$



Pore Pressure: Linearly Increasing Temperature Source (Interior) $Cv/K = 0.5$					
	$r/ro = 0$	$r/ro = 0.25$	$r/ro = 0.5$	$r/ro = 0.75$	$r/ro = 1.0$
Time	Temp rise	Temp rise	Temp rise	Temp rise	Temp rise
0.100	0.231	0.235	0.251	0.284	0.334
0.500	1.099	1.085	1.044	0.966	0.840
1.000	1.493	1.463	1.374	1.224	1.009
5.000	1.621	1.586	1.481	1.306	1.061
10.000	1.621	1.586	1.481	1.306	1.061
100.000	1.621	1.586	1.481	1.306	1.061
1,000,000	1.621	1.586	1.481	1.306	1.061
10,000,000	1.621	1.586	1.481	1.306	1.061

Figure 3.21. Pore Pressure: Linearly Increasing Temperature Source (Interior)  $Cv/K = 0.5$

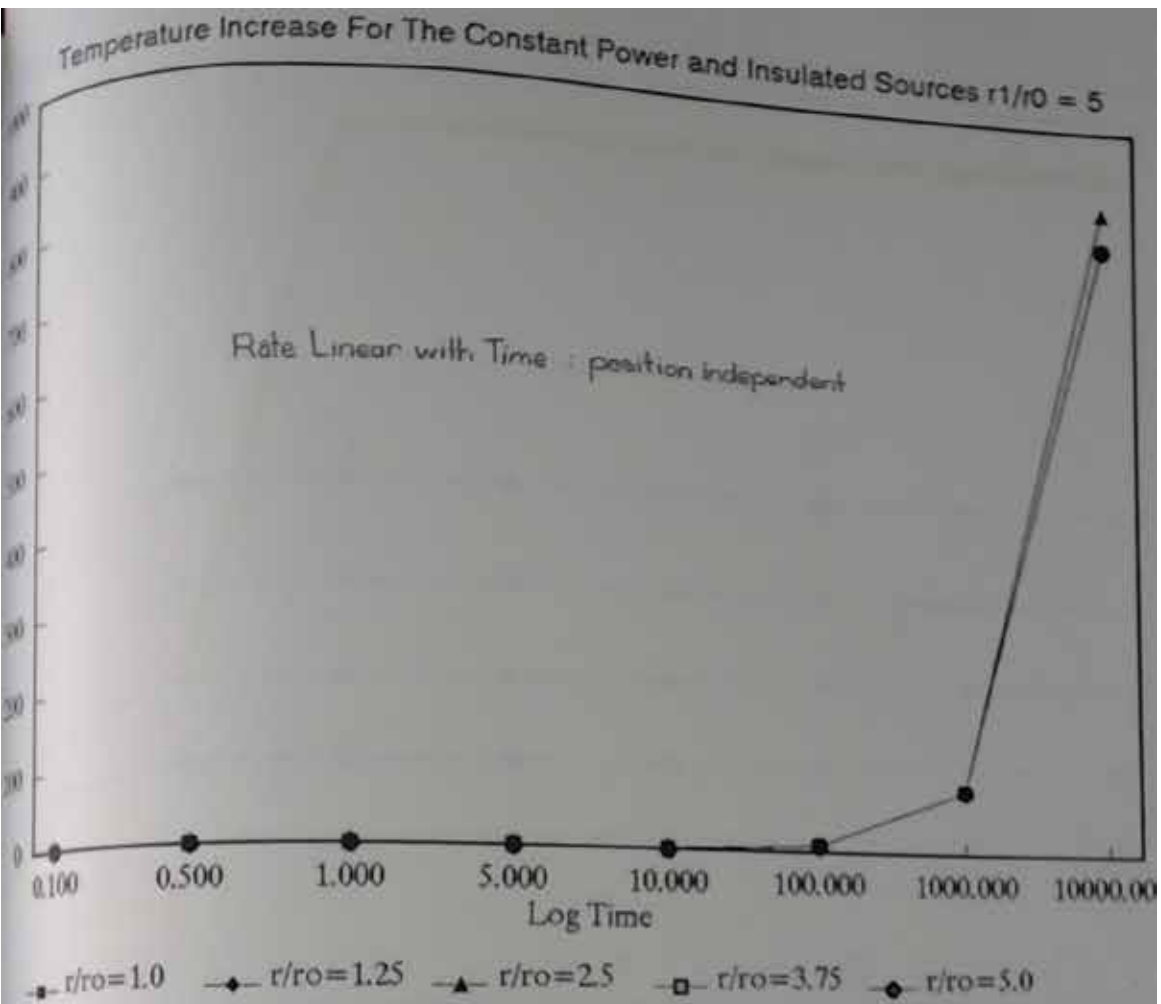
Temperature Increase For The Constant Power and Insulated Sources  $r_1/r_0 = 1.5$



Temperature Incr. For The Constant Power & Insulated Sources  $r_1/r_0 = 1.5$

Time	$r/r_0 = 1.0$	$r/r_0 = 1.125$	$r/r_0 = 1.25$	$r/r_0 = 1.375$	$r/r_0 = 1.5$
0.100	0.322	0.217	0.171	3.169	7.042
0.500	0.964	0.858	0.812	3.810	7.667
1.000	1.764	1.658	1.611	4.610	8.467
5.000	8.164	8.058	8.011	11.010	14.867
10.000	16.164	16.058	16.011	19.010	22.867
100.000	160.164	160.058	160.011	163.010	166.867
1000.000	1600.164	1600.058	1600.011	1603.010	1606.867
10000.000	16000.164	16000.058	16000.011	16003.010	16006.867

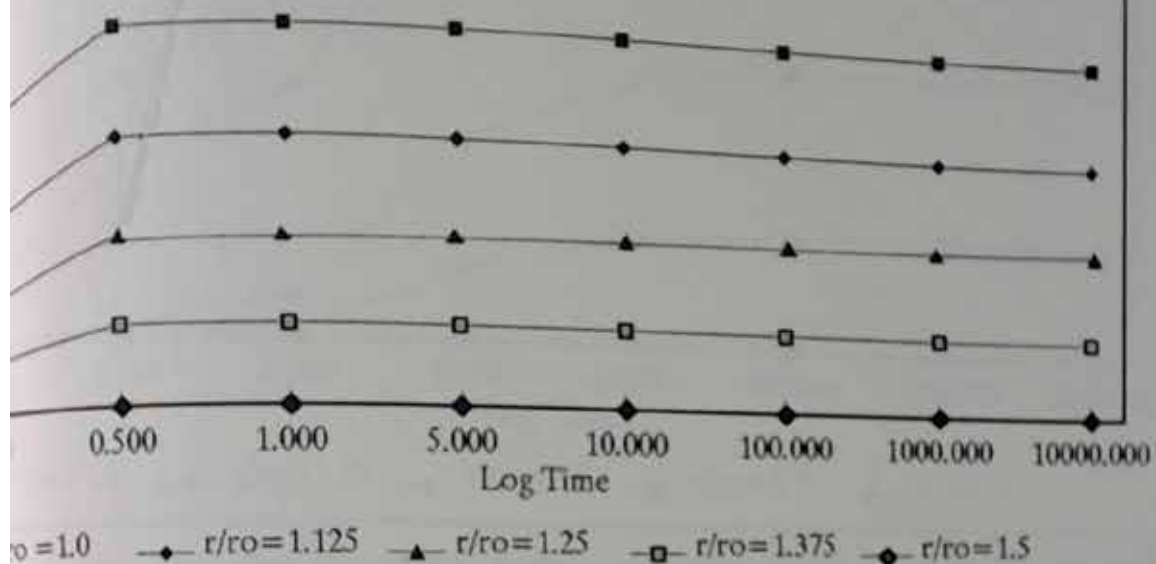
Fig. 3.22. Temperature Increase For The Constant Power and Insulated Sources  $r_1/r_0 = 1.5$



Temperature Incr. For The Constant Power and Insulated Sources $r_1/r_0 = 5$					
	$r/r_0 = 1.0$	$r/r_0 = 1.25$	$r/r_0 = 2.5$	$r/r_0 = 3.75$	$r/r_0 = 5.0$
Time	Temp rise	Temp rise	Temp rise	Temp rise	Temp rise
0.100	0.314	0.130	5.598E-05	0.000	0.000
0.300	0.617	0.408	3.208E-02	8.375E-04	1.207E-05
0.500	0.802	0.587	0.107	1.218E-02	1.590E-03
0.700	1.378	1.158	0.541	0.291	0.223
0.900	1.808	1.588	0.964	0.704	0.633
1.000	9.309	9.088	8.464	8.204	8.132
10.000	84.309	84.088	83.464	83.204	83.132
100.000	834.309	834.088	883.464	833.204	833.132

Fig. 3.23. Temperature Increase For The Constant Power and Insulated Sources  $r_1/r_0 = 5$

ture Increase For The Constant Power and Zero Temperature Sources  $r_1/r_0=1.5$

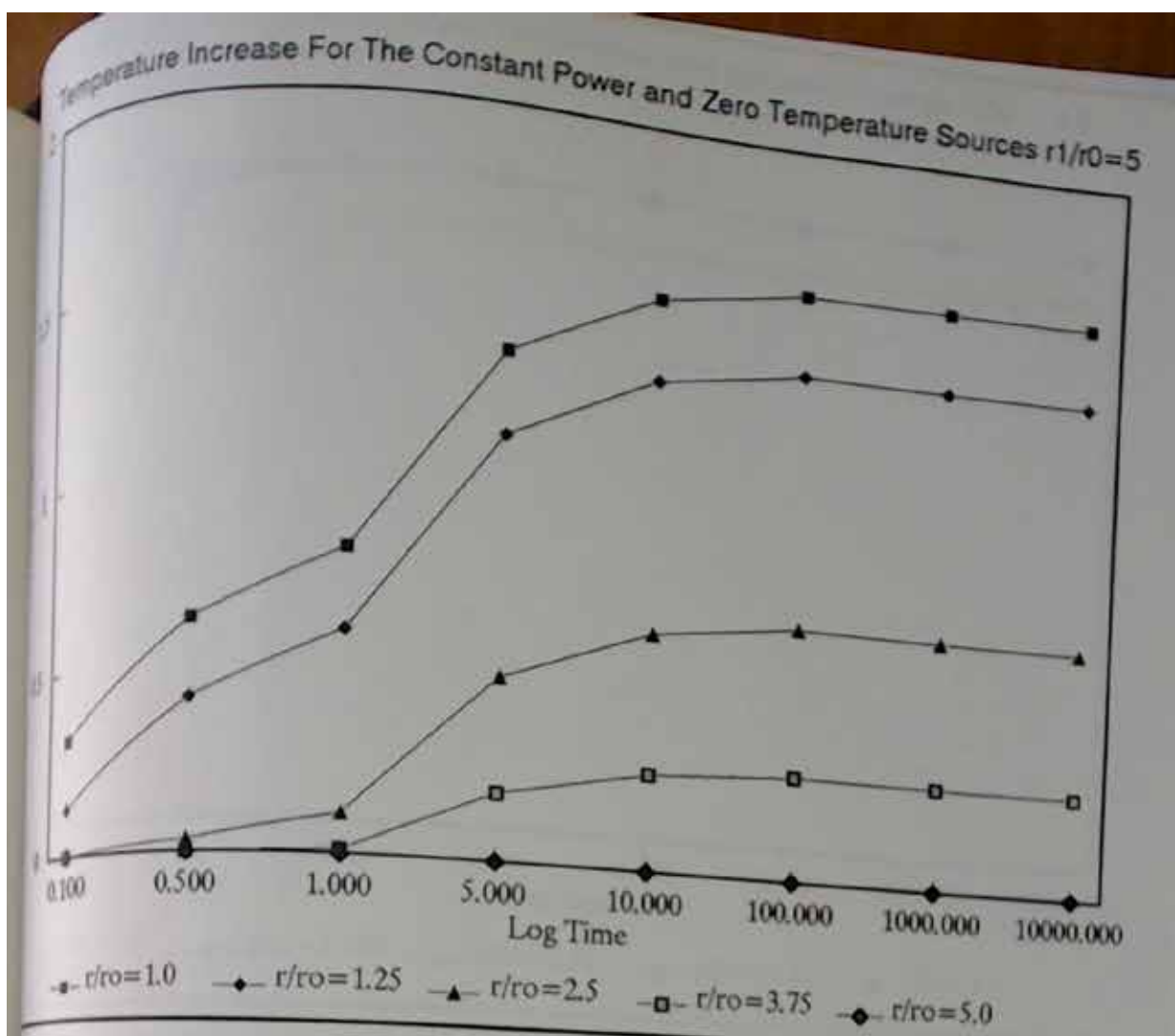


Incr. For The Constant Power and Zero Temp. Sources  $r_1/r_0=1.5$

$r_0 = 1.0 \quad r/r_0 = 1.125 \quad r/r_0 = 1.25 \quad r/r_0 = 1.375 \quad r/r_0 = 1.5$

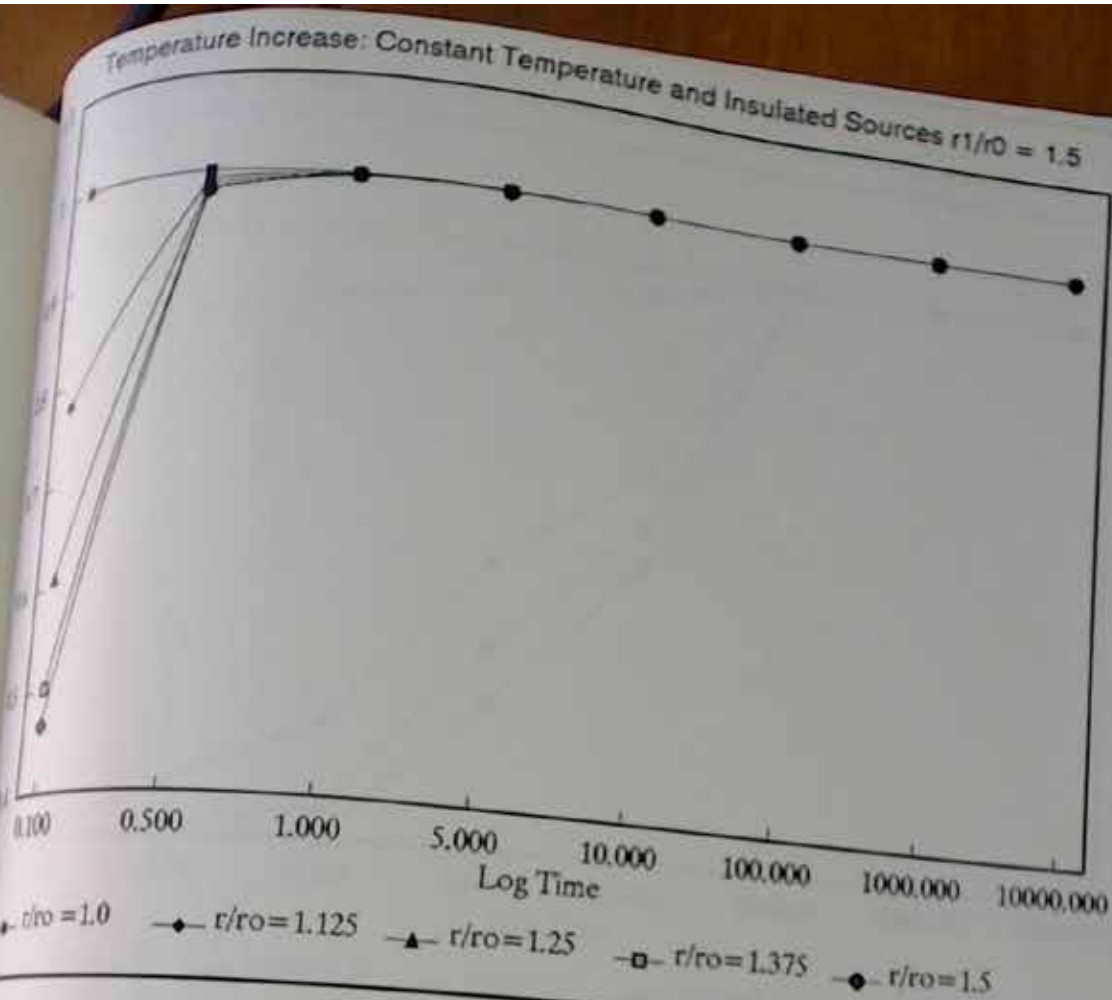
| Temp rise |
|-----------|-----------|-----------|-----------|-----------|
| 0.307     | 0.198     | 0.115     | 5.187E-02 | 0.000     |
| 0.404     | 0.287     | 0.182     | 8.667E-02 | 0.000     |
| 0.405     | 0.288     | 0.183     | 8.701E-02 | 0.000     |
| 0.405     | 0.288     | 0.183     | 8.701E-02 | 0.000     |
| 0.405     | 0.288     | 0.183     | 8.701E-02 | 0.000     |
| 0.405     | 0.288     | 0.183     | 8.701E-02 | 0.000     |
| 0.405     | 0.288     | 0.183     | 8.701E-02 | 0.000     |
| 0.405     | 0.288     | 0.183     | 8.701E-02 | 0.000     |

3.24. Temperature Increase For The Constant Power and Zero Temperature Sources  $r_1/r_0=1.5$



Temperature Increase For The Constant Power and Zero Temp. Sources $r_1/r_0=5$				
$r/r_0=1.0$	$r/r_0=1.25$	$r/r_0=2.5$	$r/r_0=3.75$	$r/r_0=5.0$
Time	Temp rise	Temp rise	Temp rise	Temp rise
100	0.314	0.130	5.598E-05	0.000
1000	0.617	0.408	3.208E-02	8.375E-04
10000	0.802	0.587	0.107	1.211E-02
100000	1.349	0.128	0.489	0.182
1000000	1.540	1.318	0.639	0.260
10000000	1.609	1.386	0.693	0.288
100000000	1.609	1.386	0.693	0.288
1000000000	1.609	1.386	0.693	0.288

Figure 3.25. Temperature Increase For The Constant Power and Zero Temperature Sources  $r_1/r_0=5$

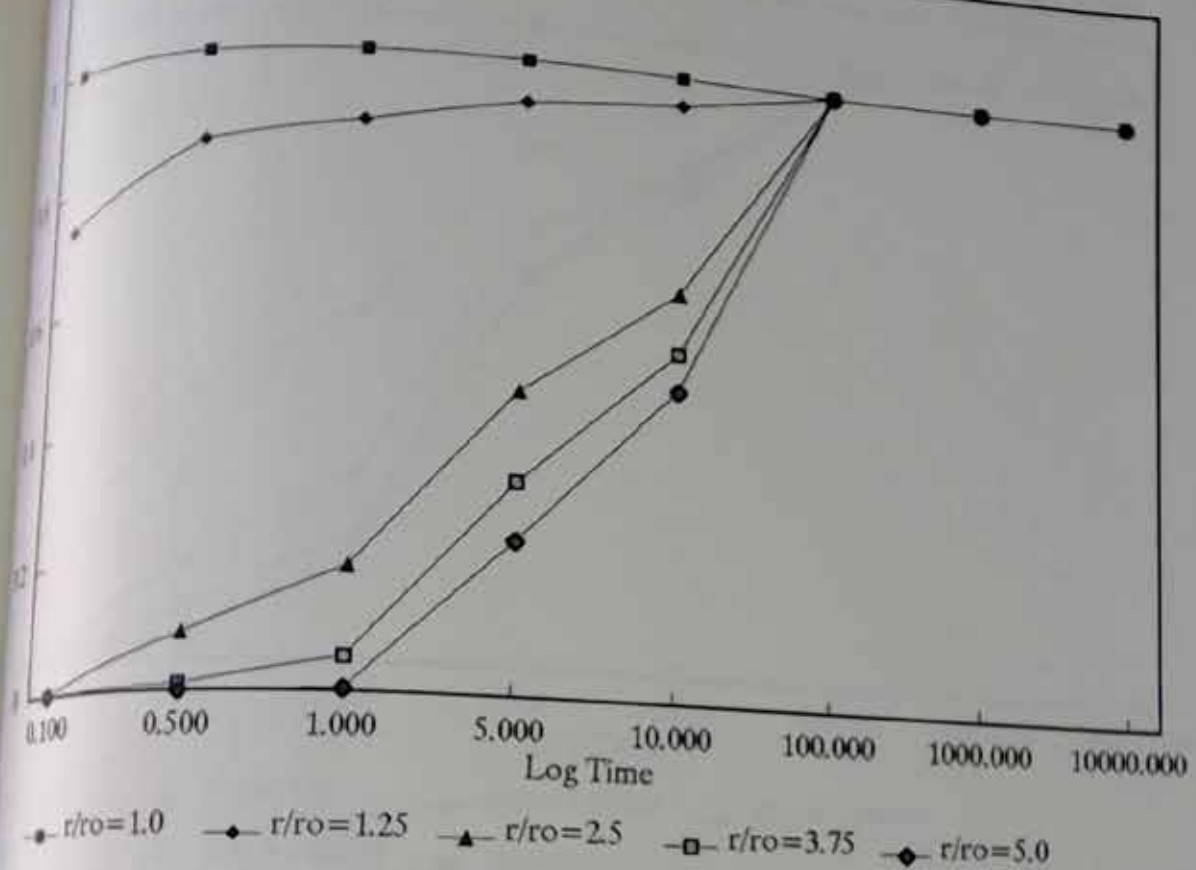


Temperature Incr: Constant Temperature and Insulated Sources  $r_1/r_0 = 1.5$

Time	$r/ro = 1.0$	$r/ro = 1.125$	$r/ro = 1.25$	$r/ro = 1.375$	$r/ro = 1.5$
100	1.000	0.779	0.609	0.503	0.467
200	1.000	0.992	0.986	0.982	0.981
300	1.000	0.999	0.998	0.997	0.999
400	1.000	1.000	0.999	0.999	0.999
500	1.000	1.000	1.000	1.000	1.000
600	1.000	1.000	1.000	1.000	1.000
700	1.000	1.000	1.000	1.000	1.000
800	1.000	1.000	1.000	1.000	1.000
900	1.000	1.000	1.000	1.000	1.000

3.26. Temperature Increase: Constant Temperature and Insulated Sources  $r_1/r_0 = 1.5$

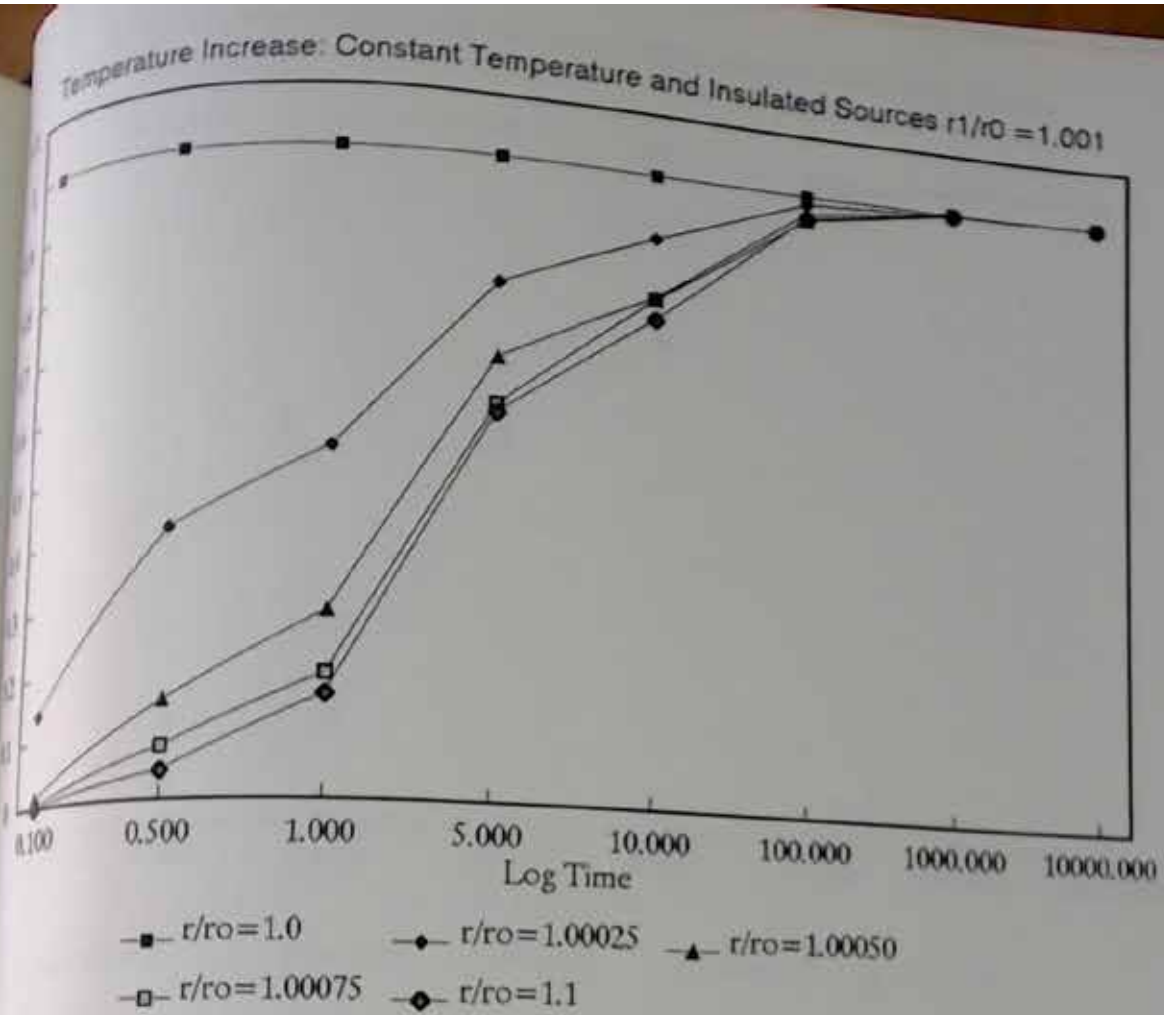
Temperature Increase: Constant Temperature and Insulated Sources  $r_1/r_0 = 5$



Temperature Increase: Constant Temperature & Insulated Sources  $r_1/r_0 = 5$

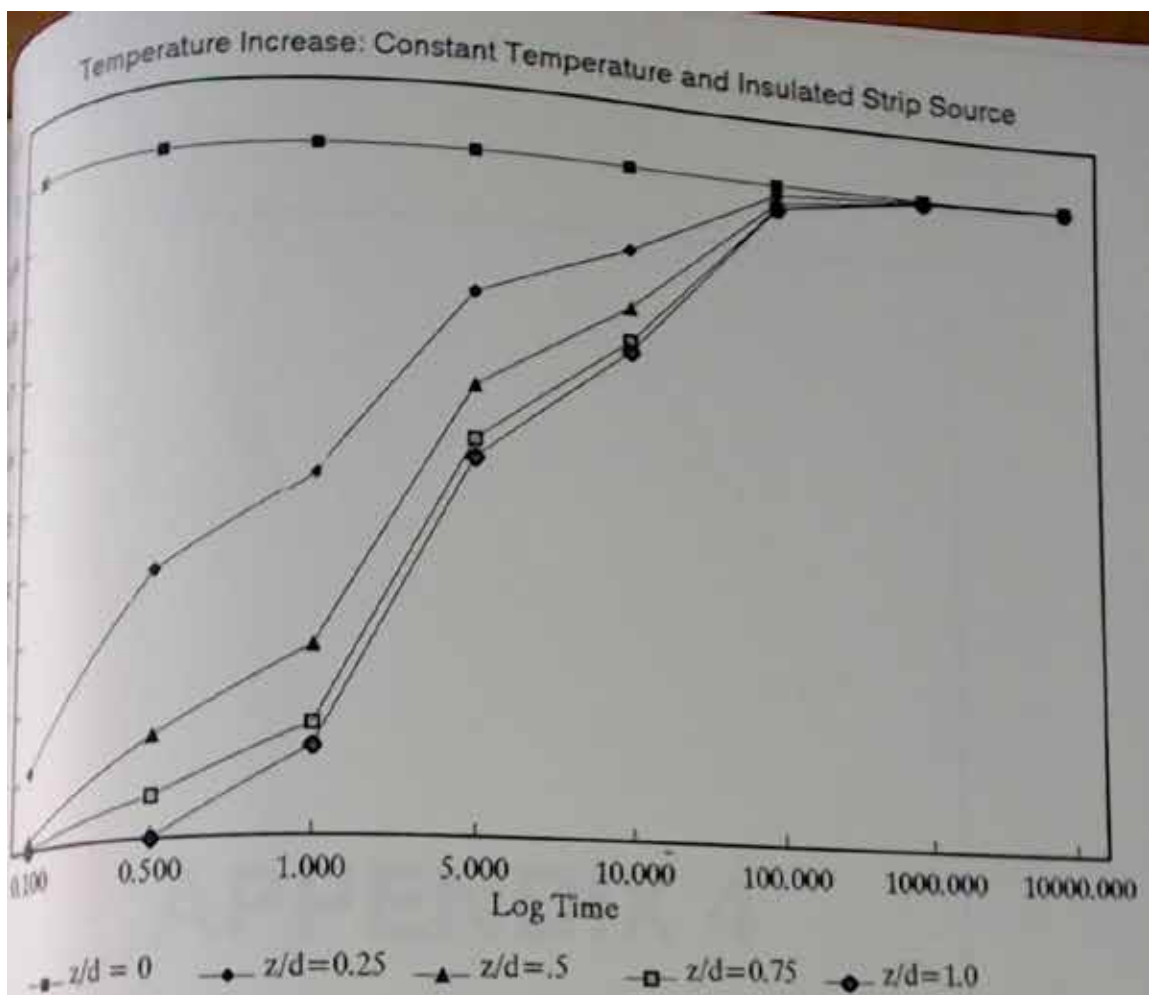
	$r/r_0 = 1.0$	$r/r_0 = 1.25$	$r/r_0 = 2.5$	$r/r_0 = 3.75$	$r/r_0 = 5.0$
Time	Temp rise	Temp rise	Temp rise	Temp rise	Temp rise
100	1.000	0.738	5.077E-04	5.985E-08	0.000
200	1.000	0.855	8.676E-02	9.793E-03	5.914E-05
300	1.000	0.884	0.190	5.275E-02	4.520E-03
400	1.000	0.930	0.468	0.327	0.238
500	1.000	0.953	0.643	0.548	0.488
600	1.000	1.000	1.000	0.999	0.999
700	1.000	1.000	1.000	1.000	1.000
800	1.000	1.000	1.000	1.000	1.000

3.27. Temperature Increase: Constant Temperature and Insulated Sources  $r_1/r_0 = 5$



Temperature Increase: Constant Temp. and Insulated Sources $r_1/r_0 = 1.001$					
	$r/r_0 = 1.0$	$r/r_0 = 1.00025$	$r/r_0 = 1.00050$	$r/r_0 = 1.00075$	$r/r_0 = 1.1$
0.1	1.000	0.141	1.406E-02	1.367E-03	2.426E-04
0.5	1.000	0.406	0.148	8.062E-02	4.316E-02
1.0	1.000	0.527	0.280	0.187	0.156
2.0	1.000	0.799	0.680	0.606	0.593
5.0	1.000	0.899	0.803	0.799	0.767
10.0	1.000	0.988	0.973	0.960	0.964
20.0	1.000	0.999	0.999	0.999	0.999
50.0	1.000	1.000	1.000	1.000	1.000

Fig. 3.28. Temperature Increase: Constant Temperature and Insulated Sources  $r_1/r_0 = 1.001$



Temperature Increase: Constant Temperature and Insulated Strip Source					
$z/d = 0$	$z/d = 0.25$	$z/d = .5$	$z/d = 0.75$	$z/d = 1.0$	
Temp rise	Temp rise	Temp rise	Temp rise	Temp rise	
1.000	0.113	1.209E-02	1.198E-03	2.027E-04	
1.000	0.380	0.145	6.003E-02	3.895E-04	
1.000	0.510	0.267	0.157	0.125	
1.000	0.786	0.646	0.566	0.541	
1.000	0.872	0.784	0.732	0.716	
1.000	0.984	0.973	0.966	0.964	
1.000	0.998	0.997	0.997	0.996	
1.000	0.999	0.999	0.999	0.999	

1.29. Temperature Increase: Constant Temperature and Insulated Strip Source

## **APPENDIX 4**

#### Appendix 4 Special Cases for Pore Pressures when $c_v = k$

The case of  $c_v = k$  for the permeable soil with a constant or exponentially declining power source

$$\text{where } \bar{u} = \frac{x}{(1 - c_v/k)} \left[ \frac{K_0(\xi' r/r_0)}{\xi' K_1(\xi')} - \frac{K_0(nr/r_0)}{n K_1(n)} \right] \cdot \frac{\bar{q}}{2\pi k}$$

where

$$n = \sqrt{\frac{sk}{c_v}} \quad \text{and} \quad \xi' = \sqrt{\frac{s}{k}} \quad \text{and} \quad c_v/k = \xi'^2/n^2$$

when  $c_v = k$  the above expression is undefined but L'Hopital's rule may be used to evaluate it.

Re L'Hopital's Rule:

$$\lim_{x \rightarrow a} \frac{f(x)}{g(x)} = \lim_{x \rightarrow a} \frac{f'(x)}{g'(x)} \quad \text{when } f(a) = g(a) = 0$$

The limit as  $c_v \rightarrow k$  is the same as  $n \rightarrow \xi'$

$$\text{Let } r = \left[ \frac{K_0(\xi' r/r_0)}{\xi' K_1(\xi')} - \frac{K_0(nr/r_0)}{n K_1(n)} \right]$$

and

$$g = (1 - \xi'^2/n^2) 2\pi k$$

Consider

$$\frac{df}{dx} = -\frac{r/r_0 K_1(nr/r_0) n K_1(n) + n K_0(n) K_0(nr/r_0) \bar{q}}{n^2 K_1^2(n)}$$

$$\frac{dg}{dn} = 4\pi K \xi'^2 n^{-3}$$

then

$$\frac{C}{q} = \frac{\chi q}{4\pi k} \frac{n^2 (r/r_0 K_1(nr/r_0) K_1(n) - K_0(n) K_0(nr/r_0))}{n K_1^2(n)}$$

in the limit as  $n \rightarrow \infty$

$$\tilde{u}_{cv \rightarrow \infty} = \frac{\chi q}{4\pi k} \left[ \frac{r/r_0 K_1(\xi' r/r_0) K_1(\xi')}{K_1^2(\xi')} - \frac{K_0(\xi') K_0(\xi' r/r_0)}{K_1(\xi')} \right]$$

$$\text{or } \tilde{u}_{cv \rightarrow \infty} = \frac{F(r/r_0 K_1(\xi' r/r_0) K_1(\xi')) - K_0(\xi') K_0(\xi' r/r_0)}{2 K_1^2(\xi')}$$

where

$$u_{cv} = \frac{\chi q}{2\pi k} \text{ for the purposes of calculating and plotting.}$$

$$\text{where } F = \frac{1}{\xi'} \text{ for constant power source, } \frac{1}{\xi'^2 + d}$$

for the exponentially declining power source.

Now the case of  $c_v = \kappa$  for a permeable soil with a constant surface temperature source is examined

Again L'Hopital's rule is used with

$$\tilde{u} = \left[ \frac{K_0(\xi' r/r_0)}{\xi' K_0(\xi')} - \frac{K_1(\xi')}{K_0(\xi')} \frac{K_0(nr/r_0)}{n K_1(n)} \right] \cdot e_0 \cdot \frac{1}{(1 - c_v/\kappa) \xi'}$$

here let

$$\begin{aligned} f &= \frac{1}{\xi' K_0(\xi')} \left[ \frac{K_0(\xi' r/r_0)}{\xi' K_0(\xi')} - \frac{K_1(\xi')}{K_0(\xi')} \frac{K_0(nr/r_0)}{n K_1(n)} \right] e_0 \\ g &= (1 - c_v/\kappa) \xi' \end{aligned}$$

then

$$\frac{df}{dn} = \lambda \frac{\alpha_0 K_0(\xi')}{K_0(\xi)} \left[ \frac{E/r_0 K_1(nr/r_0) n K_1(n) - n K_0(n) K_0(nr/r_0)}{n^2 K_1^2(n)} \right]$$

$\delta q/\delta n = 2\zeta^3 n^{-3}$  and thus

$$\frac{d\zeta}{dn} = \frac{r/r_0 K_1(\xi' r/r_0) K_1(\xi') - K_0(\xi') K_0(\xi' r/r_0)}{2\zeta K_0(\xi') K_1(\xi')}$$

where  $\zeta' = \lambda \alpha_0$  for purposes of calculation and plotting.

The results for pore pressure in these 3 cases are evaluated with appropriate forms of LTFORM and the results presented in figure 15, 16 and 17 respectively and in appendix 3.